ACTA UNIVERSITATIS SZEGEDIENSIS

ACTA MINERALOGICA-PETROGRAPHICA

TOMUS XXVI. Fasc. 1.

SZEGED, HUNGARIA
1983

NOTE TO CONTRIBUTORS

General

The Acta Mineralogica—Petrographica publishes original studies on the field of geochemistry, mineralogy and petrology, first of all studies of Hungarian researchers, papers resulted in by co-operation of Hungarian researchers and those of other countries and, in a limited volume, papers from abroad on topics of global interest.

Manuscripts should be written in English and submitted to the Editor-in-chief, Institute of Mineralogy, Geochemistry and Petrography, Attila József University, H-6701 Szeged, Pf. 651, Hungary.

The authors are responsibe for the accuracy of their data, references and quotations from other sources.

Manuscript

Manuscript should be typewritten with double spacing, 25 lines on a page and space for 50 letters in a line. Each new paragraph should begin with an indented line. Underline only words that should be typed in italics.

Manuscripts should generally be organized in the following order:

Title
Name(s) of author(s) and their affiliations, in foot-note the address of the author to whom the correspondence should be sent.
Abstract
Introduction
Methods, techniques, material studied, description of the area investigated, etc.
Results
Discussion or conclusions
Acknowledgement
Explanation of plates (if any)
Tables
Captions of figures (drawings, photomicrographs, etc.)

Abstract

The abstract cannot be longer than 500 words.

Tables

The tables should typewritten on separate sheets and numbered according to their sequence in the text, which refers to all tables.

The title of the table as well as the column headings must be brief, but sufficiently explanatory.

The tables generally should not exceed the type-area of the journal, i.e. 12.5×18.5 cm. Fold-outs can only exceptionally be accepted.

ACTA UNIVERSITATIS SZEGEDIENSIS

ACTA MINERALOGICA-PETROGRAPHICA

TOMUS XXVI

SZEGED, HUNGARIA
1983/1984

HU ISSN 0365—8066

Adjuvantibus

BÉLA MOLNÁR et TIBOR SZEDERKÉNYI

Redigit

GYULA GRASSELLY

Edit

Institutum Mineralogicum, Geochimicum et Petrographicum
Universitatis Szegediensis de Attila József nominatae

Nota

Acta Miner. Petr., Szeged

Szerkeszti

GRASSELLY GYULA

A szerkesztőbizottság tagjai

MOLNÁR BÉLA és SZEDERKÉNYI TIBOR

Kiadja

a József Attila Tudományegyetem Ásványtani, Geokémiai és Kőzettani Tanszéke
H-6722 Szeged, Egyetem u. 2—6.

Kiadványunk címének rövidítése
Acta Miner. Petr., Szeged

CONTENTS

CONTENTS

Acta Mineralogica-Petrographica. Szeged, XXVIII, 5 - 17, 1983

VARIATIONS OF BEACH SANDS WITH SEASONS, BEACH SLOPE AND SHORE DYNAMICS ON THE NILE DELTA COAST

N. M. EL-FISHAWI and B. MOLNÁR

ABSTRACT

Sandy beaches of the Nile Delta coast show a marked variation of grain size with the season and with the changing shore dynamics. Average median grain size of beach sands ranges from 1.98 ∅ in winter to 2.40 ∅ in summer. Beach face slope is shown to depend primarily on the median diameter and standard deviation of beach sediments. The highest correlation coefficient (0.908) is found between slope and median, and there is also a significant correlation (0.806) betwee nslope and sorting. Relying upon statistical analysis, it is demonstrated that the grain size of beach sands is proportional to the shore dynamics affecting Nile Delta coast. A procedure is suggested for the determination of diameter of sand grains about to be moved or added to the beach under a range of reasonable wave heights and current velocities.

INTRODUCTION

During the last three decades many studies have been carried out concerning the movement of beach sediment and its relation to the causative hydrodynamic factors [ZENKOVICH, 1967; KING, 1972; KOMAR, 1976]. Some of these investigations are based on laboratory experiments. Regarding to the threshold velocity, no measurements have obtained from the field.

The Nile Delta beach is a variable beach facing the open Mediterranean Sea for about 144 km. The presence of cusps, berms, bars and accretion and erosion forms are the main characteristic features of this beach. Its variability according to grain size parameters, beach face slope and the affecting hydrodynamic factors makes it suitable for the study of the relationship between these characteristics.

Published geological informations on the variation of beach sands with time are still few [TRASK and JOHNSON, 1955; TRASK, 1956; Coastal Erosion Studies, 1976; EL-FISHAWI *et al.*, 1976]. The present investigation, however, differs from the others. Its aim is to trace the seasonal variation of beach sands along the coast and not on the same place with different times.

Beach samples were collected along the Nile Delta coast between Rosetta and Damietta mouths *(Fig. 1A)*. Two series of samples were collected during January, 1975 and July, 1978 at 3 km intervals. Littoral currents were measured also along the coast with the same standard interval of beach samples. Repeated beach samples also were collected at different dates from local Burullus beach astride Burullus outlet *(Fig. 1B)*. At the same time, current velocities and wave heights were recorded.

TECHNIQUES

Grain size analyses were carried out by the conventional sieving method using a vibrating shaker. About 80 gm split of each sample was screened for 25 minutes using one-phi interval. The cumulative percentages were plotted on probability paper,

and grain size parameters were calculated using the formulae of FOLK an WARD [1957].

Wave heights were obtained by means of OSPOS (Offshore Pressure Operated-Suspended) wave records situated just west of Burullus outlet. Measurements of littoral current were made by simple floats whose movements were observed with time between two stations marked by poles. Only surface currents were measured.

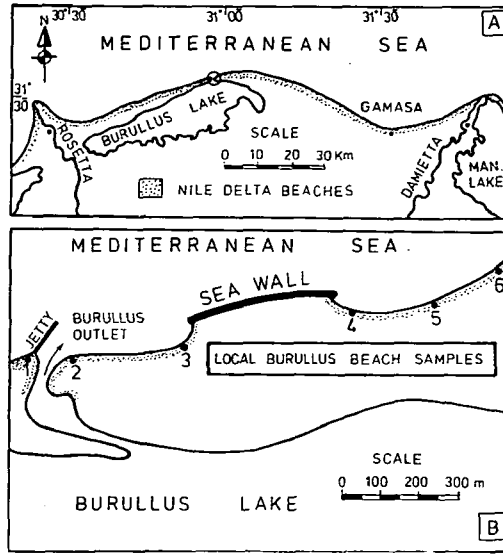

Fig. 1. A. Location map showing Nile Delta beaches.
B. Sites for beach samples — Local Burullus area

The application of statistics should be based upon an average of a large number of data. Although there are 6 times for recording wave heights per day with recording interval of 20 minutes, it is probably long enough for the wave conditions to have changed sufficiently for successive records. Data on the littoral current velocities and wave heights were averaged for each date of sampling of beach sands.

Time variation of beach sands

Many sandy beaches of the Nile Delta coast show a marked variation of grain size with the seasons and with the changing shore dynamics. The coarser sandy beaches, particularly the central part of the coast, are highly variable both from place to place and from time to time. On contrast, beaches with fine sand do not show such marked variations. It is generally true that the grain size of beach sands is larger where the wave energy is greater.

Visual analysis of the data can be made by plotting the cumulative percentages of beach sands with distance along the Nile Delta coast *(Fig. 2)*. The results obtained are suitable to support the previous studies on the variation of beach sands with time. Table 1 summarizes the main differences between winter and summer beach sediments.

TABLE 1

Average grain size of Nile Delta beach sands during winter and summer seasons

Grain size \ Season	Winter	Summer
Median diameter	1.98 ∅	2.40 ∅
Coarse + very coarse sand	14.77%	2.96%
Fine + very fine sand	43.56%	78.41%

Winter beach sediments:

During winter, 1975 it is observed that the coarse and very coarse sands are added to the beach sediments with a maximum value of 70.95% near Ayash Fort. This percentage, however, decreases east and westwards and ranges between 68% and 2% with an average of 14.77%. The percentage of fine and very fine sands varies along the coast being smaller in the central part and higher near Rosetta and Damietta mouths with an average of 43.56%. The range of grain sizes of the beach sands lies between a median diameter of 0.70 ∅ and 2.60 ∅ with an average of 1.98 ∅. During the winter season it was found that the lateral variation of grain size is highly variable along the coast.

Summer beach sediments:

During the summer 1978, the beach sediments show large differences in relation to the winter sediments. The main observation is that the coarse and very coarse sands are much reduced to very small values and they occur only astride Burullus outlet

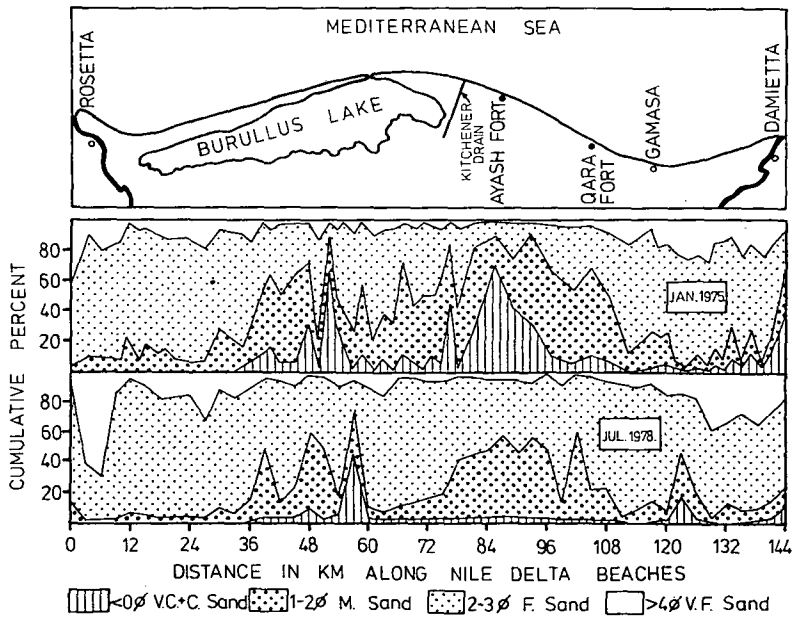

Fig. 2. Time variations of beach grain size — Nile Delta coast.

and near Gamasa. Their percentage ranges between 44% (only on one locality) and 0.02% with an average of 2.96%. On the other hand, fine and very fine sands are much increased with an average of 78.41%. The median diameter varies between 1.15 ∅ and 2.90 ∅ and averages 2.40 ∅. Grain size variations are much reduced also during summer season.

These changes between the summer and winter may be related to the fact that the beach receives more energy in winter than in summer. This is reasonable for the abundance of coarse sand in winter and fine sand in summer. The coarse materials which feed the beach during winter are available from offshore sources and are periodically added to the beach sediments [EL-FISHAWI, 1977]. The investigation of grain size distribution, as shown in *Fig. 2* deals with another character of Nile Delta beach sands. A general pattern of grain size peaks appear to remain stationary in a very narrow stretch throughout the different yearly sampling and in spite of time variation of beach sands. Two main peaks can be observed east of Burullus outlet and near Ayash Fort. This feature has been observed by Coastal Erosion Studies [1976] and EL-FISHAWI [1977]. Until now, it is difficult to explain why the peaks occur and why they remain there.

Beach face slope and beach sands

The angle of beach face is what a line joining the beach crest to the top of the steps makes with the horizontal. The angle was measured in degress with a modified protractor by the authors. Samples have been collected along Nile Delta coast from the part of the beach face subjected to wave action in order to remove the variability due to seaward variation in grain size parameters.

Table 2 illustrates the littoral current velocity, angle of beach face slope and grain size parameters of beach sands along Nile Delta coast.

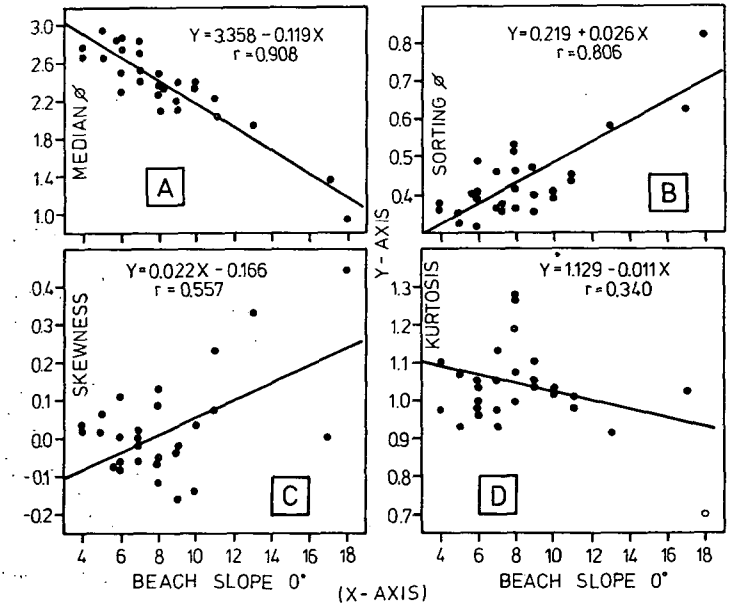

Fig. 3. Relationships between beach face slope and statistical parameters of beach sands

TABLE 2

Average current velocity, beach slope and statistical parameters of Nile Delta beach sands during 1978

Location in km.	Curr. vel. (cm/sec.)	Beach slope, 0°	Median, ∅	Sorting, ∅	Skewness	Kurtosis
3 km WBR.	32	—	3.10	0.40	—.14	1.07
6 km WBR.	55	—	3.15	0.40	—.14	1.07
9 km WBR.	41	—	2.70	0.30	0.16	1.23
15 km WBR.	51	—	2.60	0.32	0.07	1.18
18 km WBR.	40	—	2.70	0.39	0.32	1.27
24 km WBR.	42	—	2.70	0.32	0.07	1.18
27 km WBR.	35	—	2.85	0.40	0.14	1.08
33 km WBR.	45	—	2.65	0.42	0.07	0.96
39 km WBR.	44	—	2.00	0.49	0.00	0.94
45 km WBR.	31	—	2.35	0.54	0.01	1.08
48 km WBR.	38	—	1.90	0.54	—.13	0.92
54 km WBR.	34	—	2.40	0.51	—.19	1.23
57 km WBR.	42	7°	2.40	0.46	0.02	1.06
0.0 km EBR.	42	9°	2.20	0.47	—.16	1.06
3 km EBR.	55	8°	2.10	0.52	0.13	1.00
6 km EBR.	37	10°	2.40	0.41	0.04	1.04
9 km EBR.	52	7°	2.70	0.36	0.00	0.98
12 km EBR.	48	18°	0.95	0.83	0.45	0.71
15 km EBR.	45	8°	2.25	0.46	—.05	1.27
18 km EBR.	43	8°	2.50	0.41	0.09	1.08
21 km EBR.	38	9°	2.40	0.35	—.02	1.05
33 km EBR.	35	11°	2.25	0.44	0.07	0.99
36 km EBR.	31	6°	2.50	0.41	—.06	1.04
39 km EBR.	33	6°	2.30	0.40	—.06	1.01
42 km EBR.	37	9°	2.10	0.40	—.02	1.11
45 km EBR.	37	8°	2.35	0.36	—.06	1.28
48 km EBR.	34	10°	2.35	0.40	—.14	1.04
51 km EBR.	39	11°	2.05	0.45	0.24	1.02
54 km EBR.	30	7°	2.50	0.35	—.06	1.14
57 km EBR.	35	5°	2.65	0.35	0.02	0.94
60 km EBR.	31	8°	2.35	0.52	0.12	1.20
3 km EGAM.	27	7°	2.85	0.35	—.02	0.94
6 km EGAM.	27	4°	2.65	0.38	0.02	1.11
9 km EGAM.	40	13°	1.95	0.59	0.34	0.92
12 km EGAM.	33	6°	2.75	0.49	—.07	1.04
15 km EGAM.	30	5°	2.95	0.32	0.06	1.08
18 km EGAM.	34	4°	2.75	0.36	0.03	0.97
21 km EGAM.	32	6°	2.90	0.32	—.11	0.96
24 km EGAM.	47	6°	2.90	0.40	0.00	0.97
27 km EGAM.	45	17°	1.35	0.63	0.01	1.04

Figure 3 shows the relationships between beach slope and grain size parameters. For each relationship, the regression equation is calculated in the form of $Y=\alpha+\beta X$. The correlation coefficient is calculated to measure the correspondence of observations to any fitted equation.

The relationship between beach face slope and median diameter is shown in *Fig. 3A*. It is observed that the beach slope increases with increasing median diameter.

The relationship is linear, ranging from 18 degrees for a coarse diameter of 1 ∅, 11 degrees for a medium diameter of 2 ∅, to 4 degrees for a fine diameter of 3 ∅. The regression equation is $Y=3.358-0.119X$ and $r=0{,}908$ where X is the beach slope in degrees and Y is the median in phi units. The correlation coefficient 0.908 indicates a strong relationship.

Beach face slope is affected also by the degree of sorting of beach sediments as well as by the median diameter itself. Poorly sorted sand beaches are much steeper than those of well sorted ones as shown in *Fig. 3B*. The transition from a gentle slope (4 degrees) to a steep one (18 degrees) is accompanied with changing from a better sorted sand (0.35 ∅) to a poorly sorted one (0.83 ∅). The regression equation is $Y=0.219+0.026X$ and $r=0.806$ where X is the slope in degrees and Y is the sorting in phi units. The correlation coefficient 0.806 indicates that the median diameter is more effective in beach slope than the sorting parameter.

In the contrast, the relationships between beach slope and both skewness and kurtosis are not as strong as that between slope and both median and sorting. *Figure 3C* shows that when the beach slope increases the sand becomes more fine skewed. However, the correlation coefficient 0.557 does not exhibit a strong relationship. The variation of beach slope in relation to kurtosis was found to be very weak as shown in *Fig. 3D* ($r=0.34$).

The increase of beach slope with increasing grain size has been demonstrated by several field studies [BASCOM, 1951; WIEGEL, 1964; MCLEAN and KIRK, 1969; DUBOIS, 1972]. Regarding to sorting, KRUMBEIN and GRAYBILL [1965] found that well-sorted coarse-sand beaches have steeper slopes than poorly-sorted coarse-sand beaches. MCLEAN and KIRK [1969] have a wavy curved line rather than being linear for the relationship between slope and grain size. The reason may be related to the different sources of their beach sands. Nile Delta beaches gave a linear relationship indicating probably one source from the offshore zone.

An attempt was made to correlate the beach slope with the littoral current velocity. The result is shown in *Fig. 4*. It is apparent from the scatter diagram that there are two possibilities for the behaviour of the variables. The first is represented by a fitted straight line with a regression equation of $Y=0.833+0.198\,X$ and $r=0.428$. Although the correlation coefficient is low, the scatter diagram does indicate that beach slope becomes steeper with an increase in the velocity of the littoral current.

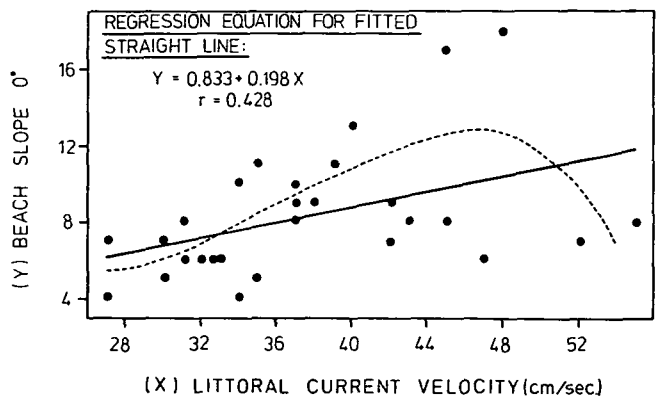

Fig. 4. Relationship between littoral current velocity and beach face slope

The second is a possibility that the beach slope increases with increasing current velocity to a critical value (48 cm/sec). Current velocity higher than this value may be destructive to the beach and will result in a steady decrease in slope. Unfortunately, the resulting scatter diagram does not exhibit a strong relationship, yet there is some suggestion of increasing slope with increasing currens velocity.

Beside the grain size parameters and littoral current, there are several variables effecting the beach slope. RECTOR [1954] found that the greater the wave steepness, the lower the beach slope. A comparison between BASCOM'S [1951] and WIEGEL'S, [1964] data for a given grain size leads to the fact that the low-energy beaches have steeper slopes than the high-energy beaches. KING [1972] showed that an increase in the wave energy will result in a decrease in slope.

Effect of current and waves on grain size of beach sands

Under the action of waves and littoral current, nearshore zone sediments are in motion and could be carried onshore to add to the beach sediments. As the orbital velocity of water flow over a bed of sediments is increased, a stage is reached when the water exerts a force on the particles sufficient to cause them to move from the bed and be transported. This stage is generally known as the threshold of sediment transport. Many equations have been proposed for the threshold of sediment motion under waves [SILVESTER and MOGRIDGE, 1971; KOMAR and MILLER, 1973]. MADSEN and GRANT [1975] and KOMAR and MILLER [1975] were able to compare the threshold under waves with the threshold under unidirectional currents. Due to the difficulties of observation and control, no measurements have been obtained from the field. Therefore, in this subject, an attempt was made to measure directly the change in beach sand diameters due to the action of littoral current velocity and significant wave height.

Correlation of beach sands with littoral current

The estimation data of littoral current velocity along Nile Delta coast and grain size parameters of beach sands as shown in table 2 were used. *Figure 5* shows the relationship of current velocity with median diameter, sorting and skewness of beach sands.

The correlation of median diameter of beach sands with littoral current velocity as shown in *Fig. 5A* gives a general view about the nature of the relationship. With decreasing current velocity, the diameter of beach sands becomes finer. It is clearly seen from the scatter diagram that the current has the ability to move both coarse and fine sediments when its velocity increases. *Figure 5B* shows that beach sands become poorly sorted with increasing current velocity. This means that well-sorted fine-sands can be deposited on the beach under low velocities of current. Both well-sorted and poorly-sorted coarse and fine sands are seen to deposite under high current velocities. Symmetrical skewed sands move under low velocities as shown in *Fig. 5C* while both coarse and fine-skewed sands can be moved under high velocities. In contrast, kurtosis gives no significant trend.

Another branch of this study has been applied on local beach around Burullus outlet. By repeated surveys at different dates, samples have been collected and currents measured under different conditions. Therefore, it is possible to estimate the change in beach sands within the same area according to the variation of littoral current velocity. Table 3 illustrates the data and *Fig. 6* shows the relationship between the variables.

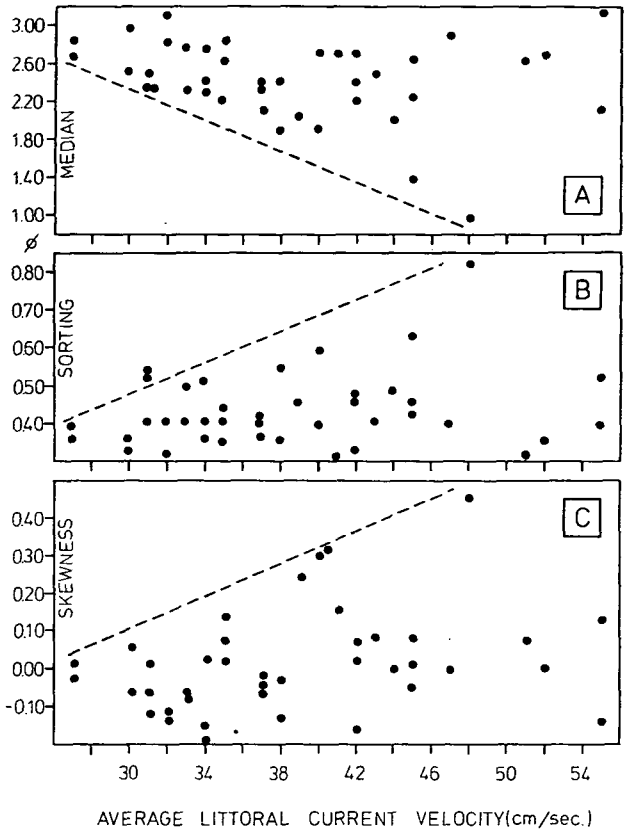

Fig. 5. Relationships between littoral current velocity and statistical parameters of beach sands along Nile Delta coast

The correlation of littoral current velocity with median diameter suggests a procedure for the acceleration of sand sizes to be transported to terminal current velocities within four intervals. The suggested procedure is to assess a suitable current velocity which initiates sediment motion for different grain size. As shown in *Fig. 6*, median diameter finer than 2.10 ∅ can be moved with velocities lower than 24 cm/sec. Median diameter ranging between 2.10—1.60 ∅ would probably be transported under current velocity ranges between 24—30 cm/sec. Sand grains with an average diameter of 1.60—1.20 ∅ tend to move with current velocity of 30—45 cm/sec. Finally, the movement of coarse sands would result with velocities over 45 cm/sec. To sum up, there is a progressive drifting of the coarser materials, from the current load and added to the beach, when the current velocity progressively decreases and vice versa.

Correlation of beach sands with significant wave height

Significant wave height is defined as the average height of the highest one-third of the waves measured over a stated interval of time, usually 20 minutes. It is designated by $H_{1/3}$. Each recording interval results in values for $H_{1/3}$, $H_{1/10}$ and H_{max}.

TABLE 3

Littoral current velocity data with relation to median diameter of local Burullus beach sands

Date	D_{50} of west B.		D_{50} of east B.			
	curr. vel. (cm/sec.)	loc. 1	curr. vel. (cm/sec.)	loc. 4	loc. 5	loc. 6
21. 2.74	37	2.35	67	2.35	2.45	2.30
6. 3.74	22	2.30	24	2.15	2.45	1.90
10. 3.74	56	1.70	36	2.25	2.00	2.50
26. 3.74	30	1.90	27	2.15	2.00	1.85
2. 4.74	36	1.90	35	2.25	2.10	2.45
	27	1.90				
9. 4.74	30	1.75	29	2.10	2.30	1.90
	25	1.75				
6. 5.74	35	1.95	34	2.20	2.10	1.60
	39	1.95				
17. 5.74	43	2.20	40	2.35	2.05	2.05
	32	2.20				
7. 7.74	27	1.60	17	2.25	2.35	2.80
4. 8.74	42	2.80	31	2.30	2.80	2.35
26. 8.74	31	2.45	31	2.35	2.05	1.25
16. 9.74	45	2.70	63	2.10	2.45	2.20
18.11.74	31	2.85	39	1.50	1.95	2.10
16.12.74	80	2.65	47	2.65	1.50	1.20
19. 1.75	18	2.10	31	2.55	2.30	1.95
12. 2.75	36	1.40	44	2.00	2.00	2.25
5. 4.75	39	1.30	48	1.50	2.10	1.10
19. 4.75	36	2.50	33	2.05	2.20	1.80

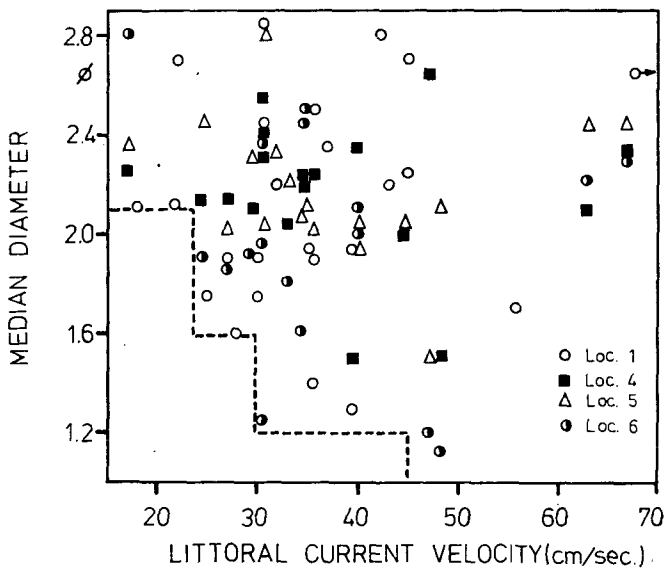

Fig. 6. Relationship between littoral current velocity and median diameter of Burullus beach sands

It was found that there is much better agreement between median diameter of beach sands and the affecting $H_{1/3}$ rather than the other wave parameters.

Table 4 summarizes the main data applied for the correlation between the two variables as shown in *Fig. 7*. The significant wave height evaluated with this scatter diagram has been used to calculate the range of grain sizes which could be set in motion by waves. It is seen that $H_{1/3}$ with an average value of lower than 35 cm is required to move median diameter of finer than 2.10 ∅. $H_{1/3}$ with an average of 60 cm would be capable of moving sediments to median diameter finer than 1.60 ∅. $H_{1/3}$ up to 90 cm moves sediments finer than 1.20 ∅. The motion of coarser grains would result with $H_{1/3}$ values higher than 90 cm.

By replotting the data shown in *Figs. 6* and *7*, a relationship between significant wave height, littoral current velocity and median diameter of beach sands can be

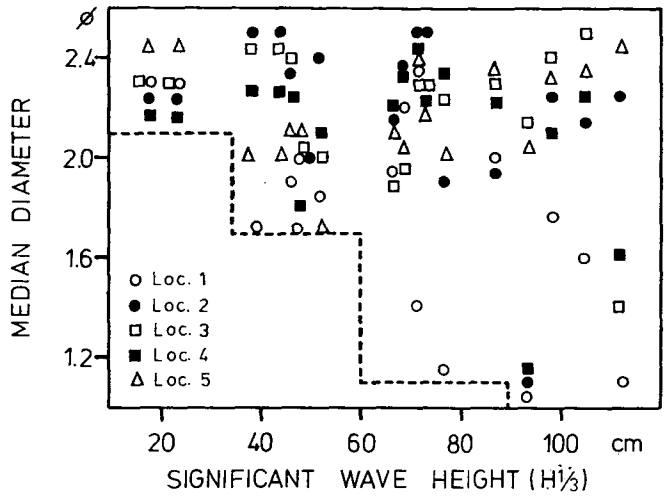

Fig. 7. Relationship between significant wave height ($H_{1/3}$) and median diameter of Burullus beach sands

obtained as shown in *Fig. 8*. This figure permitted the determination of diameter for sand grains about to be moved or added to the beach under a range of reasonable wave heights and terminal littoral current velocities. The range of grain size belonging to both wave height and current velocity was found to be nearly the same because littoral drift of beach sands is shown to depend on the longshore component of wave power which depends on the angle of wave approach.

BAGNOLD [1966] noted that grains coarser than 250 microns would probably be transported as bed load, and a significant proportion of grains finer than 250 microns by suspension. So, it can be said that sand grains coarser than 250 microns move as bed load under the action of significant wave height higher than 35 cm and current velocity of 24 cm/sec. The finer sediments move by suspensions under the action of shore dynamics with lower values than that mentioned above.

TABLE 4

Significant wave height data with relation to median diameter of local Burullus beach sands

Date	$H_{1/3}$ (cm)	Median diameter, ∅				
		loc. 1	loc. 2	loc. 3	loc. 4	loc. 5
13.12.72	48	2.00	2.00	2.00	1.80	2.10
1. 2.73	112	1.10	2.25	1.40	1.60	2.45
8. 3.73	51	1.85	2.40	2.00	2.10	1.70
3. 4.73	92	1.05	1.10	2.15	1.15	2.05
13. 8.73	72	2.35	2.50	2.30	2.45	2.35
20. 8.73	87	2.00	1.95	2.30	2.25	2.35
20. 9.73	71	1.40	2.50	2.30	2.25	2.20
30. 1.74	77	1.15	1.90	2.25	2.35	2.00
6. 3.74	19	2.30	2.25	2.30	2.15	2.45
	24	2.30	2.25	2.30	2.15	2.45
10. 3.74	39	1.70	2.50	2.45	2.25	2.00
	47	1.70	2.50	2.45	2.25	2.00
2. 4.74	46	1.90	2.35	2.40	2.25	2.10
9. 4.74	98	1.75	2.25	2.40	2.10	2.30
6. 5.74	66	1.95	2.15	1.90	2.20	2.10
17. 5.74	68	2.20	2.35	1.95	2.35	2.05
7. 7.74	105	1.60	2.15	2.50	2.25	2.35

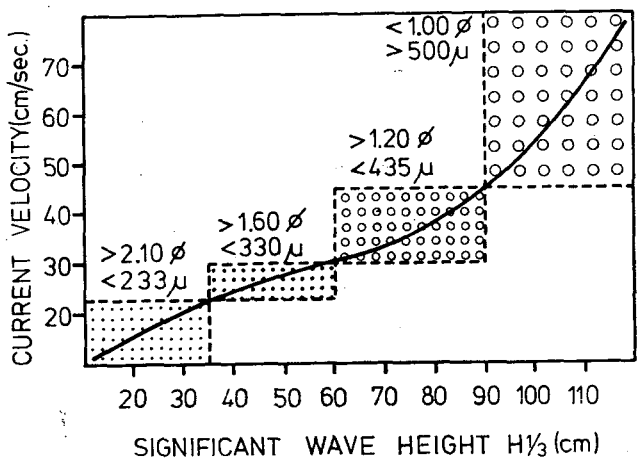

Fig. 8. Combination between significant wave height, littoral current velocity and median diameter of Burullus beach sands

CONCLUSIONS

The central part of Nile Delta beaches is highly variable. Beach sands, particularly the coarse grain beaches, show variations according to seasonal changes. In winter, beach sands are much coarser than that in summer. Great amounts of coarse and very coarse sands are added to the beach sediments during winter season from offshore sources. On the other hand, fine and very fine sands are much increased

in summer. The beach zone receives more energy in winter than that in summer and coarse sand is available where high energy can be found.

Concerning the relationship between beach face slope and grain size parameters, it was found that:

(1) Coarse and poorly sorted beach sands are much steeper than those of fine and well sortes ones.
(2) The relationship between slope and both skewness and kurtosis shows a low correlation coefficient.
(3) There is some suggestion of increasing beach slope with increasing the velocity of littoral current.

The results showed that the median diameter of beach sands, littoral current velocity and significant wave height all have diagnostic values in this study. Under the action of weak current velocity and low wave height, fine, well sorted and symmetrical skewed sands can be transported. Higher current velocities and wave heights have the ability to transport various scales of grain size parameters. When the current velocity progressively decreases, it was found that there is also a progressive drifting of the coarser materials from the current load to be added to the beach.

The correlation between beach sands and shore dynamics suggests a procedure for the sand sizes to be moved or added to the beach under these terminal values:

Median diameter of beach sands	*Littoral current velocity*	*Significant wave height*
finer than 2.10 ∅	17—24 cm/sec.	19—35 cm
finer than 1.60 ∅	24—30 cm/sec.	35—60 cm
finer than 1.20 ∅	30—45 cm/sec.	60—90 cm
finer than 1.00 ∅	45—70 cm/sec.	90—120 cm

REFERENCES

BAGNOLD, R. A. [1966]: An approach to the sediment transport problem from general physics. U. S. Geol. Surv., Prof. Pap., No. **422**, (I), 11—137.

BASCOM, W. N. [1951]: The relationship between sand size and beach face slope. Trans. Am. Geophys. Union, **32**, 866—874.

COASTAL EROSION STUDIES [1976]: Detailed Technical Report on Coastal Geomorphology and Marine Geology. UNESCO (ASRT) UNDP, Project Egypt 73/063, Alexandria, 175 pp.

DUBOIS, R. N. [1972]: Inverse relation between foreshore slope and mean grain size as a function of the heavy mineral content. Geol. Soc. Am. Bull., **83**, 871—876.

EL-FISHAWI, N. M. [1977]: Sedimentological studies of the present Nile Delta sediments on some accretional and erosional areas between Burullus and Gamasa. M. Sc. thesis, Alexandria Univ., 143 pp.

EL-FISHAWI, N. M., SESTINI, G., FAHMY, M. and SHAWKI, A. [1976]: Grain size of the Nile Delta beach sands. In: UNESCO (ASRT) UNDP-Proc. Sem. on Nile Delta Sed., Alexandria, Oct. 1975, pp. 79—94.

FOLK, R. L., and WARD, W. C. [1957]: Brazos River bar, a study in the significance of grain size parameters. J. Sedim. Petrol., **27**, 3—27.

KING, C. A. M. [1972]: Beaches and coasts. 2nd ed., London, Edward Arnold Ltd., 570 pp.

KOMAR, P. D. [1976]: Beach processes and sedimentation. Prentice-Hall, Englewood Cliffs. 429 pp.

KOMAR, P. D., and MILLER, M. C. [1973]: The threshold of sediment movement under oscillatory water waves. J. Sedim. Petrol., **43**, 1101—1110.

KOMAR, P. D., and MILLER, M. C. [1975]: Sediment threshold under oscillatory waves. Proc. 14th Conf. on Coast. Eng., pp. 756—775.

KRUMBEIN, W. C., and GRAYBILL, F. A. [1965]: An introduction to statistical models in geology. McGraw-Hill, New York, 574 pp.

MADSEN, O. S., and GRANT, W. D. [1975]: The threshold of sediment movement under oscillatory waves. A discussion. J. Sedim. Petrol., **45**, 360—361.

MCLEAN, R. F., and KIRK, R. M. [1969]: Relationship between grain size, size sorting and foreshore slope on mixed sand-shingle beaches. N. Z. J. Geol. Geophys., **12**, 138—155.

RECTOR, R. L. [1954]: Laboratory study of the equilibrium profiles of beaches. U. S. Army Corps of Eng., Beach Erosion Board, Tech. Memo. No. **41**, 32 pp.
SILVESTER, R., and MOGRIDGE, G. R. [1971]: Beach of waves to the bed of the continental shelf. Proc. 12th Conf. on Coast. Eng., pp. 580—595.
TRASK, P. D. [1956]: Changes in configuration of Point Reyes Beach, California, 1955—1956. U. S. Army Corps of Eng., Beach Erosion Board, Tech. Memo. No. **91**, 49 pp.
TRASK, P. D., and JOHNSON, C. A. [1955]: Sand variation at Point Reyes Beach, California. U. S. Army Corps of Eng., Beach Erosion Board, Tech, Memo. No. **65**.
WIEGEL, R. L. [1964]; Oceanographical engineering. Prentice-Hall, Englewodd Cliffs. 532 pp.
ZENKOVICH, V. P. [1967]: Processes of coastal development. Edinburgh and London, Oliver and Boyed, 738 pp.

Manuscript received, 27 January, 1983

NABIL M. EL-FISHAWI
Institute of Coastal Research
Alexandria, Egypt.

BÉLA MOLNÁR
Attila József University
Department of Geology and Paleontology
H-6722 Szeged,
Egyetem u. 2.
Hungary

Acta Mineralogica-Petrographica, Szeged, XXVI/1, 19—25, 1983

GENESIS OF BEACH FLAGGY MARLSTONE BOULDERS BY TRACE ELEMENTS AND ISOTOPIC MEASUREMENTS

S. N. WASSEF, M. M. ALY and M. S. ELMANHARAWY

ABSTRACT

During the prospection of Rosetta beach black sands deposits a piled deposit of marlstone boulders was found breaking the homogeneity of the beach. The genesis of this deposit was questionable. Therefore, its origin was studied by trace element and stable isotopic measurements, besides geological investigations and the study of the history of the area. The results obtained revealed that these boulders are of fresh water environment affected by the surrounding sea water rejected on beach during abnormal and strong weather conditions.

INTRODUCTION

The area of east Rosetta extends from the Rosetta estuary to Lake Burullus inlet *(Fig. 1)*. In general, this part is a delta neutral beach resulting from the delta growth seawards. The coastal area is generally flat and consists of a single berm; no rocky structures are present. The waves wash up the berm, but seldom cross it except in winter and in stormy conditions. In Rosetta area some sand dunes may interrupt the flatness of the coastal plain. The beach face slope increases from completely flat to relatively steeper nearer to Lake Burullus, and this prevents the sea water to cross the berm in this region. This part is characterized by the loss of heavy minerals and tends to have coarser grain sizes than gentle slopes which have finer particles.

The first part of this beach extends for a distance of about 10 km from the mouth. It is characterized by a complex group of lagoonal lakes of irregular variable shape according to the quantity of water crossing the beach to these lakes. The second part extends from the 10th km to Lake Burullus inlet and is characterized by its flatness and regularity except the presence of some sand dunes scattered on the beach [WASSEF, 1973].

DEPOSIT ACCUMULATION

At a distance about 38 km from Rosetta mouth, there is found an accumulation of carbonate rocky fragments on the nearshore area *(Fig. 1)*. This deposit is an anomalous one breaking the homogeneity and the sandy nature of the beach. The size of the rocky fragments ranges between a few cm length to more than 30 cm; the fragments consist of one rock type. Some of the rocky fragments are elongated while others are rounded. This deposit is mixed with shells and foraminiferal organisms stuck to the fragment faces. It starts from the berm as far as about 60 m towards the backshore and extends about 1 km parallel to the beach line. The boulders are hard, greyish in colour, and mostly flat (*Figs. 2* and *3)*.

The flat boulders tend to remain lying on their larger side. It seems that joints or stratification divided them into homogeneous but flat or oblong bodies during disintegration. The rounding, however perfect, will but not lead to sphericity but must then result in a disky, triaxial ellipsoid [PETTIJOHN, 1957].

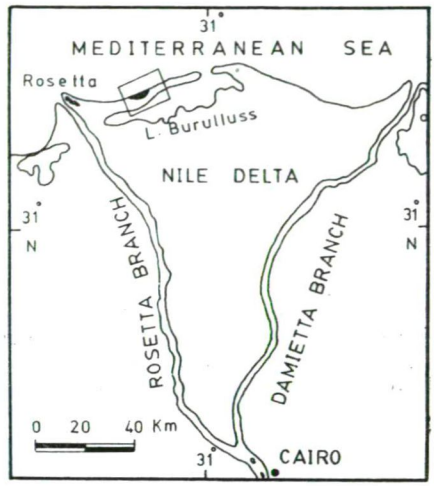

Fig. 1. Location map of the marlstone on Rosetta beach

Fig. 2. General view of the marlstone boulders accumulation on Rosetta beach

CHEMICAL INVESTIGATION

Three samples have been chosen to represent this deposit to be analyzed. The chemical investigation was done by dissolving a crushed weighed part from every sample in 5% HCl. The result showed an average residue (clay) of about 36% of the total weight. The average of the dissolved carbonates was about 64%.

According to PETTIJOHN [1957] it is known that an indurated mixture of clay materials and calcium carbonate, normally containing 25 to 75% clay is marlstone. Then the deposit accumulated on beach consists of flaggy marlstone boulders.

GEOLOGICAL INVESTIGATION

From the geological point of view, this deposit is the only rocky medium on a uniform sandy beach. The grain size analysis of the beach sand below (1 m depth) showed no difference in size from the abundant grains of the whole beach, where the

Fig. 3. A photograph showing the size of the flaggy marlstone boulders on beach (relative to 30 cm rule)

average value of the median is 2.69 ∅ [WASSEF, 1973]. Besides, there are no marlstone fragments buried in beach sands. This leads to the conclusion that this deposit is a surface one coming from sea. This idea is supported by the observation of some pieces of different sizes sliding up on the beach face slope coming from sea.

There are two suggested sources likely to feed this deposit. One is the submerged old marine rocks, and the other is the River Nile branch. Because of the large size of the deposit components, it is excluded that the actual Rosetta Nile branch is the

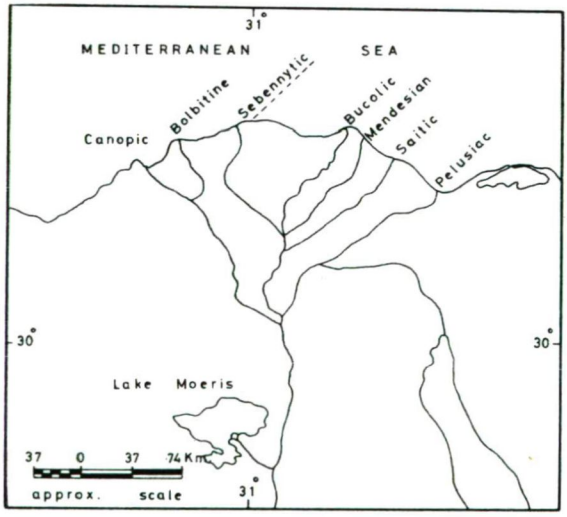

Fig. 4. Map showing the old Nile branches (BALL, 1942, after HERODOTUS 450 B. C.)

source due to the long distance between the mouth anf the deposit location. The transportation of fragments of this size cannot be realized for this long distance (38 km) along the beach. The rejection of these heavy pieces on beach indicates high erosion conditions in the area, and abnormal weather conditions especially in winter. These conditions are sufficient to push these boulders as far as the berm. During. the occasional storms and abnormal conditions, the water covers this area violently and the erosion due to change of sea level takes place [McKee, 1959].

From the historical geology of the area, there was an old Nile branch called the Sebennytic branch mentioned by Ball [1942], after Herodotus 450 B. C. *(Fig. 4)*. This old branch is suggested to be one of the sources of this deposit. The ancient site of this old branch estuary is coinciding approximately with the area of the deposit.

To arrive at a decisive conclusion about the origin of this deposit, whether marine or fresh water, two methods have been applied, the trace element analysis beside the oxygen and carbon isotopic measurements.

TRACE ELEMENT ANALYSIS

Among the methods which can be used to differentiate between marine and fresh water sediments, the geological methods are considered the most important. A frequently used geochemical method is the trace element analysis and the consideration of relation between elements which are distinctive with respect to the environment of sedimentation. Some binary relations are very decisive in differentiation between marine and fresh water environments.

Keith and Degens [1959] showed that the binary relation between boron and gallium is useful as a geochemical criterion for the differentiation between fresh water and marine sediments *(Fig. 5)*. Potter *et. al* [1963] used the boron-vanadium relation as an environmental discriminator between marine and fresh water sediments. This relation is used to get the respective environment of the investigated

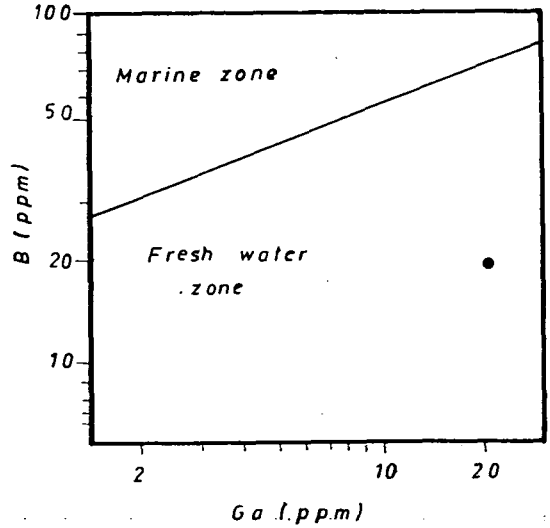

Fig. 5. The location of the average value of boron-gallium content

deposit *(Fig. 6)*. DEGENS *et al.* [1958] explained a triangular diagram using boron-gallium-rubidium ternary relation by which they differentiate between marine and fresh water sediments *(Fig. 7)*.

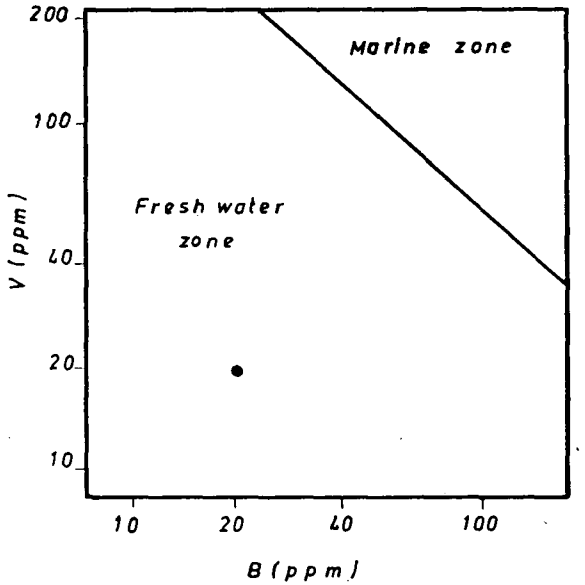

Fig. 6. The location of the average value of vanadium-boron content

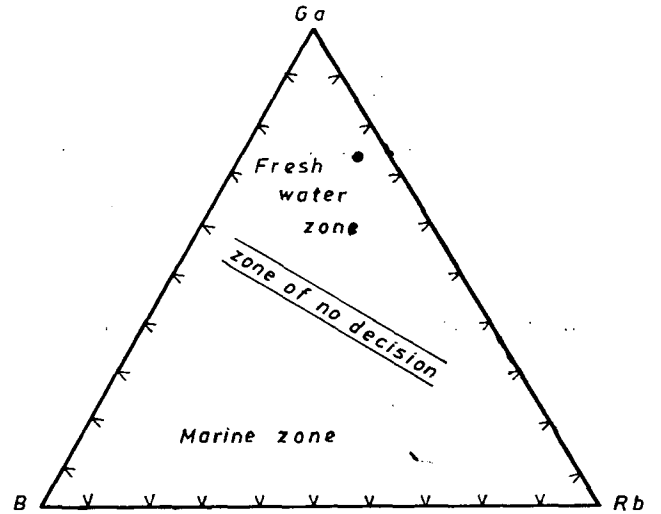

Fig. 7. The location of the average value of boron-gallium-rubidium content

ISOTOPIC MEASUREMENTS

The isotopic analysis of carbonates can be used to determine the environmental origin of the studied carbonate samples.

In this study the isotopic measurements of oxygen and carbon isotopes were

carried out with a micromass 602C mass spectrometer according to the method described by McCrea [1950] and Bowen [1966]. The method is briefly: acid decomposition of carbonates under vaccum (10^{-6} Torr) using 100 % orthophosphoric acid. The $^{13}C/^{12}C$ ratio is measured on mass range 45—46, and the $^{18}O/^{16}O$ ratio is measured on mass range 44—46 with an accuracy of $\pm 0.01‰$. The standard used in this analysis is Solnhofen L. S., NB—20 [Bowen, 1966]. The obtained results are referred to PDB—1.

Keith and Weber [1964] noticed a distinct difference between the isotopic ratios for carbon and oxygen between the marine and the fresh water shells. The $\delta^{13}C$ values for the marine shells range from $+5.2$ to $+1.7‰$ (relative to PDB—1). The fresh water Molluscan shells have relatively depleted $\delta^{13}C$ values ranging from -0.6 to $-15.2‰$. Similar differences were noted in the ^{18}O results. Epstein [1951] and Lowenstam [1953] provided an isotopic temperature scale which can be used to determine the environmental temperature in which the shells have grown. According to Keith and Weber [1964], for the Jurassic and younger samples the best discrimination between marine and fresh water limestone is given by the following equation:

$$Z = a(\delta^{13}C + 50) + b(\delta^{18}O + 50) \quad (1)$$

where a and b are 2.048 and 0.498, respectively. Limestones with a Z value above 120 would be classed as marine, those with Z below 120 as fresh water, and those with Z nearer to 120 as intermediate. Clayton [1961] described the isotopic fractionation between the $CaCO_3$ and the water in contact, and concluded that the isotopic composition of $CaCO_3$ can be affected by the surrounding water.

RESULTS

Elemental Relations

Table 1 shows the trace elements present in the marlstone samples. These elements are estimated using both emmission spectroscopy and X-ray fluorescence techniques.

Applying the average result of the boron-gallium binary relation of Keith and Degens [1959], the location is in the fresh water zone *(Fig. 5)*. For the vanadium-boron relation of Potter *et al.* [1963], the average result is located in the middle of the fresh water zone *(Fig. 6)*. From the triangular gallium-boron-rubidium diagram [Degens *et al.*, 1958], the result occupied a spot in the fresh water zone *(Fig. 7)*.

Isotopic Data

Applying the equation 1, the obtained average Z value for the samples equals 122.57 (Table 2), which indicates an intermediate value between the marine and

Table 1

Trace elements present in the samples collected (in ppm)

Sample No	Ga	V	B	Rb	Ge	Pb	Sn	Zn	Be	Ti	Cr
1	18	20	20	57	4	5	5	50	1	2000	22
2	22	20	21	55	5	5	5	42	2	2000	32
3	20	20	19	59	6	5	5	58	1.5	2000	36
Average	20	20	20	57	5	5	5	50	1.5	2000	30

fresh water carbonates. The value is not contradicting the result obtained by the trace element technique. This Z value is not indicating a typical marine sediment, but fresh water results affected by the surrounding sea water in contact with these rocky samples [CLAYTON, 1961]. The average environmental temperature is calculated to be 26 °C, which indicates warm deposition environment.

TABLE 2

Analytical isotopic data of the studied marlstone samples

Sample No	$\delta^{18}O$ [‰]	$\delta^{13}C$ [‰]	Z value	Environmental temperature (°C)
1	−2.18	−1.64	122.85	24
2	−2.74	−1.68	122.49	28
3	−2.39	−1.82	122.38	26
Average	−2.44	−1.71	122.57	26

CONCLUSION

The flaggy marlstone boulders present on Rosetta beach are of fresh water environment, mostly related to the old Sebennytic branch of the Nile, and are not of the present day Rosetta branch. This large size deposit is rejected on beach by the abnormal weather conditions from a relatively nearer source indicating high erosion conditions in this area.

REFERENCES

BALL, J. [1942]: Egypt in the classical geographers. Survey and Mines Department, Cairo.

BOWEN, R., [1966]: Methods in geochemistry and geophysics. Elsevier Publishing Company, Amsterdam, p. 251.

CLAYTON, R. N., [1961]: Oxygen isotope fraction between calcium carbonate and water. J. Chem. Phys., **34**, pp. 724—726.

DEGENS, E. T., E. G. WILLIAM, and M. L. KEITH, [1958]: Environmental studies of carboniferous sediments. Part II: Application of geochemical criteria. Bull. Amer. Assoc. Petrol. Geol., **42**, pp. 981—997.

EPSTEIN, S. [1951]: A mass spectrometer for the measurements of small difference in isotope abundance ratios. Nat. Bur. Stand. (U.S.) Circ. **522**, (CA 47, 10341), pp. 133—139.

LOWENSTAM, H. A. [1953]: Temperature-shell growth relations of recent and interglacial Pleistocene shoalwater biota from Bermode. J. Geol., **61**, pp. 424—438.

KEITH, M. L. and E. T. DEGENS, [1959]: Geochemical indicators of marine and fresh-water sediments. In: ABELSON, P. H. (Ed.), Researches in geochemistry. John Wiley & Sons, Inc.

KEITH, M. L., and WEBER, J. N. [1964]: Carbon and oxigen isotopic composition of selected limestones and fossils. Geochim. Cosmochim. Acta **28**, pp. 1787—1816.

MCCREA, J. M. [1950]: On the isotopic chemistry of carbonates and the paleo-temperature scale. J. Chem. Phys., **18**, pp. 849—857.

MCKEE, E. D. [1959]: Storm sediments on Pacific Atoll. J. Sed. Petr., **29**, p. 354.

PETTIJOHN, F. J. [1957]: Sedimentary rocks. 2nd edition. Harper & Broth.

POTTER, P. E., SHINP, N. F. and WITTERS, J. [1963]: Trace elements in marine and fresh water argillaceous sediments. Geochim. Cosmochim. Acta **27**, pp. 669—694.

WASSEF, S. N. [1973]: Distribution of monazite in Rosetta and Damietta beach sands and its conditions of sedimentation. Ph. D. Thesis, Ain Shams University, Cairo.

Manuscript received, 30 September, 1983

S. N. WASSEF
M. M. ALY
M. S. ELMANHARAWY
Nuclear Materials Corporation
Cairo, Egypt

Acta Mineralogica-Petrographica, Szeged XXVI/1, 27—32. 1983

INFRARED SPECTROPHOTOMETRIC STUDY OF THE EGYPTIAN ECONOMIC BEACH MINERALS AS WELL AS THEIR ALTERNATION AND WEATHERING PRODUCTS

LIALA A. GUIRGUIS and SAMIR N. WASSEF

ABSTRACT

An infrared spectrophotometric method is indicated by which the quantitative mineralogy of any beach black sand sample can be quickly, accurately and reproducibly determined regardless of the degree of alternation or the degree of weathering the sample has undergone.

From standard calibration curves obtained by using individual pure minerals, and with the aid of a synthetic mixture of the diagnostic minerals, the quantities and types of minerals present in the unknown samples can be rapidly determined.

INTRODUCTION

The importance of the Egyptian delta beach sands stems from the presence of several economic minerals by appreciable tenors and the large extension of the deposit. These minerals are garnet, zircon, monazite, rutile, ilmenite, magnetite and hematite. The average frequencies of these minerals are: garnet 3.25%, zircon 3.5%. monazite 0.16%, rutile 1.25%, ilmenite 39%, magnetite 15%, and hematite 4%. The rest are gangue minerals composed mainly of green silicates, quartz, and feldspars [WASSEF, 1965, 1973].

The use of the infrared absorption spectrophotometer has found added usage in the mineralogical fields [KELLER *et al.*, 1952; LAUNER, 1952; TUDDENHAM and LYON, 1959; MONTEL, 1971]. The method has several distinct advantages. The sample can be taken directly in powdered form, excellent spectra can be obtained with samples that would be judged amorphous by X-ray diffraction, the petrography of a sample can be determined even if that sample is a small grain or rock chip. Moreover, certain mineral impurities are clearly detectable in the spectra of some minerals to be determined.

EXPERIMENTAL

1) The pure mineral samples were prepared from on ore-dressing concentrate sample. Every mineral sample is purified by passing on heavy liquid (bromoform) to separate the light contaminations and highly altered grains. Using the stereomicroscope the clean and pure mineral needed are removed by a needle and collected. The collected grains are rinsed by ethyl alcohol and thus made ready for the analysis.

2) Infrared absorption spectra were obtained with KBr and CsI disks containing from 0.25 to 2% of the sample in question. These samples were preground under alcohol, mixing well with KBr or CsI in an electrical vibromill, weighing out enough of the blend to form a 12 mm diameter disk of the desired thickness and pressing under 12.5 tons pressure in a vacuum die. The absorption curves were obtained using

a Beckman Mod. 4240 double beam infrared spectrophotometer equipped with a dry air purge for the region 400—200 cm^{-1}. The spectrum was measured in the range 4000—200 cm^{-1}.

RESULTS

Figs. 1a and *1b* show the infrared spectrogram of the bromoform-sink Egyptian beach sample. Their absorption data are plotted in Table 1. It can be seen that the spectrum is very complicated especially with weak overtone and combination bands. The critical bands used for identification of each of the minerals are labelled *(Fig. 1)*.

Since the instrument used in this study operates on the double beam principle, a synthetic mixture can be used in the reference beam and its absorption pattern will be removed from the final spectrogram of the unknown sample by simultaneous compensation. Thus, we can reproduce the individual curves for each of the seven minerals shown in *Fig. 2*. The amount of the calculated constituent minerals are: Garnet 3.0%, zircon 3.15%, monazite 0.14%, rutile 1.45%, ilmenite 42.0%, magnetite 13.5%, and hematite 5.4%. A detailed description of the individual infrared absorption spectral data have been given in Table 2.

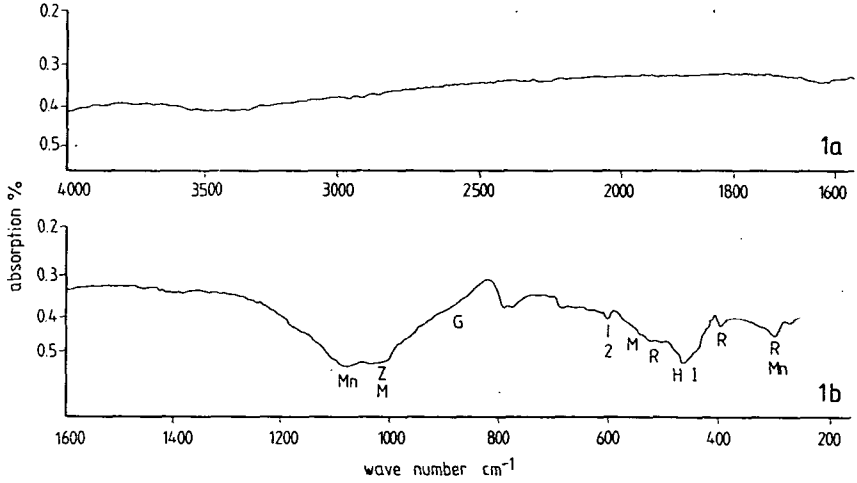

Fig. 1. IR-spectra of the Egyptian beach heavy fraction minerals, Sp. G.>2.85, in the range of 4000—200 cm^{-1}. H: hematite, M: magnetite, I: ilmenite, R: rutile, Mn: monazite, Z: zircon and G: garnet

TABLE 1

Infrared absorption data of the Egyptian beach heavy fraction minerals. Sp. Gr. 2.85 g/cm³

Sample	Frequency ranges and absorption magnitudes
Bromoform sink Sp. Gr. 2.85 g/cm³	260 w, 300 w, 325 w, 330 w, 400 w, 450 w, 460 w, 530 w, 535 w, 545 w, 560 w, 577 w, 615 m, 625 wsh, 630 wsh, 655 w, 685 w, 855 s, 910 w, 930 w, 960 w, 1000 w, 1040 w, 1050 w, 1060 w, 1250 w ,1280 w, 1370 w, 1430 w, 1470 w, 1640 m, 1650 m, 1690 w, 1720 w, 1770 w, 1830 m, 1980 w, 2020 w, 2200 w, 2300 m, 2700 m, 3250 bs, 3250—4000 mb.

Absorption magnitudes; s (strong), m (medium), w (weak), sh (shoulder), b (broad).

TABLE 2

Infrared absorption data from separated Egyptian economic beach minerals

Mineral and symbol	Frequency ranges and absorption magnitudes (cm^{-1})
Almandine-pyrop Garnet (G)	385 m, 460 s, 488 s, 577 s, 650 wsh, 885 s, 910 s, 975 s, 1000 wsh, 1060 wsh, 1100 vwsh, 1140 vwsh, 1420 w, 1450 w, 1625 w, 2738 w, 3380 mb.
Zircon (Z)	315 m, 385 m, 445 s, 600 m, 618 m, 860 sh, 910 s, 1000 bs
Monazite (Mn)	300 m, 495 sh, 545 m, 563 m, 590 wsh, 625 w, 910 w, 1050 xbs, 3000 b
Rutile (R)	300 m, 400 m, 460 sh, 535 s, 570 m, 1040 w.
Ilmenite (I)	325 m, 400 w, 420 w, 460 m, 485 w, 530 s, 570 sh, 590 sh, 630 sh, 760 sh, 810 w, 875 w, 1425 w, 1440 w, 1600 w, 2200 w, 3200—3600 w.
Magnetite (M)	490 m, 575 s, 1000 m, 2200 xbs.
Hematite (H)	333 w, 470 s, 560 s, 630 sh, 1060 w.

Absorption magnitudes; s (strong,) m (medium), w (weak), sh (shoulder), b (broad), x (extra), v (very).

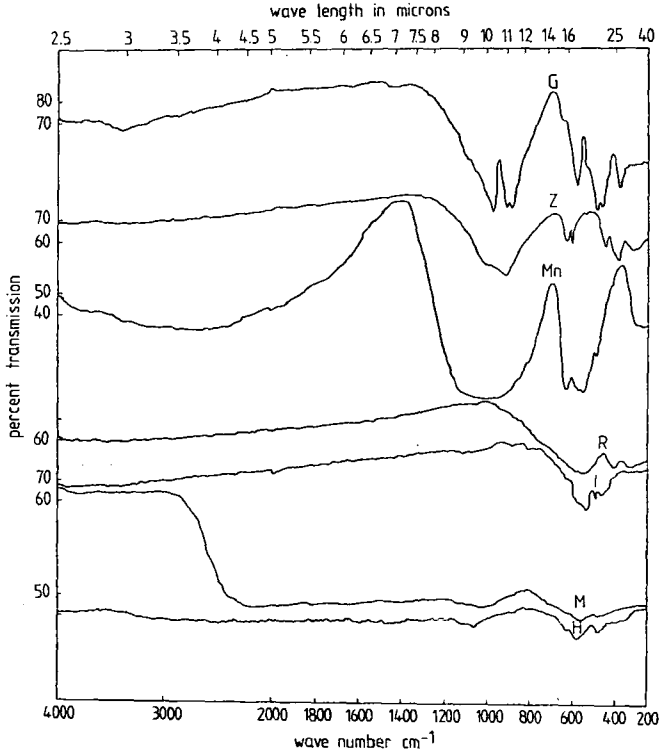

Fig. 2. IR-spectra of the Egyptian economic beach minerals. H: hematite, M: magnetite, I: ilmenite, R: rutile, Mn: monazite, Z: zircon and G: garnet

Almandine-Pyrope Garnet

The free silicates ion has a tetrahedral symmetry and belongs to point group T_9. Its nine normal modes of vibration are, in HERZBERG's [1964] notation, v_1 (non degenerated), v_2 (doubly degenerated), v_3 and v_4 (each triply degenerated).

In the garnet sample examined a medium peak at 385 cm^{-1} shifted from 415 cm^{-1} is due to the substitution of the larger ion of Fe^{2+} with the smaller Mg^{2+}; this band is attributed in part to the v_2 of SiO_4 tetrahedra and an unspecified mode of MgO_6 octahedra.

The strong band at 460 cm^{-1} is due to Fe_2O_3 [GORE, 1972]. This is clearly seen in the spectra of hematite, magnetite and ilmenite while the strong bands at 488 and 577 cm^{-1} could be assigned to v_4.

Silicates absorb strongly in the range 800—1100 cm^{-1} (v_3). However, the shape of the absorption bands differ considerably between the different silicates. Thus, in case of garnet the peak at 909 cm^{-1} splits into two peaks at 885 and 910 cm^{-1}, respectively, and there is a strong peak at 975 cm^{-1} while there are two small shoulders at 1000 and 1060 cm^{-1}.

The infrared shifted spectrum suggests that the SiO_4 tetrahedra in these silicates garnets are strongly affected by the metal oxide bonds and alteration products.

It is interesting to notice that the garnet spectrum herein matches that given by OMORI [1971] for almandine-pyrope garnet from Nijosan, Osaka Prefecture, Japan, except for the two carbonate bands at 1420 and 1450 cm^{-1} which could be due to small alteration to calcite or the presence of calcite in the pitted garnet grains.

There is more than one way of fitting the hydroxyl ion as it is clear from the bands at 1625 cm^{-1}, 2738 cm^{-1} and 3380 cm^{-1} which may be due to alteration.

Zircon

The bands at 910 and 1000 cm^{-1} are transitions to crystal field split v_3 levels. There is also a large crystal field splitting in v_4 whose observed crystal levels are 600 cm^{-1} and 445 cm^{-1}.

The band at 385 cm^{-1} is an external rotary mode in which the silicates ion executes partial rotation about the „*a*" axis while the band at 315 cm^{-1} is an external or lattice mode involving the translatory motion of the positive zirconium ion with respect to the negative silicate ion.

The main difference between garnet and zircon as orthosilicate minerals is that the SiO_4 tetrahedra in garnet share corners with an octahedron and edges with a dodecahedron [GIBBS and SMITH, [1965], whereas in zircon the tetrahedron and ZrO_8 dodecahedra share edges [ROBINSON *et al.*, 1971].

Monazite

In the spectrum of monazite an extra broad band occurs due to ionic phosphate vibration PO_4^{-3} with an absorption maximum at 1050 cm^{-1} caused by P—O stretching vibration [COLTHUP *et al.*, 1964].

The 625 cm^{-1}, 545 cm^{-1}, 495 cm^{-1} and 300 cm^{-1} bands appear in the spectrum of the standard monazite sample and according to MCDEVIT and WILLIAM [1964], this could be due to a group of rare earth oxides. The broad absorption band around 3000 cm^{-1} may be due to hydrogen bound in water.

Rutile

The spectrum of rutile shows a strong band at 535 cm^{-1} and a medium one at 400 and 300 cm^{-1} which is due to Ti—O stretching vibration. It is interesting that the weak band at 1040 cm^{-1} is well defined in the spectrum of the synthetic rutile and hematite, and this may show exsolution intergrowth of rutile-hematite. A medium band at 570 cm^{-1} may also confirm the presence of hematite.

Ilmenite

The curve has an absorption band around 530 cm^{-1} which may be due to TiO linkage and two medium absorption bands at 460 cm^{-1} and 325 cm^{-1} which may be due to FeO linkage. The studied ilmenite also absorbs over a wide range starting at 590 cm^{-1}. Thus there is a carbonate band at 1425 cm^{-1} and 1440 cm^{-1}. Hydroxyl lattice group bands appear at 1600 cm^{-1} and 2200 cm^{-1}. There is an amount of loosely bound water evidenced by the water band at 3200—3600 cm^{-1}. These could be due to the beginning of ilmenite alteration to leucoxene.

Magnetite

Magnetite shows a strong band at 575 cm^{-1} which is due to Fe_3O_4 linkage. The 490 cm^{-1} and 1000 cm^{-1} bands could be due to Fe_2O_3 mineral impurity. Some alteration to hydrated minerals is evidenced by the OH lattice group vibration at 2200 cm^{-1}.

Hematite

The strong band at 560 cm^{-1} is the mean value of brands of almost equal intensities reported by McDevit and William [1964] at 540 cm^{-1} and 590 cm^{-1}. Another strong band appears at 470 cm^{-1} which is due to Fe_2O_3 [Gore, 1972], but the weak bands at 333, 630, and 1060 cm^{-1} could be due to some rutile impurity.

CONCLUSION

Many of the beach samples given to the petrologist for identification are altered beyond recognition, but we now have a very powerful tool to aid in the rapid qualitative and quantitative determination of the mineralogy of such samples, as shown from the obtained results which are in harmony with the known black sands composition.

REFERENCES

Colthup, N. B., Lawrence, H. D., and Wiberieg, S. E. [1964]: Introduction to infrared and Raman spectroscopy. Academic Press, New York, London.

Gibbs, G. V., and Smith, J. V. [1965]; Refinement of the crystal structure of synthetic pyrope. Amer. Mineral., **50**, 2032—2039.

Gore, R. C.: [1972]: Infrared spectral interpretation. J. Hully Association 112.

Herzberg.G. [1964]: Infrared and Raman spectra of polyatomic molecules. Princeton, Van Nostrand.

Keller, W. D., Spotts, J. H. and Biggs, D. L. [1952]: Infrared spectra of some rock-forming minerals. Am. J. Sci., **250**, 453—471.

Launer, P. J. [1952]: Regularities in the infrared absorption spectra of silicate minerals. Amer. Mineral., **37**, 774—784.

Montel, G. [1971]: Sur les structures de quelques apatites d'interet biologique et leur imperfections, Bul. Soc. Fr. Mineral. Cristallogr., **94**, 300—313.

McDevit, T., and William, L. [1964]: Infrared absorption study of metal oxides in the law frequency region (700—240 cm^{-1}). Spectrochimica Acta **20**, 799—808.

OMORI, K. [1971]: Analysis of the infrared absorption spectrum of almandine-pyrope garnet from from Nijosan, Osaka Prefecture, Japan. Amer. Mineral., **56**, 841—849.
ROBINSON, K., GIBBS, G. V., and RIBBLE, P. H. [1971]: The structure of zircon: A comparison with garnet. Amer. Mineral, **56**, 782—790.
TUDDENHAM, W. M., and LYON, R. J. P. [1959]: Relation of infrared spectra and chemical analysis of some chlorites and related minerals. Anal. Chem., **31**, 370—380.
WASSEF, S. N. [1965]: Correlation of the sedimentation conditions of the Mediterranean beach east of Damietta to the Suez Canal by heavy minerals and isotopes applications. M. Sc. thesis, Faculty of Science, Ain Shams Univ., Cairo, Egypt.
WASSEF, S. N. [1973]: Distribution of monazite in the black sands of Rosetta and Damietta and its conditions of sedimentation. Ph. D. Faculty of Science, Ain Shams Univ., Cairo, Egypt (1973).

Manuscript received, 19 April, 1983

LIALA A. GUIRGUIS,
SAMIR N. WASSEF
Nuclear Materials Corporation,
Cairo, Egypt

Acta Mineralogica-Petrographica, Szeged XXVI/1, 33—49. 1983

THE STABLE CARBON ISOTOPE COMPOSITION OF THE HYDROCARBON AND CARBON DIOXIDE COMPONENTS OF HUNGARIAN NATURAL GASES

I. KONCZ

ABSTRACT

The results of carbon isotope ratio measurements for 79 natural gas occurrence of Hungary were interpreted. On the base of carbon isotope ratios characteristic to methane and its distribution with depth genetic groups were determined which differ from each other in the character of the generation process and the type of organic material. The change of carbon isotope ratio with depth and the degree of transformation can be attributed to the common effect of kinetic isotope effect and vertical migration in the case of the methane component of natural gases of thermogeneous origin arising from the same type of organic material and trapped in Neogene reservoir rocks. Carbon isotope ratios referring to strong vertical migration are in general in connection with the high carbon dioxide content of natural gases. It could have been established from the carbon isotope ratios of carbon dioxide that the bulk of carbon dioxide originated from the deeper zones of the lithosphere as a consequence of regional metamorphism of carbonate rocks.

INTRODUCTION

The Pannonian basin is an intermontaneous sinking between the mountain arches of Alps, Carpathians and Dinaric mountains, which is filled up with continuously formed Neogene sediments of Molassic character [SZALAY, KONCZ, 1981]. The base of Neogene formations is formed from Mezozoic and Paleozoic sedimentary rocks with varied evolution. A sediment mass of 7000 meter thickness accumulated in the Neogene sinkings. The sinking of basin parts started in the middle Miocene and became more intensive in the lower Pliocene. The depth of the boundary of Pliocene/Miocene in a part of the Neogene sinkings is 3400—4500 meters, while in the other part is between 1000—2500 meters (average value: 1500 meters). In this latter case Miocene sediments of great thickness were formed. The velocity of sediment formation was 200—500 meters (in average 300—400 meters), and 100—250 meters (in average 100—150 meters) per million years, respectively. The geothermic gradient varies between 0.036—0.055 °C/meter according to present measurements. The velocity of heating up calculated from the present geothermic gradients and velocity of sedimentation varies between 9—18°C/million years. This value in the parts of the basin with different sedimentation conditions is 14—18 and 9—12 °C/million years, respectively.

The vitrinite reflections (R_0) measured from Neogene sedimentary rocks and evaluated by the Dow method gave a linear relationship with depth in the coordinate system lg R_0—m $\times 10^4$ with a slope of 1.7—3.1 [Dow, 1978, MÁFKI, MTA GKL, KBFI Reports]. The slope of the lg R_0 — depth function is 1.7—2.2 (average 2.0) for the parts of the basin where Miocene sediments are thin, while for thick Miocene sediments the slope is 3.1 *(Fig. 1)*. The slope of lg R_0 — present temperature functions – expressed in lg R_0/ °C $\times 10^3$ units – is 3.6—5.2 (average: 4.4) and 6.3, respective-

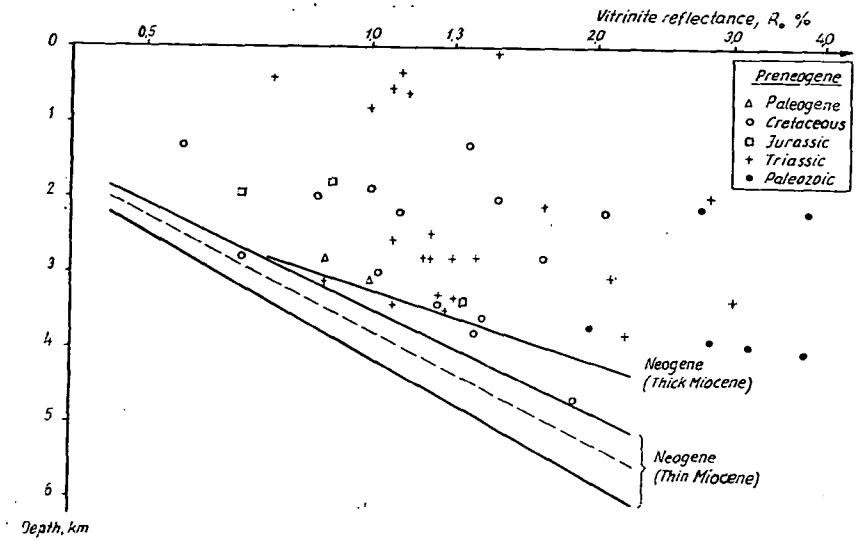

Fig. 1. Relation between the vitrinite reflection and depth in Neogene and older sediments.

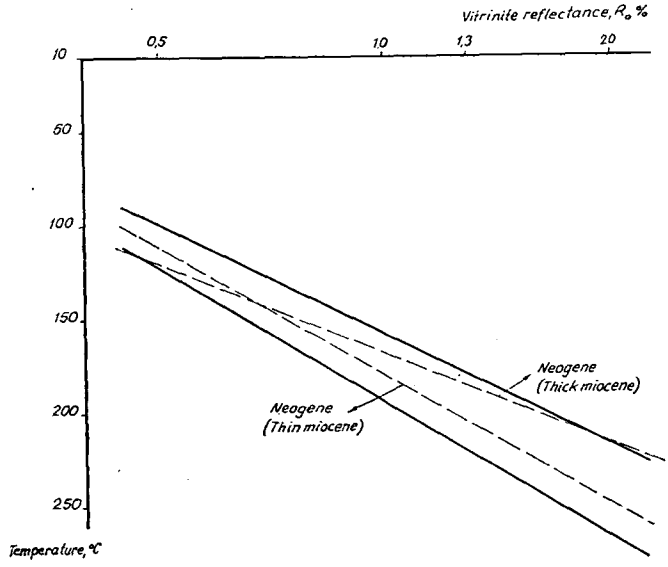

Fig. 2. Relation between the vitrinite reflection and present temperature in the Neogene sediments

ly *(Fig. 2)*. The present temperature of Neogene sediments can be assumed as identical with the maximum temperature reached.

Based on vitrinite reflections, those depth- and temperature boundaries can be determined in Neiogene sediments, which correspond to the stages of catagenic transformation of organic matter [Dow, 1978], (Table 1). The vitrinite reflections for

TABLE 1

Depth and temperature boundaries of the stages of catagenic transformations in the Neogene sediments

Stage	R_0%	Depth, km	Temperature, °C
Beginning of crude oil formation	0.5	2.1—2.5	100—123
Beginning of wet gas formation	1.0	3.3—4.2	160—190
End of crude oil formation			
Beginning of dry gas formation	1.3	3.6—4.8	180—220
End of wet gas formation	2.0	4.2—5.8	220—270

sediments older than Neogene are of course greater, than for Neogene sediments, or at least approximate those of the Neogene *(Fig. 1)*. This indicates, that a part of pre-Neogene sediments reached only in the Neogene those conditions under which they could generate hydrocarbons. This fact increases the hydrocarbon perspectives of pre-Neogene sediments.

The known Hungarian natural gas accumulations are in the depth interval of surface — 5.5 kilometers. The composition of natural gases varies in a wide range. One of their characteristics is the occurrence of carbon dioxide in a wide concentration range (0—0.98 cu.m/cu.m). This variety of composition which probably indicates a genetic heterogenity, justifies the study of their origin by means of the stable carbon isotope composition of carbonaceous components (hydrocarbons, carbon dioxide).

PREVIOUS WORKS

HOLCZHACKER *et al.* [1981] published the carbon isotope distribution of hydrocarbon components of Hungarian natural gases as well, as its change with depth and carbon dioxide concentration. The maximum depth of biogenetic methane occurrence was determined as 950 meters, while the minimum depth of thermogeneous methane arising from catagenic transformations was determined in 800 meters. The tendentious change of carbon isotope ratio of methane, the enrichment of ^{13}C with depth was attributed to the kinetic isotope effect.

NAMESTNIKOV has pointed out by means of the hydrocarbon composition of the natural gases in the Pannonian basin that the main zone of crude oil formation is in a depth interval of 1.6—3.2 kilometers.

KERTAI attempted first to clear the origin of carbon dioxide based on the carbon isotope composition of carbon dioxide of Hungarian natural gases and on their geologic environment [KERTAI, 1972]. He supposed that the significant carbon dioxide reserves are in connection with the metamorphic base and are the product of the regional metamorphism of carbonates.

TÖRÖK studied the composition distribution in natural gas reservoirs containing carbonated and nitrogeneous natural gases. His gravitational — migration model explained the distribution and distribution types of carbon dioxide within one reservoir and reservoirs located above each other. The depth of „source "can also be determined but the origin of carbon dioxide has not been treated [TÖRÖK, 1979].

CORNIDES and KECSKÉS [1982] and KECSKÉS *et al.* [1981] studied the carbon isotope ratio of Slovakian mineral waters rich in carbon dioxide and came to the conclusion that the problem of carbon dioxide origin in the Carpathian basin can be solved only taking into account the carbon dioxide of juvenile origin, too.

HOLCZHACKER *et al.* [1981] came to the conclusion from the low negative carbon isotope ratio of the methane of highly carbonated natural gases that the methane associated with carbon dioxide was formed at high temperature and in a great depth.

ANALYTICAL PROCEDURES

The carbon dioxide was extracted from the samples by barium-hydroxide. The barium carbonate was prepared with filtration, washing and drying for mass spectrometric measurements. The gas for measurement was made in vacuum with ortophosphoric acid.

The hydrocarbons of carbon dioxide-free gas samples were transformed to carbon dioxide in ampoules containing catalisator and copper oxide (CuO) previously heated in vacuum.

The measurements of isotope ratios were performed on a VARIAN—MAT86 mass spectrometer. Carbon dioxide made of the Stringocephalenkalk von Rübenland carbonate with ortophosphoric acid was used as a standard. The results are converted into PDB standard. The standard deviation of measured data is $\pm 0.25‰$.

The methane was not preparatively separated from the hydrocarbons of natural gases, so the carbon isotope ratios relate to the total amount of hydrocarbons of the given gas. It is known that the carbon isotope ratio of hydrocarbons heavier than methane is a lower negative value [FUEX, 1977]. To prevent greater deviations only the carbon isotope ratio of such gases was evaluated in which the share of hydrocarbons heavier than methane was not higher than 10 per cent. Assuming the highest carbon isotope ratio, $-25‰$, for the C_2 components the maximum deviation is $+2‰$. This little deviation can be neglected near the wide carbon isotope ratio range of the methane, so it was assumed that the carbon isotope ratio measured for the hydrocarbon constituents of a natural gas approximately represents the carbon isotope ratio of the methane.

The preparation of the samples and the mass spectrometric measurements were performed in the Central Research and Development Institute of Mining by K. HOLCZHACKER, P. A. PETIK, É. MEDGYES.

SAMPLE LOCATIONS

The gas samples give information from 79 natural gas accumulations of Hungary. The areal arrangement of gas reservoirs is shown on *Fig. 3.* 67 per cent of the gas samples originated from Neogene reservoirs, 22 per cent from Mezozoic reservoirs covered with Neogene sediments and 11 per cent from Paleozoic reservoirs. The depth interval of the Neogene reservoirs extends from the surface till 5.3 kilometers. The Mezozoic and Paleozoic gas samples originated from a depth interval of 1.8—4.4 and 1.5—3.9 kilometers, respectively.

RESULTS AND DISCUSSION

The carbon isotope ratios of the hydrocarbons

It is known from the literature that the carbon isotope ratio of the methane shows marked differences depending upon the character of the generation process. The thermogenic methane which is the results of catagenic transformation of the organic matter is much more richer in ^{13}C, than the biogenic methane of bacterial

origin. The boundary between biogenic and thermogenic methane is determined empirically based upon the distribution of carbon isotope ratios. The carbon isotope ratio range of the biogenic methane was determined by FUEX [1977] between −50‰ and −90‰, while ALEKSEEV [1977] established a range of −55‰ and −95‰; the same range for thermogenic methane is, according to FUEX, −20‰ ——60‰, while

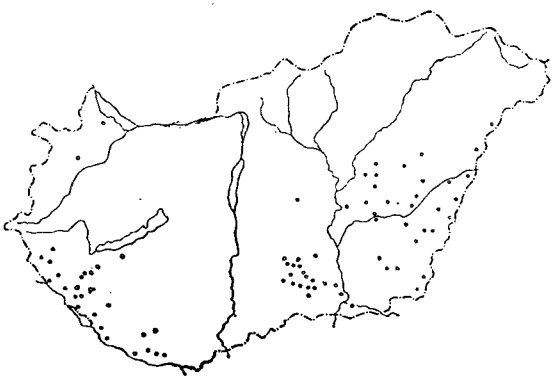

Fig. 3. The natural gas reservoirs studied in Hungary

ALEKSEEV has put it between −36‰ and −58‰, The isotope ratio range in the simultaneous presence of thermogenic and biogenic methane is −50‰ −60‰ (FUEX] and −55‰——65‰ [ALEKSEEV].

These empirical boundaries in Hungarian natural gases are (*Figs. 4* and *5a*):

— biogenic: −65‰ and −81‰ (group „C")

— biogenic+thermogenic: −59‰ and −65‰ (group „D"),

— thermogenic: −22‰ and −59‰ (groups „A" and „B").

The maximum depth of occurrence of natural gases containing methane of biogenic origin (groups „C" and „D") is 1 kilometer. Maximum reservoir temperatures are 45—60 °C.

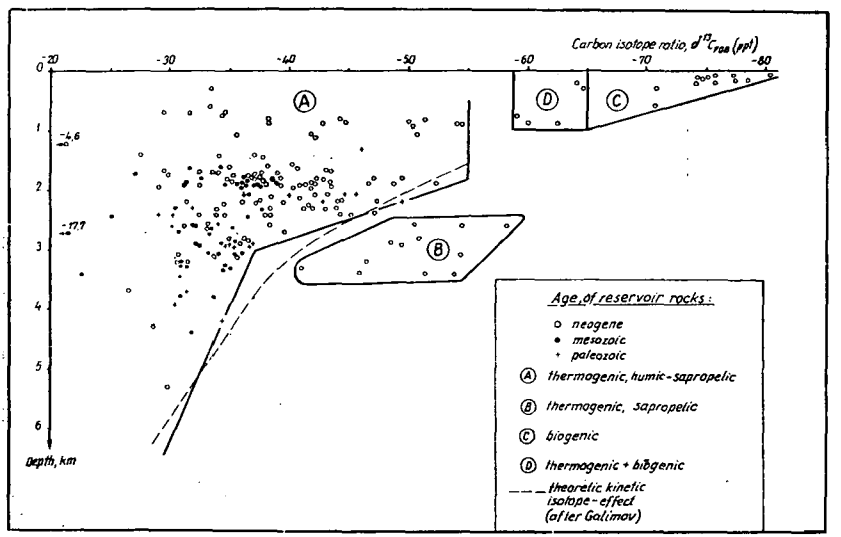

Fig. 4. The carbon isotope ratios of the hydrocarbons of natural gases as a function of depth.

The isotope ratios of thermogenic methanes are determined mainly by the type of the organic matter and the kinetic isotope effect. The methane arising from humic type organic matter is richer in ^{13}C than the methane of sapropelic origin [SCHOELL, 1980]. At the same degree of transformation this difference is 10—15‰. It can be concluded from the carbon isotope ratio distribution of thermogenic methane of the Hungarian natural gases that the high negative values at depths greater than 2.5 kilometers are the consequence of the presence of methane originated from sapropelic type of organic matter (*Figs. 4* and *6.* group „B").

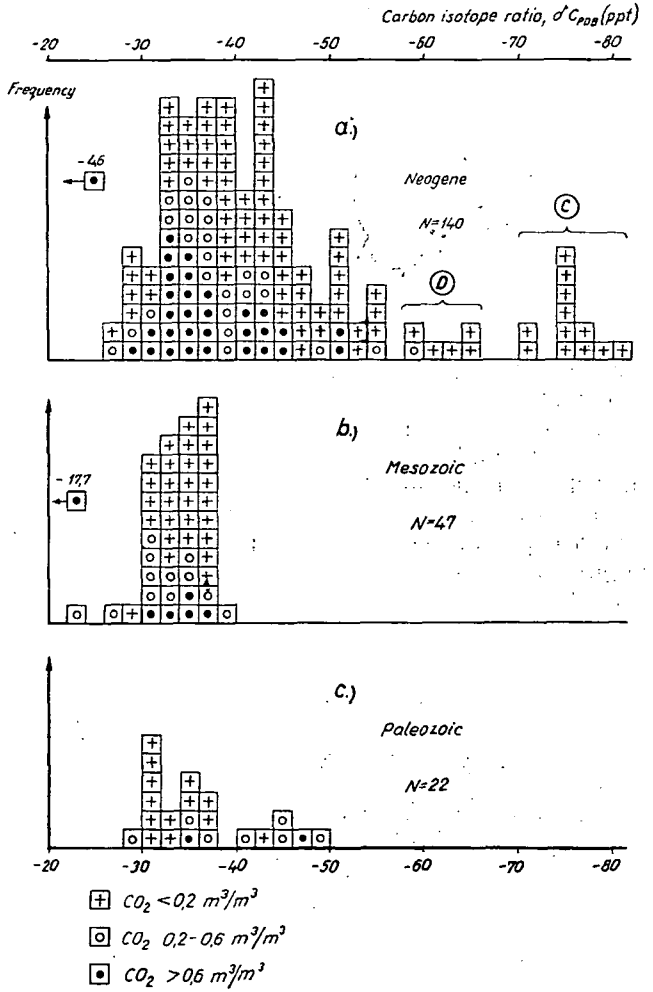

Fig. 5. The carbon isotope ratio distribution of natural gases of reservoir rocks with different age

The change of carbon isotope ratio distribution with depth in the group „A" can be attributed to the kinetic isotope effect. With the increase of depth the ^{13}C enriches in the methane and approximates the carbon isotope ratio range of the generating source, the kerogene [GALIMOV, 1973], PRASOLOV and LOBKOV, 1977], *(Figs.*

4, 6, 7d). Because of the vertical migration, not the autochtonous methane is present in general in the natural gas accumulations, but only a quasi autochtonous methane, which underwent only minor vertical displacement, and syngenetic with the kerogene. That is why the kinetic isotope effect has the form of an envelope curve in the upper region of the carbon isotope ratio distribution at high negative limit values

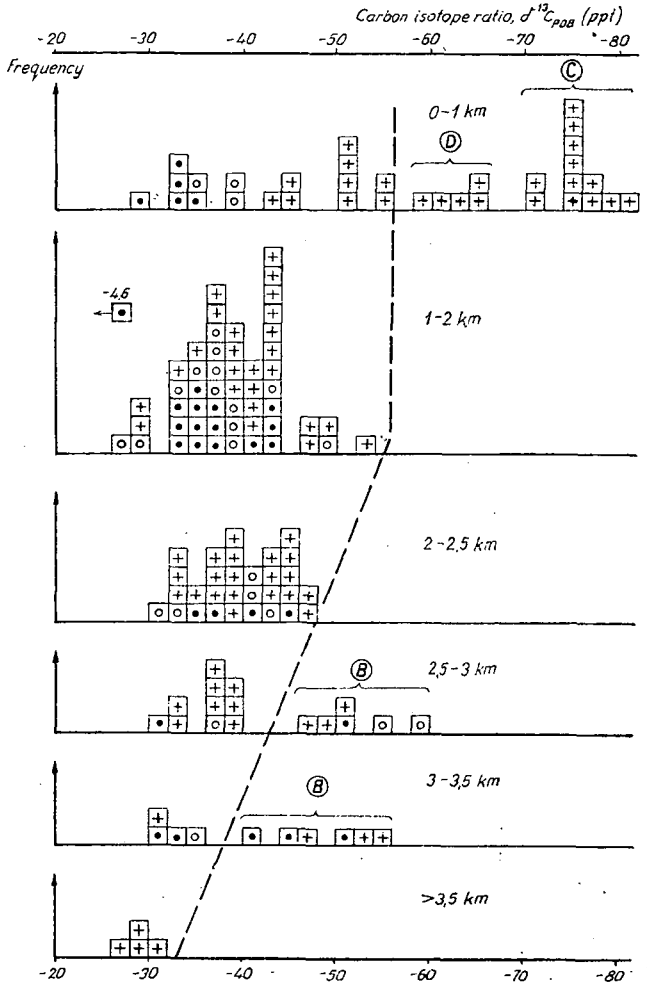

Fig. 6. The carbon isotope ratio distribution of the hydrocarbons in natural gases of Neogene reservoir rocks in different depth intervals

[PRASOLOV and LOBKOV, 1977]. The limiting curve obtained by GALIMOV'S theorethical calculations and adapted to the geothermic conditions of the Pannonian basin, representing the effect of the kinetic isotope effect is shown in *Fig. 4*. This is in good agreement with the boundary line plotted by us on the base of upper limit values. It must be mentioned, however, that the correlation of kinetic isotope effect with formation temperature and depth is only a rough approximation, as the effect is determined by such parameters e.g. vitrinite reflection, which reflect the grade of transformation

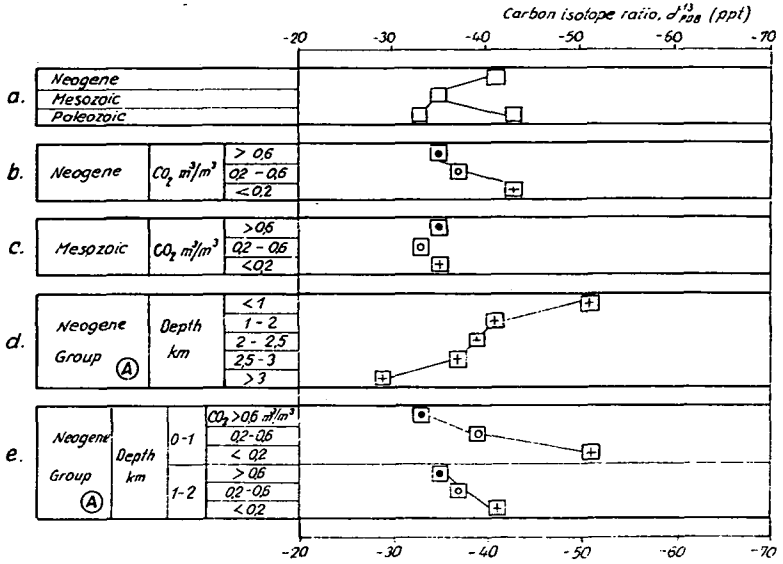

Fig. 7. The median of carbon isotope ratio distributions of the hydrocarbons of Hungarian natural gases

degree of transformation of the organic matter in sediments with different age *(Fig.* and the simultaneous effect of time and temperature [SCHOELL, 1980]. The influence of migration after the formation upon the carbon isotope ratios can be neglected beside the effects of the organic matter type and kinetic isotope effect.

The change of carbon isotope ratio with depth in the natural gases of group „A" is very remarkable. The carbon isotope ratio of methane, in several cases associated with a high concentration of carbon dioxide in relatively shallow formations (depth 0—1 kilometer) corresponds to a depth of formation greater than 3 kilometers. This indicates that in the surrounding of these accumulations there was a significant vertical migration.

There are characteristic differences in the carbon isotope ratio distribution correlated with the age of the reservoir rocks *(Fig. 5)*. The thermogenic methane of the Neogene reservoir rocks has a wider carbon isotope ratio range (−25‰ + −56‰) than that of the Mezozoic reservoir rocks (−20‰ − −30‰) where the distribution range is only 10‰. There are two populations in the carbon isotope ratio distribution of the methane originating from Paleozoic reservoir rocks: one of them is in the range of −28‰ and −38‰, the other −40‰ and −50‰. Although the age of the reservoir rocks is not equal to that of the mother rocks, the differences between the carbon isotope ratio distributions are in connection with the higher degree of transformation of the organic matter in the Mezozoic and Paleozoic sediments, which has been expressed with the vitrinite reflection values *(Fig. 1)*. The population originating from Paleozoic reservoir rocks and characterized with methane enriched in ^{12}C has resulted probably from the migration of the methane which has been generated in Neogene sediments. The population enriched in ^{13}C was taken as characteristic to the methane syngenetic with sediments older than Neogene. The median of carbon isotope distribution ratios indicates a Neogene — Mezozoic — syngenetic Paleozoic sequence in the enrichment of ^{13}C. This seems to show also a relationship with the

7a). This relationship, however, can be explained also with the assumption that the type of organic matter shifted towards the humic type. As we have no data about the type of organic matter, the effect of the degree of transformation and the type of organic matter can not be unequivocally separated.

The relatively great number of carbon isotope ratios for methane and the great depth interval of Neogene reservoirs has allowed the correlation of carbon isotope ratio distributions with depth *(Fig. 6)*. The carbon isotope ratios can be correlated with the stages of the transformation of organic matter by means of the vitrinite reflections belonging to given depth intervals (Table 2). The width of carbon isotope ratio intervals decreases with the depth: at a depth less than 1 kilometer this range is 54‰, while at depth greater than 3.5 kilometers it decreases to 6‰ parallelly with the enrichment of ^{13}C. In shallow depth (< 1 km) genetically separable gas accumulations has been found which contain methane of biogenic origin (group „C") and both biogenic and thermogenic methane (group „D"). In the depth range of 2.5—3.5 kilometers are found those natural gas accumulations with methane of thermogenic origin which has been formed from sapropelic type of organic matter (group „B"). The carbon isotope ratio distribution of the methane in the natural gases of the group „A" which gives the bulk of the data, reflects the simultaneous effect of the vertical migration and kinetic isotope effect. The width of the range of carbon isotope ratios decreases from 28‰ (depth < 2 kilometers) to 6‰ (depth > 3 kilometers). Parallelly with this phenomenon the median of the carbon isotope ratio distributions according

TABLE 2

Vitrinite reflection ranges and stages corresponding to the depth ranges in Neogene sediments

Depth range km	Vitrinite reflection range R_0%	Stage
0—2	0.2—0.5	Immature
2.0—2.5	0.5—0.6	Beginning of crude oil formation
2.5—3.0	0.6—0.8	The main phase of crude oil formation
3.0—3.5	0.8—1.2	The main phase of crude oil formation and beginning of wet gas formation
>3,5	>1.2	Formation of wet and dry gas

to the kinetic isotope effect shift towards less negative values with the increase of depth *(Fig. 7a)*. In depth greater than 3 kilometers only syngenetic methane exists with carbon isotope ratios corresponding to the carbon isotope ratio of dry gas formed in great depth, and geothermal methane, respectively [FUEX, 1977]. The increase of carbon isotope ratio range with decreasing depth can be attributed to the effect of vertical migration.

One of the characteristics of the Hungarian natural gas accumulations is the frequent occurrence of carbon dioxide in a wide concentration range. It frequently occurs that in the same pool and depth interval the carbon isotope ratio of the methane in natural gases with high carbon dioxide concentration is a significantly less negative value, than that of the methane coexisting with a low carbon dioxide concentration (Table 3). This fact indicated the discrimination of the carbon isotope ratios of the methane depending upon the carbon dioxide concentration of the natural gas *(Figs. 5, 6, 7)*. The dependence of the carbon isotope ratio of the methane from the carbon

TABLE 3

The change of the carbon isotope ratio of methane with carbon dioxide concentration

Depth km	CO_2 m^3/m^3	The carbon isotope ratio of methane $^{13}C_{PDB}$ ‰
3.1—3.4	0.05	−46.4
	0.51	−22.6
0.7—0.9	0.11	−44.9
	0.93	−29.5

dioxide concentration has occurred only in Neogene gas accumulations; this phenomenon has not been observed in the gases of Mezozoic reservoirs *(Figs. 7b, 7c)*. The greatest deviations have been found in the natural gases of the shallow (<1 kilometer) Neogene reservoirs *(Fig. 7e)*. The above mentioned deviations decrease with the increase of depth and are not significant under 2.5 kilometers. These facts indicate that the methane of natural gases with high carbon dioxide concentration is not syngenetic with the methane of natural gases with low carbon dioxide concentration and has migrated together with the carbon dioxide to the present accumulation. This statement is not equivalent with that one that the methane of natural gases with high carbon dioxide concentration is syngenetic with the carbon dioxide, because the carbon dioxide during its vertical migration is able to extract the hydrocarbons from the rocks. The anomally low negative carbon isotope ratio of the methane of natural gases with high carbon dioxide concentration in shallow reservoirs proves a marked vertical migration and an open structure. This assumption has been supported by the practical experience that such natural gas accumulations have been formed in the surrounding of structural lines, deep faults [TÖRÖK, 1979].

Two anomalous carbon isotope ratios have to be interpreted in connection with the high carbon dioxide content: −4.6‰ and −17.7‰. It can be supposed in these cases that the methane associated with the high carbon dioxide content was formed from inorganic (carbonate) carbon; the carbon dioxide formed during regional metamorphism or the juvenile carbon dioxide was hydrogenated with water in the hot zones of the lower part of the earth's crust or in the upper part of the earth's mantle [GUCALO, 1980; KRAVCOV, 1980].

THE CARBON ISOTOPE RATIO OF THE CARBON DIOXIDE

The frequent occurrence of carbon dioxide in Hungary and the wide range of carbon dioxide content of natural gases has made possible the study of carbon dioxide origin by means of carbon isotope ratios.

Carbon dioxide can arise from different sources and in different processes in the different zones of the earth. The primary sources of the carbon dioxide are the exogenous (atmospheric) and endogenous (from the material of the earth's mantle) juvenile carbon dioxide. The atmospheric carbon dioxide can be divided into two groups with markedly different carbon isotope ratios: one of it contains inorganic carbon (the bulk of carbonates) independent of the metabolism of living organisms, the other is composed of so called organic carbon as a result of the metabolism of living organisms. Several processes form carbon dioxide from the exogenous carboniferous material containing organic and inorganic carbon (Table 4). The

TABLE 4

The transformation of organic and inorganic carbon of exogene origin into carbon dioxide

Geosphere		The quality of carbon	The process of carbon dioxide formation
Biosphere		Organic carbon	Oxidation (with atmospheric oxygen, microbic)
Lithosphere	Upper part of the earth crust		The microbic oxidation of hydrocarbons
			Oxidation (with atmospheric oxygen)
			Diagenesis, catagenesis
			Contact metamorphism
		Inorganic carbon	Hydrolysis
			Dissolution with CO_2 of different origin
			Contact metamorphism
	Lower part of the earth crust, upper part of the earth mantle	Organic and inorganic carbon	Regional metamorphism

microbial and atmospheric oxidation as well as the diagenetic transformations of the organic matter is going on in shallow depth, and accordingly at low temperatures. Higher temperature and greater depth are necessary for the catagenic processes of organic material and the hydrolysis of carbonates. In the lower part of the earth's crust and in the upper part of the earth's mantle in the pressure- and temperature range corresponding to the greenschist-, epidote- and epidote-amphibolite rock facies, during regional metamorphism carbon dioxide arises both from the organic carbon existing in graphit state and the inorganic carbon of the carbonates. Significant amount of carbon dioxide arises from the impure carbonates simultaneously with the formation of epidote and tremolite [HOEFS and MORTEANI, 1979; KREULEN, 1980]. The hydrogenation of carbon dioxide arising from the decomposition of carbonates during regional metamorphism may result such methane the carbon isotope ratio of which is in the range of inorganic carbon [GUCALO, 1980; KRAVCOV, 1980]. As it was previously shown similar situation has been found in the Hungarian gas accumulations, too. The contact metamorphism and the dissolution of carbonates, on the contrary, can not be adapted to predetermined depth- and temperature ranges.

The lower part of the earth's crust and the upper part of the earth's mantle is able to generate carbon dioxide more than four order of magnitude, the magmatic rocks of anatectic origin generate carbon dioxide more than one order of magnitude, than the sedimentary rocks [SOKOLOV, 1971]. These data indicate that gas accumulations with high carbon dioxide concentration have been formed mainly from carbon dioxide generated in the lower part of the earth's crust and in the upper part of the earth's mantle. This means that the source of the bulk of carbon dioxide is mainly the juvenile carbon dioxide and the carbon dioxide generated by regional meta-

morphism [KERTAI, 1972; HOEFS and MORTEANI, 1979; KREULEN, 1979; PANKINA, 1979; MAXIMOV *et al.*, 1980; PANKINA *et al.*, 1978].

The determination of the origin of carbon dioxide by means of carbon isotope ratios is difficult, however, because the carbon dioxides of different origin, which can be well distinguished by carbon isotope ratios, may mix within a given geosystem, or may be generated simultaneously from different sources. During the regional metamorphism carbon dioxide with different carbon isotope ratios is generated simultaneously from carbon of graphite state and from carbonates. The mixture of such carbon dioxide is richer in ^{12}C depending upon the concentration of the graphite, than the carbonates are. This effect can be so marked that the carbon dioxide originated from the regional metamorphism can be distinguished from the juvenile carbon dioxide [HOEFS and MORTEANI, 1979]. The alternative origin hypotheses of different authors have been based on these problems. The most frequent origin hypotheses are: a) juvenile, b) regional metamorphism of carbonates and graphite and c) the mixture of the above mentioned. Further complications are caused by the vertical migration, because in this process the carbon dioxide is able to dissolve carbonates, or to blend with the carbon dioxide of organic origin which has been formed in different processes (oxidation, catagenesis). In the former case the carbon dioxide enriches in ^{13}C, in the latter one in ^{12}C. It is evident from these difficulties, that the reliable determination of carbon dioxide origin can not be performed only by means of the carbon isotope ratios, which, although they are extremely useful and necessary, can only be used with limited validity without geologic interpretation.

The carbon isotope ratios of the carbon dioxide of Hungarian natural gases have been in the range -1.1% — $-18.1‰$. The median of the frequency distribution is at $-5‰$ and $-6‰$, the boundaries of probable values interval — median $\pm$ standard deviation — are at -4 and $-9‰$, respectively *(Fig. 8a)*. The carbon isotope ratio distribution has shown a dependence upon carbon dioxide concentration. The greatest significant deviation has occurred at natural gases having a carbon dioxide concentration lower and higher than 0,6 cu.m/cu.m. The statistical test used has been the KOLMOGOROV—SMIRNOV's no-parameter-method with a reliability of 95 per cent. The difference between the two distributions depending upon the concentration of carbon dioxide has had a character, that in natural gases with high carbon dioxide concentration (higher than 0.6 cu.m/cu.m) carbon dioxide with an isotope ratio higher than $-10‰$ did not occur (*Figs. 8b* and *8c*). Therefore it can be concluded that in natural gases containing carbon dioxide with an isotope ratio higher than $-10‰$ the proportion of carbon dioxide formed from organic carbon is higher. The range of the probable carbon isotope ratio distribution of carbon dioxide in natural gases with high carbon dioxide content is between $-4‰$ and $-7‰$, which corresponds to the carbon isotope ratio of juvenile carbon dioxide, $-4‰$ and $-8‰$ [KREULEN, 1980; EGLINTON and MURPHY, 1969; KROPOTOVA, 1979; PUCHELT and HUBBERTEN, 1980]. However, these carbon isotope ratios could be also the result of mixing carbon dioxides formed during the regional metamorphism of carbonates and graphite.

The carbon isotope ratios of the carbonates of Hungarian sedimentary rocks are in the range of $+4‰$ and $-4‰$ [HOLCZHACKER *et al.*, 1981]. The proportion of carbon dioxide with a carbon isotope ratio of less than $-4‰$ increases, while the proportion of carbon dioxide with a carbon isotope ratio higher than $-10‰$ decreases with the depth (Table 5). This trend can be interpreted in such a way that the carbon dioxide rich in ^{13}C blends with the carbon dioxide of organic origin rich in ^{12}C as the

depth decreases; the source of carbon dioxide rich in ^{13}C is in greater depth in the litosphere.

There is no significant deviation between carbon isotope ratio distributions of carbon dioxides originating from reservoir rocks of different age (*Figs. 9* and *10*). However, the frequency of high negative carbon isotope ratios ($> -10‰$) characteristic of carbon dioxide of organic origin is relatively high at the carbon dioxides

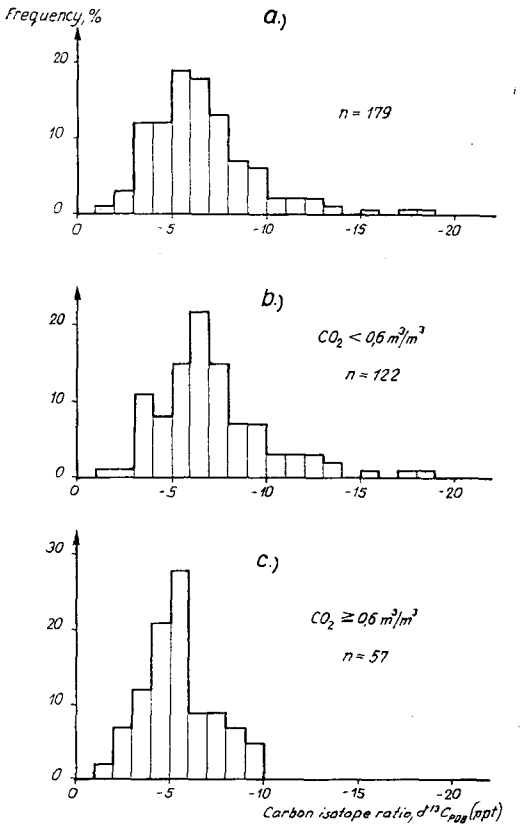

Fig. 8. Carbon isotope ratio distributions of the carbon dioxide of Hungarian natural gases

TABLE 5

The change of the carbon isotope ratio distribution of the carbon dioxide with depth

Depth, km	Frequency, per cent	
	$> -4‰$	$< -10‰$
< 1.5	4	19
1.5—2.0	12	8
2.0—2.5	12	10
2.5—3.0	19	4
> 3.0	32	6

of Neogene reservoir rocks (13 %). This frequency for the carbon dioxides of Mezozoic and Paleozoic reservoir rocks is only 2—6 per cent.

An important conclusion can be drawn concerning the origin of carbon dioxide if the carbon isotope ratio distributions are plotted as a function of carbon dioxide

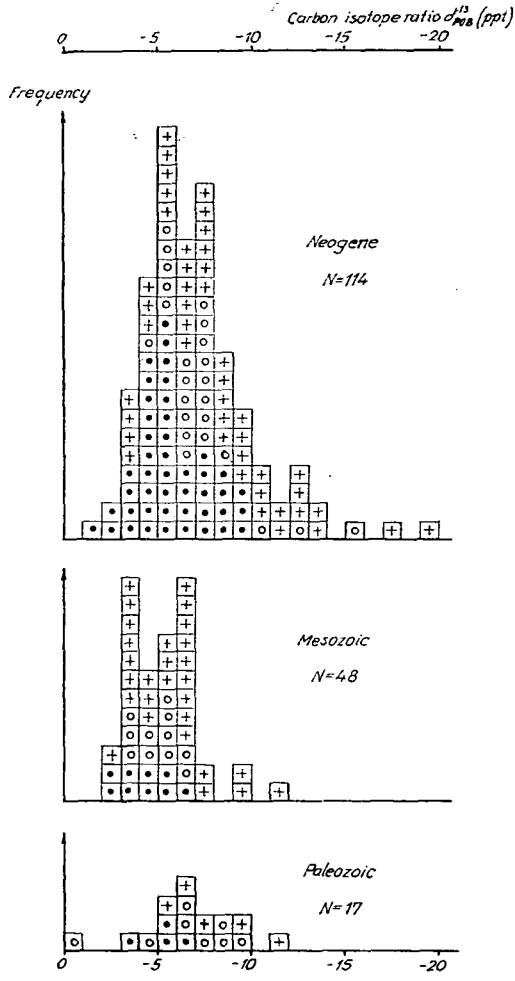

Fig. 9. The carbon isotope ratio distributions of the carbon dioxide of natural gases from reservoir rocks of different ag

concentration for reservoir rocks of different age (*Figs. 10b, c* and *d*). The carbon dioxide enriches in ^{13}C with the increase of carbon dioxide concentration and the carbon isotope ratio approximates the range of carbonates. It can therefore be concluded, that the bulk of carbon dioxide has been formed in the lower part of the earth's crust during the regional metamorphism of carbonates as it has been supposed earlier by KERTAI [1972].

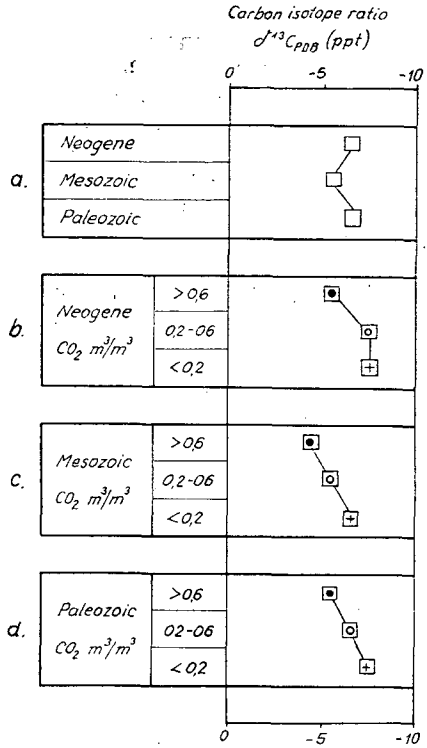

Fig. 10. The median of the carbon isotope ratio distribution of the carbon dioxide

CONCLUSIONS

1. The Hungarian natural gases can be divided into four genetic groups based on the carbon isotope ratio distribution of the methane as a function of depth: biogenic origin (group „C"); mixture of biogenic and thermogenic methane (group „B"); methane of thermogenic origin formed from sapropelic organic matter (group „D"); and the bulk of methane which has also thermogenic origin and has been formed from humic sapropelic organic matter (group „A").
2. The differences in the carbon isotope ratio distributions for reservoir rocks of different age indicate, that the methane of Mezozoic reservoir rocks has either a higher degree of transformation or originates from a more humic organic matter. The origin from an organic matter of higher degree of transformation seems to be proved by the vitrinite reflections of the Mezozoic reservoir rocks. The carbon isotope ratio distribution of the methane of Paleozoic reservoir rocks shows two populations: one of them is in the range of carbon isotope ratio of the methane of Mezozoic reservoir rocks, the other is probably of Neogene origin.
3. The change of carbon isotope ratio distribution with depth for the methane of Neogene reservoir rocks (group „A") indicates a kinetic isotope effect. The consequence of vertical migration is the increase of carbon isotope ratio ranges with decreasing depth. Carbon isotope ratios reflecting the effect of vertical migration occur frequently simultaneously with high carbon dioxide concentrations. The carbon isotope ratio distribution of methane associated with a carbon dioxide content

higher than 0.6 cu.m./cu.m. differs significantly from that of the methane of natural gases with low carbon dioxide concentration in a depth less than 2 kilometers. The methane of natural gases with high carbon dioxide concentration is enriched in ^{13}C. Such carbon isotope ratios of the methane of natural gases with high carbon dioxide content also occur, which indicate the anorganic carbonate origin of the methane.

4. There are significant differences in the carbon isotope ratio distribution of the carbon dioxide with the concentration. The share of carbon dioxide enriched in ^{12}C, i. e. of organic origin, is greater in natural gases with low carbon dioxide content. With the increase of carbon dioxide concentration the carbon isotope ratio distribution of the carbon dioxide shifts towards the enrichment in ^{13}C. This indicates that the bulk of carbon dioxide resulted from the regional metamorphism of carbonates.
5. The change of carbon isotope ratio distribution with depth indicates that the bulk of carbon dioxide originates from the deeper zones of the lithosphere. The carbon dioxide enriches in ^{13}C with increasing depth and decreases the frequency of carbon isotope ratios indicating the presence of carbon dioxide of organic origin.

ACKNOWLEDGEMENTS

I acknowledge the management of the Hungarian Oil and Gas Trust and the Hungarian Hydrocarbon Institute to permit the publication, as well as the Central Research and Development Institute of Mining for the measurements of carbon isotope ratios.

REFERENCES

ALEXEEV, F. A. [1977]: Zum Zoning der Erdöl- und Erdgasgenese in der Lithosphäre nach isotopengeochemischen Untersuchungen. Zeitschrift für angewandte Geologie **25,** No **8,** 379—382.

CORNIDES, I., KECSKÉS, Á. [1982]: Deep-seated carbon dioxide in Slovakia: the problem of its origin, Geologicky Zbornik-Geologica Carpathica **33,** No 2, 193—190.

DOW, W. G. [1977]: Kerogen studies and geological interpretations, Journ. Geochem. Exploration **7,** 79—99.

EGLINTON, G., MURPHY, M. T. J. [1969]: Organic Geochemistry. Springer-Verlag, Berlin—Heidelberg—New York.

FUEX, A. N. [1977]: The use of stable carbon isotopes in hydrocarbon exploration. Journ. Geochem. Exploration **7,** 155—188.

GALIMOV, E. M. [1973]: Izotopi ugleroda v neftegazovoj geologii. Nedra, Moscow.

GUCALO, L. K. [1980]: O razgruzke metana mantii v vodah termalnih istochnikov Kamchatki. Geohimija **3,** 351—358.

HOEFS, J., MORTEANI, G. [1979]: The carbon isotopic composition of fluid inclusions in Alpine fissure quartzes from the western Tauern Window (Tirol, Austria). Neues Jahrb. Mineral., 123—134.

HOLCZHACKER, K. *et al.*, [1981]: A stabil szénizotóparány-adatok felhasználási lehetőségei. Kőolaj és Földgáz **14,** (114), No 6., 178—186.

KECSKÉS, Á. *et al.*, [1981]: Tömegspektrométeres izotópadatok geológiai értelmezésének problémái széndioxid-genetikai vizsgálatok példáján, MTA Kémiai Közlemények **56,** 365—371.

KERTAI, GY. [1972]: A kőolaj és földgáz vegyi összetétele és keletkezése. Akadémiai Kiadó, Budapest.

KRAVCOV, A. I. [1980]: Geologija i geohimija prirodnih gazov v zonah glubinnih razlomov i formirovanije mestorozdenij gorjuchih gazov i nefti, in Degazacija zemli i geotektonika. Nauka, Moscow, 189—199.

KREULEN, R. [1980]: CO_2 rich fluids during regional metamorphism on Naxos (Greece): carbon isotopes and fluid indusions. Am. Journ. Science **280,** 745—771.

KROPOTOVA, O. I. [1979]: Geohimija endogennogo ugleroda v svete izotopnih dannih, in Razdelenije elementov i izotopov v geohimicheskih processov. Nedra, Moscow, 130—149.

MÁFKI, MTA GKL, KBFI reports about vitrinite reflectance measurements. (Manuscripts)

MAXIMOV, S. P. *et al.* [1980]: Izotopnih sostav ugleroda CO_2 gazov Zapadnoj Sibirii v svjazi s ego genezisom. Geohimija **7**, 992—998.
PANKINA, R. G. *et al.* [1978]: Genezis CO_2 v neftjanih popitnih gazah (po izotopnomu sostavu ugleroda). Geologija Nefti i Gaza **2**, 38—43.
PANKINA, R. G. *et al.* [1979]: Izotopnij sostav ugleroda CO_2 v uglevodorodnih skoplênijah v aspekte ego genezisa. ZFI-MITT, **26**, 103—104.
PRASOLOV, E. M., LOBKOV, V. A. [1977]: Ob uslovijah obrazovanija i migracii metana (po izotopnomu sostavu ugleroda). Geohimija **1**, 122—135.
PUCHELT, H., HUBBERTEN, H. W. [1980]: Vulkanogenes Kohlendioxid: Aussagen zur Herkunft aufgrund von Isotopenuntersuchungen. ZFL-MITT, **30**, 198—210.
SCHOELL, M. [1980]: The hydrogen and carbon isotopic composition of methane from natural gases of various origins. Geochim. Cosmochim. Acta **44**, 649—661.
SOKOLOV, V. A. [1971]: Geohimija prirodnih gazov. Nedra, Moscow.
SZALAY, A., KONCZ, I. [1981]: Genese und Migration der Kohlenwasserstoffe in den Neogen-Depressionen des Pannonischen Beckens Ungarns. Zeitschrift für angewandte Geologie **27**, 226—272.
TÖRÖK, I. [1979]: Összetétel-eloszlások széndioxid- és nitrogéntartalmú földgáztelepeken. Kőolaj és Földgáz, **12** (112), 129—134.

Manuscript received, 15 July, 1983

I. KONCZ
Hungarian Hydrocarbon Institute
Section for Geochemistry
H-8801 Nagykanizsa, Vár u. 9.
Hungary

Acta Mineralogica-Petrographica, Szeged, XXVI/1, 51—71, 1983

COMPARISON OF THE LOPATIN METHODS AND THEIR CRITICAL EVALUATION

I. KONCZ

ABSTRACT

There are significant differences among the results of the LOPATIN methods used for estimating the vitrinite reflectance. These differences made it justified to compare and to critically evaluate these methods. Four methods have been compared: two methods by LOPATIN published in 1971 and 1976, resp., and the methods of KARPOV an WAPLES. In addition to the differences caused by deviations of geosystems used for the correlation, the LOPATIN methods basically differ from each other in the character of the correlation relationship and in the reaction kinetic principles employed.

The author thinks that the linear relationship between the logarithm of the vitrinite reflectance and that of the time-temperature index is better founded. For describing the geosystem published by Dow, the reaction kinetic principle is more adequate that are characterized by the following features: the activation energy does not depend on the temperature and, as a result of this, the change of the reaction rate by 10 °C decreases with the increase of the temperature. This reaction kinetic principle is used by LOPATIN in his method published in 1976.

INTRODUCTION

It is a generally accepted and proved fact that the hydrocarbons of the earth's crust form from the organic matter of the sedimentary rocks, i. e. from the kerogen, decisively as a result of thermal effects.

The composition of products originating in the course of the thermal decomposition is closely connected to the maturity of kerogen. (The composition of the decomposition products are denoted by the terms crude oil, wet gas, dry gas). For the quantitative characterization of the kerogen maturity, generally the reflectance of the vitrinite forming a part of the organic matter of sedimentary rocks is used. That is why the values of the vitrinite reflectance measured and estimated by calculation methods supply useful informations for judging potential hydrocarbon prospects. The estimation of the vitrinite reflectance by calculation methods plays an important part in judging the hydrocarbon prospects in sedimentary basins known in a small degree and, by comparing the measured and estimated values, in the paleogeothermal reconstruction.

Similarly to the kerogen, the change of the properties of vitrinite (volatile matter content, reflectance) is a result of a thermal decomposition originating under the thermal influence. The thermal decomposition process of vitrinites was first studied on coals. HUCK, KARWEIL [1955] and KARWEIL [1956] have stated that the thermal decomposition of vitrinites can be described by reaction kinetic relationships and, consequently, not only the temperature but also the time plays a role. BOSTICK [1973] extended this statement to vitrinites in sedimentary rocks. The thermal decomposition consists of the joint effect of very complicated, serial and parallel reactions. The reaction kinetic relationships permit the description of this complicated process in a

formal kinetic way which is characteristic of the total process. with apparent constants (with apparent activation energy, frequency factor and reaction order).

Resulting from the formal kinetic description, the abovementioned apparent reaction kinetic constants can be determined by comparing them with the well-known geosystems (correlation).

Extrapolating the kinetic constants arising from the laboratory model experiments may give rise to significant errors because of the deviation of the time factor by several orders of magnitude [SNOWDON, 1979]. LOPATIN [1971] has published a simple calculation method for estimating the vitrinite reflectance which has been modified in 1976. KARPOV [1975] and WAPLES [1980] have published another calculation method the basic principle of which is similar to that of LOPATIN'S method. The deviations of the results obtained for the same geosystems with the methods of identical basic principle that has been demonstrated in this article, have made justified a critical evaluation of Lopatin's methods.

THE COMMON THEORETICAL BASES OF LOPATIN'S METHODS

In the sedimentary rocks, the thermal decomposition of the vitrinite takes place under non-isothermal conditions; the rate of reaction calculated by using Arrhenius' equation is the function of time, too:

$$k(t) = A \cdot e^{-\frac{E}{RT(t)}}. \tag{1}$$

Where: k = rate of reaction, million years^{-1},
t = geological time, million years,
A = frequency factor, million years^{-1},
E = activation energy,
R = universal gas constant,
T = absolute temperature, Kelvin.

LOPATIN'S methods decompose the non-isothermal transformation into a series of isothermal transformations andy the form the actual non-isothermal transformation as a total of these isothermal transformations. Within the temperature interval $T+\Delta T$, the rate of reaction is considered as constant, and, assuming the kinetically first-order reaction. by means of the so-called "cooking" time Δt_i, spent in the temperature interval $T+\Delta T$, the transformation is calculated using the following formula:

$$ln\frac{c_{Ti}}{c_{Ti+\Delta T}} = k_i . \Delta t_i. \tag{2}$$

Where: $c_{T_i}/c_{T_i+\Delta T}$ = transformation module of vitrinite,
k_i = rate of reaction belonging to the lower or upper temperature limit of the temperature interval $T_i+\Delta T$,
Δt_i = time spent in the temperature interval $T_i+\Delta T$.

Instead of the absolute rate of reaction, the LOPATIN'S methods make use of the relative rate of reaction, i. e. the so-called temperature factor of the rate of reaction, γ_i, which is the quotient of the absolute rate of reaction, belonging to the interval $T_i+\Delta T$ (k_i) and to a so-called reference temperature (T_R) chosen arbitrarily (k_R):

$$\gamma_i \equiv \frac{k_i}{k_R}. \tag{3}$$

Eqn. 2 can be written in the following modified version by introducing the relative rate of reaction:

$$\ln \frac{C_{T_i}}{C_{T_i+\Delta T}} = k_R \cdot \gamma_i \cdot \Delta t_i \tag{4}$$

By summarizing the elementary isothermal transformations calculated in this way, the transformation approximating the non-isothermal transformation, from the beginning of the sediment formation up to the present situation, can be produced:

$$\ln \frac{C_{To}}{C_T} \approx \sum_{To}^{T} \ln \frac{C_{Ti}}{C_{Ti+\Delta T}} = k_R \sum_{To}^{T} (\gamma_i \cdot \Delta t_i). \tag{5}$$

Where: T_o = temperature pertaining to the beginning of the sediment formation,
T = temperature pertaining to the present situation,
c_{To}/c_T = ratio of the non-isothermal transformation.

The sum of the elementary transformations is the index of the maturity time temperature (TTI):

$$\mathrm{TTI} \equiv \sum_{To}^{T} (\gamma_i \cdot \Delta t_i). \tag{6}$$

By introducing this definition, the non-isothermal transformation can be expressed as:

$$\ln \frac{C_{To}}{C_T} \approx k_R(\mathrm{TTI}). \tag{7}$$

Based upon reaction kinetic considerations, the methods after LOPATIN first determine the temperature factors, γ_i, pertaining to the isothermal sections, thereafter, they fix the "cooking" time (Δt_i) belonging to the individual isothermal sections on geosystems of relatively well-known heat history. The products temperature factor/"cooking" time ($\gamma_i \Delta t_i$) proportional to the isothermal transformations are summarized and, by doing so, the time/temperature index (TTI) is obtained. This index is correlated with the vitrinite reflectance values measured in known geosystems. Thus, the relationship between the vitrinite reflectance (R) and the time/temperature index is obtained.

The basic conditions of a well applicable relationship of general validity, R/TTI, are as follows:

1) The temperature factors of the reaction rate should be appropriate; they should describe the thermal decomposition of the vitrinite.
2) The vitrinite reflectance values measured in the known geosystems should meet the measure of the actual transformation of the vitrinite.
3) The thermal history of the known geosystems should comply with the actual thermal history.

The differences among LOPATIN's methods are derived from the differences among the geosystems used for the correlation that are considered as known or that are really known. A further deviation is that various temperature factors are used. Last not least, there is a difference concerning the character of the relation R/TTI, the magnitude of the temperature intervals suitable for the isothermal transformations and the reference temperature.

LOPATIN'S METHODS AND THEIR DIFFERENCES

This article encompasses the following problems of the differences among LOPATIN's methods:

— characteristics of the geosystems used for the correlation;
— character of the relationship, R/TTI;
— magnitude of the temperature factor and of the temperature intervals corresponding to isothermal transformations as problems connecting with each other;
— reference temperature.

1) Characteristics of the geosystems used for the correlations

LOPATIN [1971]: Drilling Münsterland—1, vitrinite reflectance: 1—5%.

LOPATIN [1976]: 38 coal layers, in the Soviet Union, USA and FRG; vitrinite reflectance: 0.3—5.5%.

KARPOV [1975]: 111 measuring results from various parts of the Soviet Union: vitrinite reflectance: 0.3—4.3%.

WAPLES [1980]: 402 measuring data obtained from 31 well, (no region indicated); vitrinite reflectance: 0.4—6%.

In all probability, the correlation approaches the actual relation, all the more the higher is the difference as to the time and the temperature and the vitrinite reflectance range. Considering these facts, LOPATIN's method [1971] can be regarded as uncertain, although this publication includes this basic idea that can be judged as right from that time. At the same time, LOPATIN's correlation published in 1976 based on a significantly larger amount of facts is less known and less accepted, presumably because the researchers, such as WAPLES, dealing with this topic, have accepted the redoubling of the reaction rate per 10 °C, whereas LOPATIN has changed this view point.

2) Character of the relationship, R/TTI

LOPATIN [1971]: $R = 1.301 \lg (TTI) - 0.5282.$
LOPATIN [1976]: $\lg R = 0.4762 \lg (TTI) - 1.1638.$
KARPOV [1975]: $\lg R = 0.1974 \lg (TTI) - 0.9852.$
WAPLES [1980]: $\lg R = 0.2645 \lg (TTI) - 0.4841.$

With the exception of LOPATIN's calculation method published in 1971, a linear relationship between the logarithm of the vitrinite reflectance and that of the time/ /temperature index was established in the other methods.

3) Magnitude of the temperature factor and of the temperature intervals corresponding to isothermal transformations

In his paper published in 1976, LOPATIN considered the value of the activation energy as a constant (41.84 kJ/mol) independently of the temperature and he chose the magnitude of the temperature intervals of isothermal phases starting from 50 °C in a way so that the reaction rate should be doubled. In case of a constant activation energy, the value of the temperature/intervals necessary for the doubling of the reaction rate (ΔT_i) can be calculated using the following formula:

$$\Delta T_i = \frac{1.378\, T_i}{10\,000 - 1{,}378 \cdot T_i}. \qquad (8)$$

TABLE 1

Temperature limits suitable for the doubling of reaction rate at a constant activation energy (41.84 kJ/mole)

Temperature limits (°C)

LOPATIN [1976]	According to Eqn. 8
50	50
65	65.8
80	81.6
100	99.8
120	120.0
145	142.5
170	167.2
200	196.2
230	228.6

Table 1 demonstrates the temperature limits calculated by Eqn. 8 and determined by LOPATIN [1976].

LOPATIN's method is equivalent to the method according to which, in case of a constant activation energy, the change of the reaction rate per 10 °C (r) is a function of the temperature. (1976) With the increase of the temperature, the change of the reaction rate diminishes in conformity with the following relationship:

$$\lg r_i = \frac{21850}{T_i(T_i+10)}. \tag{9}$$

Where:

$$r_i = \frac{k_{T_i+10}}{k_{T_i}}.$$

The temperature factors can be obtained under the same conditions using the following formulae:

$$\lg\gamma_i = 2185 \cdot \frac{T_i - T_R}{T_i \cdot T_R}. \tag{10}$$

Fig. 1 shows the change of the reaction rate *vs.* temperature (Eqn. 9) on the basis of Eqn. 9. According to GOLITSYN [1973], the change of the topochemical reaction rate per 10 °C encountered in the diffusion range amounts to values between 1.2 and 1.5. (In *Fig. 1*, values suggested by GOLITSYN are indicated.)

The majority of the authors, such as LOPATIN [1971], KARPOV [1975], WAPLES [1980] chose the magnitude of the temperature intervals corresponding to isothermal transformations as having a value of 10 °C in the whole temperature interval of the non-isothermal transformation. This seemingly arbitrary selection was accounted for by the fact that, according to VAN'T HOFF's rule, the chemical reaction rates taking place as a result of thermal effects are doubled per 10 °C:

$$r = \frac{k_{T_i+10}}{k_{T_i}} = z. \tag{11}$$

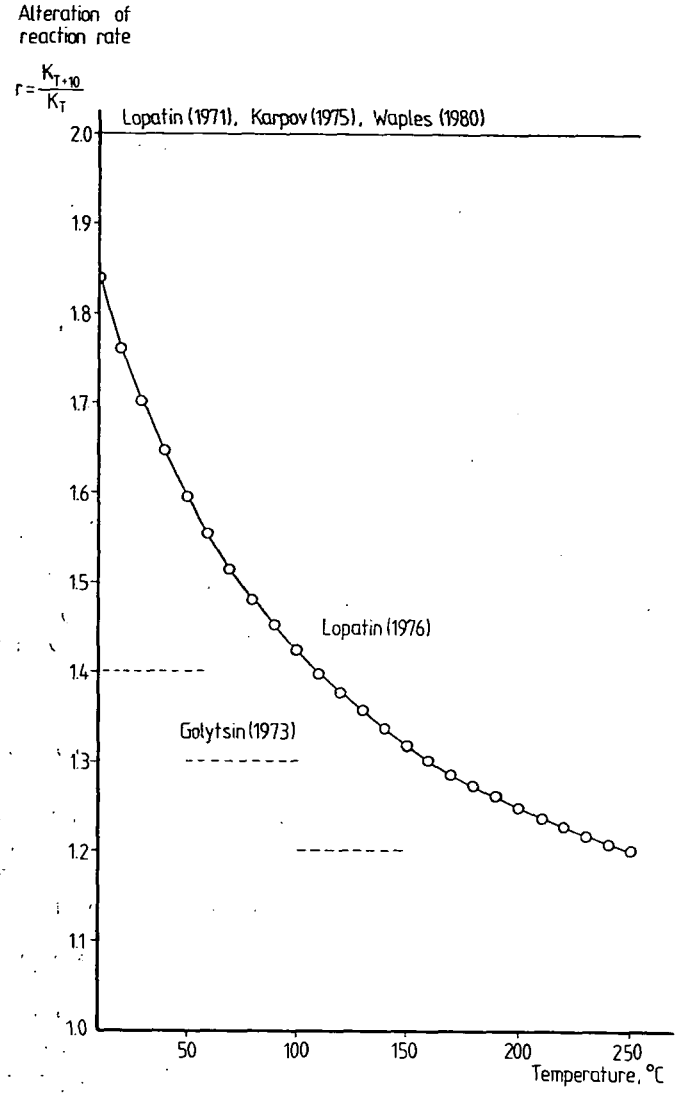

Fig. 1. Relationship between changes in the reaction rate by 10 °C and the temperature at a constant activation energy (41.84 kJ/mole)

Assuming the validity of VAN'T HOFF's rule, the temperature factors belonging to the individual isothermal sections can be obtained using the following simple relationship:

$$\gamma_i = z^N \text{ or } \lg\gamma_i = N \lg z \tag{12}$$

Where:

$$N = \frac{T_i - T_R}{10}. \tag{13}$$

Based upon the relationships to be demonstrated hereinafter, the condition of doubling the reaction rate per 10 °C results in the change of the activation energy with the increase of the temperature:

$$\lg r_i = \frac{1}{2.303\,R}\left(\frac{E_{T_i}}{T_i} - \frac{E_{T_i+10}}{T_i+10}\right). \tag{14}$$

$$\lg r_i = \frac{1}{2.303\,R}\left[\frac{T_i(E_{T_i} - E_{T_i+10}) + E_{T_i}\cdot 10}{T_i(T_i+10)}\right]. \tag{15}$$

Since $r=2$ and $\lg r>0$, the difference of activation energy, resulting from Eqn. 15, $(E_T - E_{r+10})$ should be positive giving

$$E_{T_i} > E_{T_i+10}. \tag{16}$$

Thus, the doubling of the reaction rate per 10 °C involves the decrease of the activation energy.

Eqn. 14 should be considered as the equation describing the relationship activation energy/temperature corresponding to the doubling of the reaction rate per 10 °C. Accordingly, the function of activation energy *vs.* temperature can be expressed as:

$$E = -\frac{2.303\,R\lg z}{10}\cdot T^2. \tag{17}$$

Starting from a specified temperature, T_0, the change of the activation energy (ΔE) can be calculated using Eqn. 17:

$$\Delta E = \frac{2.303\,R\lg z}{10}\cdot T_o^2 - \frac{2.303\,R\lg z}{10}\cdot T^2. \tag{18}$$

Where: $\Delta E = E_T - E_{T_0}$ and $T > T_o$

Fig. 2 shows the activation energy difference as a function of the temperature in case the reaction rate is doubled per 10 °C.

Therefore, LOPATIN's methods differ from each other in two alternative solutions:

a) the change of the reaction rate per 10 °C does not depend on the temperature, the activation energy is not constant but it is a function of the temperature,
b) the change of the reaction rate per 10 °C is not constant but it depends on the temperature, the activation energy is independent of the temperature.

4) Reference temperature

LOPATIN [1971]: 373 K (100 °C).
LOPATIN [1976]: 323 K (50 °C).
KARPOV [1975]: 283 K (10 °C).
WAPLES [1980]: 373 K (100 °C).

Even if the discrepancies of the geosystems used for the correlation are disregarded, it can be stated that there are two methods of LOPATIN's fundamental principle that are identical in all the parameters enumerated above. That is why the discrepancies arising from the differences of the geosystems cannot be determined by comparing the constants of the relationships R(TTI).

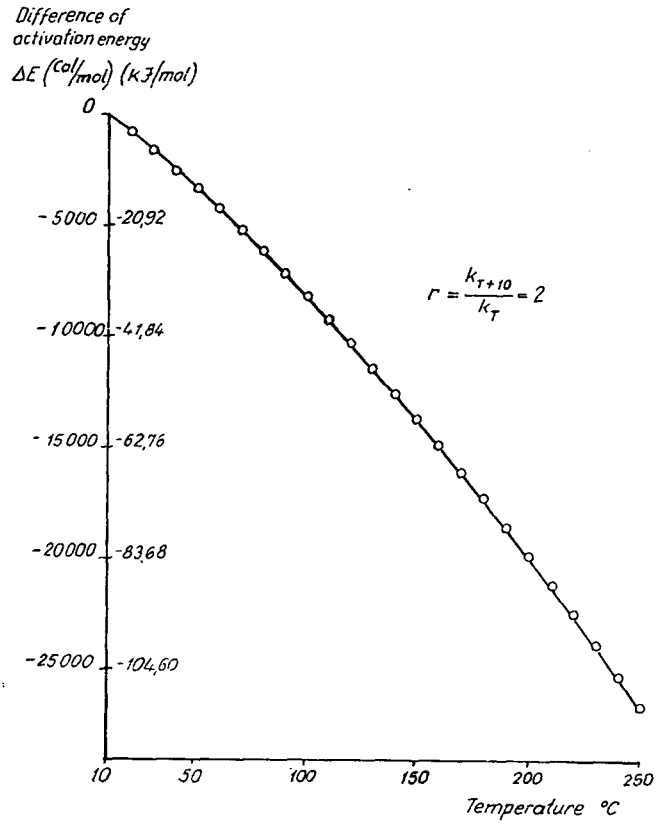

Fig. 2. Relationship between the activation energy difference and the temperature in case of the doubling of the reaction rate by 10 °C

A COMPARISON OF THE RESULTS OBTAINED BY LOPATIN'S METHODS ON THE SAME GEO-CONDITIONS

To perform the comparison, the identity of the following three geo-conditions, i. e. the heating rate, ξ, the sedimentation, as well as the temperature, T_i belonging to the beginning of the transformation, T_0 and to the end of the transformation must be ensured. These considerations can be accounted for in the following way:

Heating rate in the isothermal sections:

$$\xi \equiv \frac{\Delta T_i}{\Delta t_i}. \tag{19}$$

Where: ξ = heating rate. (°C/million years);
ΔT_i = temperature range of the isothermal section which is (10 °C) identical in the whole temperature range of the non-isothermal transformation with LOPATIN's [1971]. KARPOV's [1975] and WAPLES' [1980] methods; it is changing with LOPATIN's method [1976], with the increase of the temperature, it amounts to 15, 20, 25 and 30 °C;

Δt_i = time spent in the temperature interval, ΔT_i, of the isothermal sections, million years.

From Eqn. 19, Δt_i figuring in the time/temperature index can be expressed as:

$$\Delta t_i = \frac{\Delta T_i}{\xi_i}. \tag{20}$$

If, in conformity with the identical geo-conditions, the heating rate is independent of the time (and of the temperature), then

$$\Delta t_i = \frac{\Delta T_i}{\xi}. \tag{21}$$

If ΔT_i is constant (10 °C), then

$$\Delta t = \frac{10}{\xi}. \tag{22}$$

For the whole time and temperature range of the non-isothermal transformation, it can be written

$$\sum \Delta t_i = t \text{ and } \sum \Delta T_i = \Delta T$$

Where:

$$\Delta T = T_i - T_o \cdot$$

In this case, according to Eqn. 21:

$$t = \frac{T_i - T_o}{\xi}. \tag{23}$$

If the initial and final temperatures of the non-isothermal transformation, as a geo-condition, are constant and the heating rate is also constant, then the length of time of the transformation is constant, too. Therefore, all the parameters figuring in the calculation of the transformation are constant, they do not depend on the temperature provided the geo-conditions are identical. Presuming the heating rate and the subsidence rate, (λ), are constant, then in the total time and temperature range of the non-isothermal transformation, the geothermal gradients, G, should also be constant and independent of time and temperature since

$$\xi = G \cdot \lambda. \tag{24}$$

Using LOPATIN's methods, the value of the vitrinite reflectance can be calculated by means of the following equations, provided there are identical geo-conditions:

$$\text{LOPATIN [1971]: } R = 1.301 \left(\lg \sum_{T_0}^{Ti} \gamma_i - \lg \xi \right) + 0.773 \tag{25}$$

$$\text{LOPATIN [1976]: } \lg R = 0.4762 \left(\lg \sum_{T_0}^{T_i} (\gamma_i \Delta T_i) - \lg \xi \right) - 1.1638 \tag{26}$$

$$\text{KARPOV [1975]: } \lg R = 0{,}1974 \left(\lg \sum_{T_0}^{T_i} \gamma_i - \lg \xi \right) - 0{,}7878 \tag{27}$$

$$\text{WAPLES [1980]: } \lg R = 0{,}2645 \left(\lg \sum_{To}^{Ti} \gamma_i - \lg \xi \right) - 0{,}2196 \tag{28}$$

The number of the vitrinite reflectance values belonging to various final temperature values as well as the possibility of the comparison is reduced to a great extent by the fact that LOPATIN's method [1976] and the other methods can be compared at a limited number of final temperature values (7 values) and there is a considerably large difference among the comparable temperature values ranging from 20 to 50 °C. That is why isometamorphic temperatur values needed to attain the same vitrinite reflectance value seemed to be expedient to compare LOPATIN's methods at identical geoconditions. The vitrinite reflectance values serving as basis for the comparison were given by vitrinite reflectances authoritative from the view-point of hydrocarbon formation using Dow's values [1978]: 0.6; 1.0; 1.35; 2.0%.

To realize this method, it was necessary to determine the relationship between vitrinite reflectance and temperature, i. e. the function $R(T)$. The function $R(T)$ can be calculated by using the temperature factors in case of LOPATIN's [1971], KARPOV's [1975] and WAPLES' [1980] methods and b using the temperature function of the logarithm, of the sums of the products $\gamma_i \Delta T_i$ in case of LOPATIN's method [1976]. (The summation is done uniformly starting from 10 °C.)

$$\text{LOPATIN [1971] and WAPLES [1980]: } \lg \sum_{To}^{Ti} \gamma_i = 0.0302 \cdot T - 11.256 \tag{29}$$

$$\text{KARPOV [1975]: } \lg \sum_{To}^{Ti} \gamma_i = 0.0304 \cdot T - 8.350 \tag{30}$$

$$\text{LOPATIN [1976]: } \lg \sum_{To}^{Ti} (\gamma_i \Delta T_i) = -2563 \frac{1}{T} + 9.308 \tag{31}$$

In case of all methods with the exception of LOPATIN's method [1976], the logarithm of the sum of the temperature factor can be linearized by the temperature and, in case of LOPATIN's method, [1976] by the reciprocal value of the temperature, starting from 60 °C.

Using the above equations, the isometamorphic values necessary for attaining the various vitrinite reflectance values can be calculated by means of the following relationships:

$$\text{LOPATIN (1971): } T = 25.45 \, (R + 1.301 \lg \xi + 13.871) \tag{32}$$

$$\text{LOPATIN [1976]: } T = \frac{1221}{3.268 - \lg R - 0.4762 \lg \xi} \tag{33}$$

$$\text{KARPOV [1975]: } T = 166.7 \, (\lg R + 0.1974 \lg \xi + 2.436) \tag{34}$$

$$\text{WAPLES [1980]: } T = 125.2 \, (\lg R + 0.2645 \lg \xi + 3.197) \tag{35}$$

The temperature values determined by using the above relationships are shown in Table 2. The temperature values necessary to attain the identical vitrinite reflectance values are demonstrated as a function of the logarithm of the heating rate in *Figs. 3, 4, 5* and *6*.

TABLE 2

Isometamorphic temperature values calculated by LOPATIN'S *methods*

ξ(°C/million years)	R %	Temperature (°C)			
		LOPATIN [1971]	LOPATIN [1976]	KARPOV [1975]	WAPLES [1980]
0.3	0.6	78	54	79	82
	1.0	88	74	116	110
	1.35	97	88	138	126
	2.0	114	107	166	148
1.0	0.6	95	77	96	99
	1.0	105	101	133	127
	1.35	114	116	155	144
	2.0	131	139	183	165
3.0	0.6	111	101	112	115
	1.0	121	129	149	143
	1.35	130	146	170	159
	2.0	147	173	199	181
15.0	0.6	134	144	135	138
	1.0	144	178	172	166
	1.35	153	201	193	183
	2.0	170	234	222	204

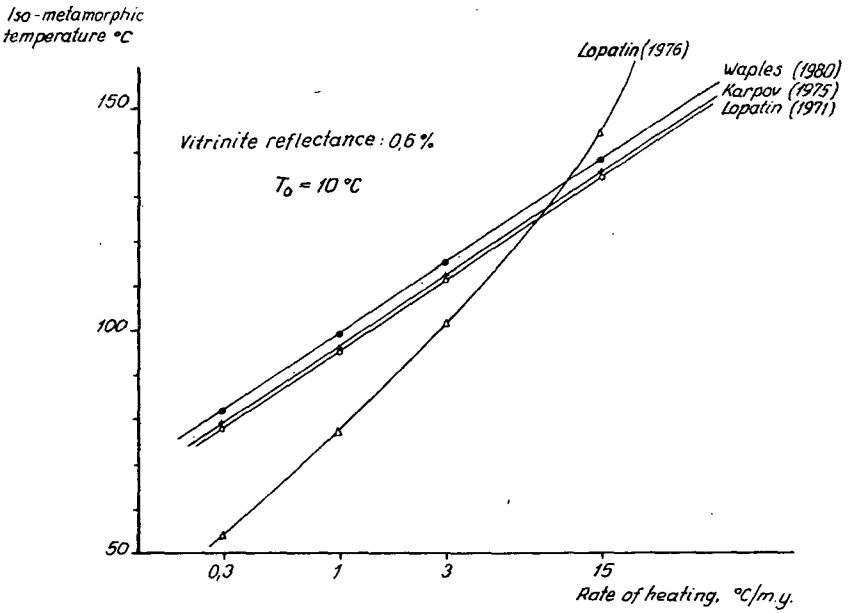

Fig. 3. Relationship between the isometamorphic temperature values belonging to the 0.6% vitrinite reflectance and the logarithm of the heating rate (at $T_0 = 283$ K, values calculated by using LOPATIN'S methods)

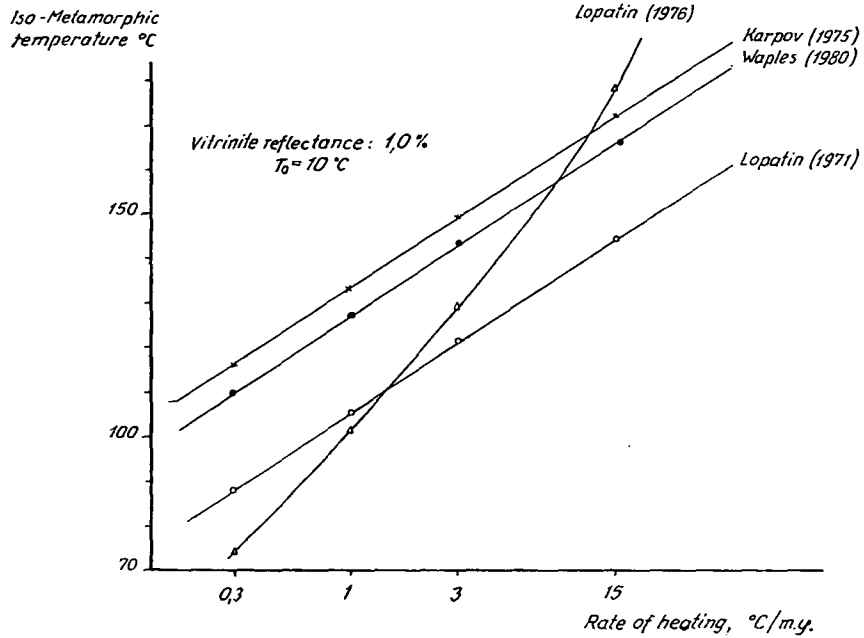

Fig. 4. Relationship between the isometamorphic temperature values belonging to the 1% vitrinite reflectance and the logarithm of the heating rate (at $T_0 = 283$ K, values calculated by using LOPATIN's methods)

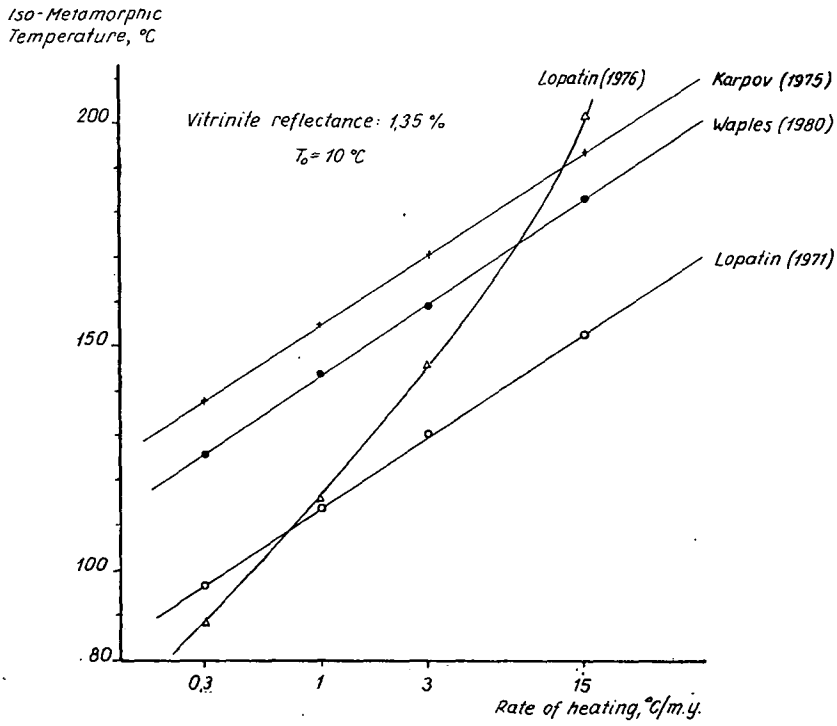

Fig. 5. Relationship between the isometamorphic temperature values belonging to the 1.35% vitrinite reflectance and the logarithm of the heating rate (at $T_0 = 283$ K, values calculated by using LOPATIN's methods)

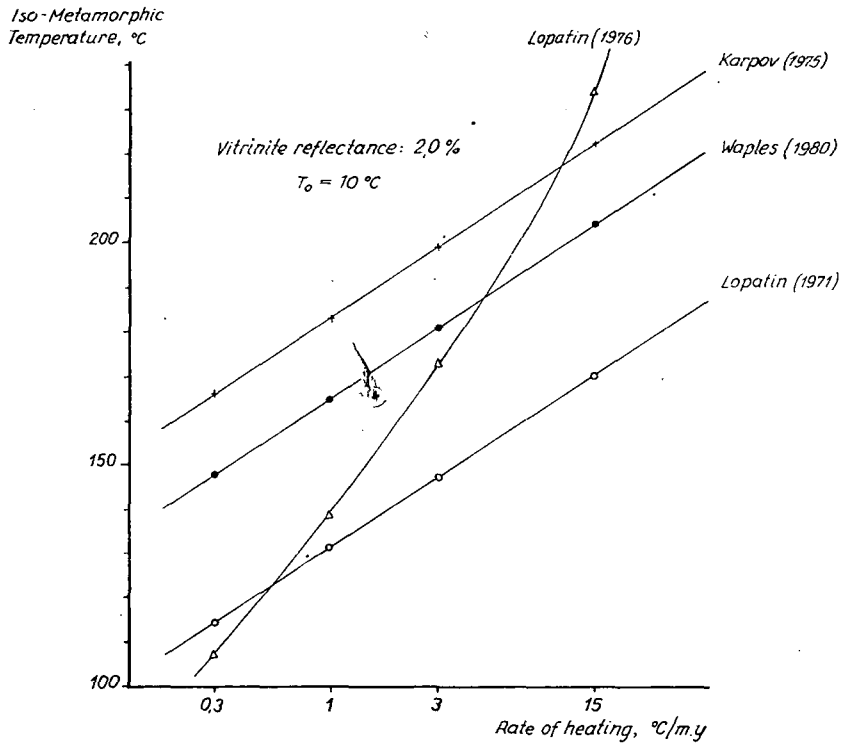

Fig. 6. Relationship between the isometamorphic temperature values belonging to the 2% vitrinite reflectance and the logarithm of the heating rate (at T_0=283 K, values calculated by using LOPATIN's method, 1976)

On the basis of the Figures, the following can be stated:

1) With methods [LOPATIN, 1971; KARPOV, 1975; WAPLES, 1980] using the doubling of the reaction rate by 10 °C and, consequently, the activation energy changing depending on temperature, the temperature values (isomorphic) needed to attain the identical vitrinite reflectance values are linear function of the logarithm of the heating rate. The slope of the linear functions suitable for the various methods is identical, the different temperature values are caused by the differences of the axial section of the linear relationship.
2) In case of LOPATIN's method [1976] which is different from the temperature and uses a constant activation energy, the reciprocal of the isometamorphic temperature values supplies a linear relationship with the logarithm of the heating rate, see *Fig. 7.*
3) The isometamorphic temperature values calculated by using the various methods at identical geoconditions show significant discrepancies. In case the vitrinite reflectance is equal to 0.6, the methods using the temperature-dependent activation energy result in nearly identical isometamorphic temperature values. With vitrinite reflectance values higher than 0.6, the differences grow considerably with the increase in vitrinite reflectance. At the same conditions (vitrinite reflectance, heating rate), the isometamorphic temperature values show an increase in the order of LOPATIN's [1971], WAPLES' [1980] and KARPOV's methods [1975].

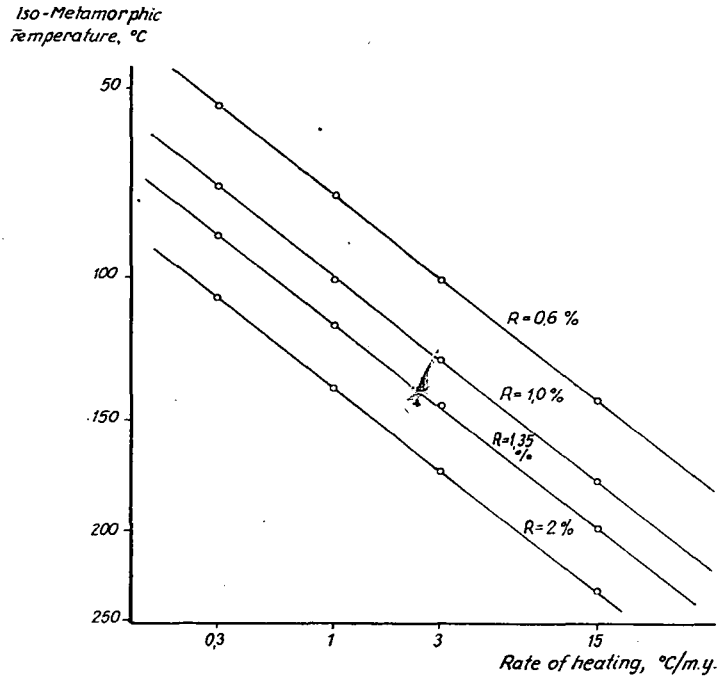

Fig. 7. Relationship between the reciprocal of the isometamorphic temperature values and the logarithm of the heating rate (at $T_0 = 283$ K, values calculated by using LOPATIN's methods)

PROBLEMS CONNECTED TO THE CHARACTER OF THE RELATIONSHIP BETWEEN TIME-TEMPERATURE INDEX AND VITRINITE REFLECTANCE

The relationship between time-temperature index and vitrinite reflectance is expressed by $R = a \lg(\mathrm{TTI}) + b$, or $\lg R = a \lg(\mathrm{TTI}) + b$, where a and b are constant. The question arises which of the relationships is correct. To answer this question the relationship between the vitrinite reflectance and the concentration ratio (c_{T_0}/c_T) figuring in Eqn. 7, characteristic of the vitrinite transformation should be examined.

It can be assumed on good grounds that the concentration of the reactive groups of the vitrinite is proportional to the volatile matter content of the vitrinite (I):

$$C = f \cdot I \tag{36}$$

The concentration ratio is equal to the volatile matter content ratio:

$$\frac{C_{T_0}}{C_T} = \frac{I_{T_0}}{I_T}. \tag{37}$$

The vitrinite reflectance-volatile matter content values that are related to each other published by KÖTTER [1960], can be correlated in the 0.18—3.0% vitrinite reflectance range and in the 0.055—0.6 volatile matter content rate by using the following linear relationship:

$$\lg I = -0.3696\, R - 0.1512. \tag{38}$$

Where I: the volatile matter content of the vitrinite (g/g).

Fig. 8 shows the curve appropriate to the correlation equation. The values serving as a basis of the correlation equation were taken from KÖTTER's publication [1976] and the points indicated from the paper of TEICHMÜLLER [1971].

The prevailing surface value of the vitrinite reflectance belonging to the beginning of the sediment formation can be expressed as:

$$\lg I_{T_0} = -0.3696\, R_{T_0} - 0.1512. \tag{39}$$

After Dow [1977], the surface value of the vitrinite reflectance falls between 0.18 and 0.20%; for this reason, a 0.19% value of the vitrinite reflectance was taken as a sur-

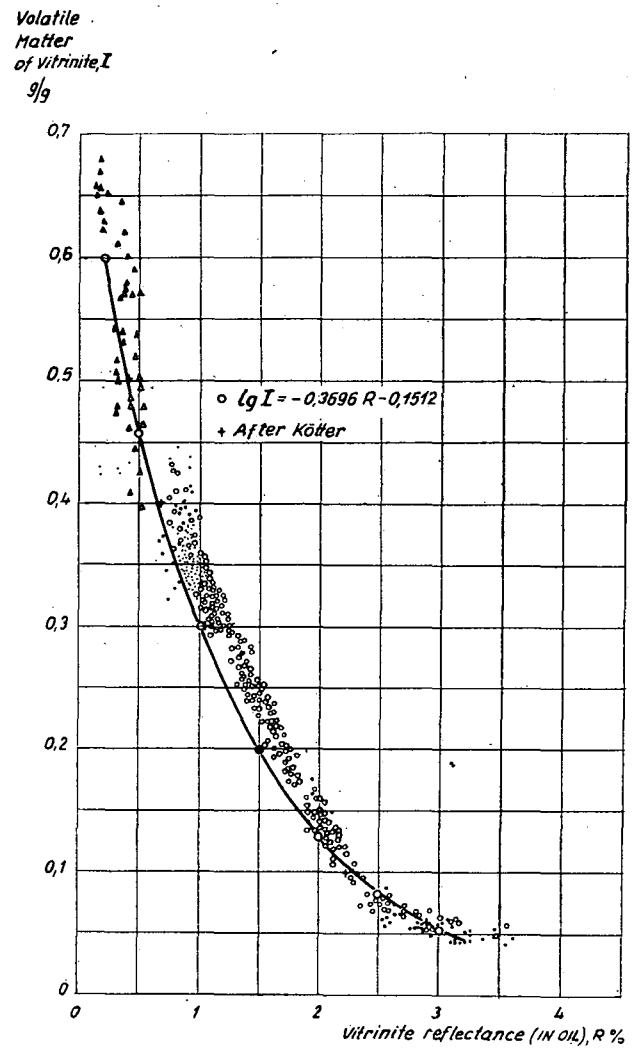

Fig. 8. Relationships between the vitrinite reflectance and the volatile matter content after KÖTTER (1960) and TEICHMÜLLER (1971) and a relationship suitable to the correlation equation determined for KÖTTER's data.

face value in the following expressions to which a 0.6 value of the volatile matter content belongs in accordance with Eqn. 38.
By using Eqns. 38 and 39, the relationship of the volatile matter content and the concentration ratio and the vitrinite reflectance may be written as:

$$\lg \frac{I_{T_o}}{I_T} = \lg \frac{C_{T_o}}{C_T} = 0.3696\,(R_T - R_{T_o}). \tag{40}$$

Based upon Eqn. 7, a relation between the time-temperature index as well as the vitrinite reflectance can be obtained in the following way:

$$\ln \frac{C_{T_o}}{C_T} = 2.303 \lg \frac{C_{T_o}}{C_T} = 0.8512\ \Delta R \tag{41}$$

where: $\Delta R \equiv R_T - R_{T_o}$ is an increment of the vitrinite reflectance.

$$0.8512\ \Delta R = k_R(\mathrm{TTI}) \tag{42}$$

$$\lg \Delta R = \lg(\mathrm{TTI}) + \lg k_R + 0.070$$

In the vitrinite reflectance range of 0.6 to 2%, the following relation exists between the increment of the vitrinite reflectance and the vitrinite reflectance:

$$\lg \Delta R = 1.2506 \lg R - 0.1032 \tag{43}$$

Using the correlation Eqn. 43 in the context of Eqn. 42 gives:

$$\lg R = 0.800 \lg(\mathrm{TTI}) + 0.800 \lg k_R + 0.1385 \tag{44}$$

Since the absolute reaction rate belonging to the reference temperature is constant if the identical methods are used, the following general formula holds true of the relationship between the time-temperature index and the vitrinite reflectance:

$$\lg R = a \lg(\mathrm{TTI}) + b$$

This result also means that the relationship R (TTI) playing a role in LOPATIN's method [1971] which establishes a linear relation between the vitrinite reflectance and the logarithm of the TTI values, cannot be considered as correct in the 0.6—2.0% vitrinite reflectance range.

It is expedient to investigate to what conclusions the formula of the relation R (TTI) leads, that can be considered as correct, at identical geoconditions.

Comparing Eqns. 26—28 and 29—31, it can be stated that the following relationships exist between the vitrinite reflectance and the temperature:

With KARPOV's [1975] and WAPLES' [1980] methods:

$$\lg RY = (\mathrm{constant})_1 \cdot T + (\mathrm{constant})_2. \tag{45}$$

With LOPATIN's method [1976]

$$\lg R = -(\mathrm{constant})_1 \cdot \frac{1}{T} + (\mathrm{constant})_2. \tag{46}$$

In Eqns. 45 and 46, $(\mathrm{constant})_1$ is a constant independent of temperature and heating rate; whereas $(\mathrm{constant})_2$ depends on the heating rate and independent of temperature. In case the heating rate can be considered as constant during the temperature

history, which is equivalent to that fact that, in the course of the temperature history, the surface temperature, the geothermal gradient and the subsidence rate were constant, then

$$T = T_o + \frac{\xi}{\lambda} \cdot Z \tag{47}$$

elucidates that the general form of Eqn. 45 can be expressed as:

$$\lg R = (\text{constant}) \cdot Z + (\text{constant}). \tag{48}$$

and that of Eqn. 46:

$$\lg R = -(\text{constant}) f\left(\frac{1}{Z}\right) + (\text{constant}). \tag{49}$$

Where: Z = depth

$f\left(\frac{1}{Z}\right)$ = function of the reciprocal of the depth.

Therefore, Eqn. 48, in which the relationship between the logarithm of the vitrinite reflectance and the depth is linear, is characteristic of methods using the doubling of the reaction rate by 10 °C and changing the activation energy *vs.* temperature. This relationship is widely used in spite of the fact that its effectiveness is bound to various conditions, such as the doubling of the reaction rate by 10 °C, permanence of the geoconditions mentioned during the temperature history and the vitrinite reflectance range between 0.6 and 2.0%.

Eqn. 49 differs from the previous ones and it is a result of reaction kinetical considerations prevailing in LOPATIN's method [1976] which seems to be expedient to try in geosystems in the future.

PROBLEMS OF THE TEMPERATURE FACTOR

The problems of the temperature factor are solved by LOPATIN's methods basically in two ways. These two solutions and their consequences can be symbolized in the following way:

1) The change of the reaction rate by 10 °C is independent of the temperature it is constant, its value is 2 ⇄ the activation energy depends on the temperature, and decreases with its growth

2) The change of the reaction rate by 10 °C depends on the temperature and decreases with the growth of the temperature ⇄ the activation energy is independent of the temperature, it is constant

The consequence of solution 1) is that the following relationship exists between the vitrinite reflectance, the temperature and the heating rate in case there is a constant surface temperature and heating rate during the temperature history:

$$\lg R = (\text{constant}) \cdot T - (\text{constant}) \lg \xi + (\text{constant}). \tag{50}$$

The consequence of solution 2):

$$\lg R = -(\text{constant}) \cdot \frac{1}{T} - (\text{constant}) \lg\xi + (\text{constant}). \tag{51}$$

Starting from Eqns. 50 and 51, there is a possibility for comparing the consequences of the two above solutions with the behaviour of the geosystems. In case of solution 1), the relationship between the isometamorphic temperature and heating rate can be expressed as:

$$T = (\text{constant}) \lg\xi + (\text{constant}). \tag{52}$$

In case of solution 2):

$$\frac{1}{T} = -(\text{constant}) \lg\xi + (\text{constant}). \tag{54}$$

On the basis of Eqns. 50 and 51, the difference of temperature values belonging to the identical vitrinite reflectance values ($\Delta T_{R1\ R2}$), in the case of solution 1) (constant heating rate) is given by

$$\Delta T_{R_1R_2} = (\text{constant}). \tag{54}$$

In case of solution 2):

$$\Delta T_{R_1R_2} = (\text{constant}) \cdot T_1 \cdot T_2. \tag{55}$$

Where: $\Delta T_{R_1R_2} \equiv T_2 - T_1$, T_1 = isometamorphic temperature belonging to vitrinite reflectance R_1 and T_2 = that belonging to vitrinite reflectance R_2.

From Eqn. 54 it can be seen that for solution 1) the difference of the isometamorphic temperature values do not depend on heating rate; in case of solution 2), resulting from Eqn. 55, it is dependent of the heating rate, since on the basis of Eqns. 52 and 53, it can be seen that the isometamorphic temperature is a function of the heating rate.

For comparing the conclusions and geosystems arising from the reaction kinetic considerations of LOPATIN's methods, the data published by Dow [1978] seem to be appropriate (see Table 3) because the present surface temperatures are identical, the sediment formation is continuous and the available data meet a rather wide interval of the heating rate. We cannot prove the constancy of the prevailing surface temperature and of the heating rate, the comparison, however, is not impeded by this circumstance since it results in an error of the same magnitude for all methods.

Fig. 9 demonstrates the difference of the isometamorphic temperature values belonging to vitrinite reflectance values of 0.6 and 1.35% ($\Delta T_{R_1R_2}$) *vs.* the logarithm of the heating rate. This figures includes temperature differences, too, which were supplied by LOPATIN's various methods dor these same vitrinite reflectance values. It can be stated that — according to data of the geosystems published by Dow — the difference of the isometamorphic temperature values is a function of the heating rate. Therefore, solution 2) of chosing the temperature factors stands nearer to the description of the behaviour of geosystems published by Dow; in this case, the process of the vitrinite transformation can be better approached by assuming an activation energy that does not depend on the temperature. In the geosystem published by Dow, the methods are more suitable for estimating vitrinite reflectance which select the temperature factors in a way so that their change by 10 °C should decrease with

TABLE 3

Isometamorphic temperature values of the geosystem published by DOW (1978)

ξ (°C/million years)	Temperature (°C)		Temperature difference (°C) ΔT_{R1R2}
	$R = 0.6\%$	$R = 1.35\%$	
0.64	84	118	34
1.34	97	137	40
2.76	113	164	51
5.59	131	198	67
10.3	143	221	78
29.0	164	257	93

the increase in the temperature. Such a method is LOPATIN's calculation method published in 1976. The methods suitable to solution 1) [LOPATIN, 1971; KARPOV, 1975 and WAPLES, 1980] seem to be less appropriate for describing the behaviour of geosystems published by DOW. Checking of this statement appears to be expedient on several geosystems having similar series of data to that published by DOW.

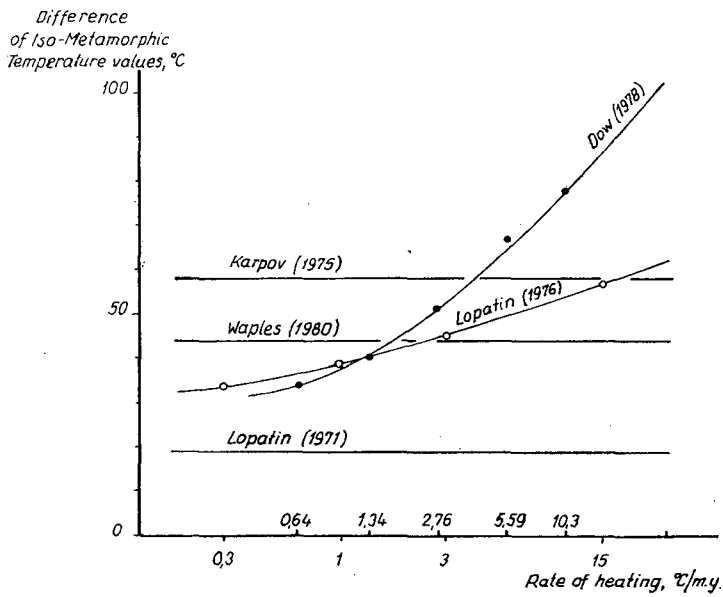

Fig. 9. Relationship between the difference of the isometamorphic temperature values belonging to the 0,6 and 1,35% reflectances and the logarithm of the heating rate

CONCLUSIONS

Based upon a comparison and critical evaluation of LOPATIN's methods, the following can be said:

1) The correct relationship between the vitrinite reflectance and the time-temperature index, in a vitrinite reflectance range of 0.6 to 2.0% that is important for hydrocarbon formation, is of the following type:

$$\lg R = (\text{constant}) \cdot \lg(\text{TTI}) + (\text{constant})$$

The relationships of this type correspond to LOPATIN's [1976], KARPOV's [1975] and WAPLES' methods [1980]. LOPATIN's method [1971] according to which there is a linear relationship between the vitrinite reflectance and the logarithm of the time-temperature index, is not acceptable. A farther modification of the latter method underlines this statement. The modified version is of identical type to the relationship published above.

2) Starting from the surface value of the vitrinite reflectance (0.19 %), there is a linear relation between the logarithm of the vitrinite reflectance increment and that of the time-temperature index throughout the full range of the vitrinite reflectance:

$$\lg \Delta R = (\text{constant}) \cdot \lg(\text{TTI}) + (\text{constant}).$$

3) The linear relationship between the logarithm of the vitrinite reflectance and that of the time-temperature index is valid from vitrinite reflectance values ranging from 0.6% to 2.0%. For the range important for hydrocarbon genesis (0.6—2.0%), the logarithm of the vitrinite reflectance increment and that of the vitrinite reflectance can be linearized by using the following relationship:

$$\lg \Delta R = 1.2506 \lg R - 0.1032.$$

4) For the description of the behaviour of the geosystem published by DOW, the temperature factors of LOPATIN's method [1976] are more suitable. The methods [LOPATIN, 1971; KARPOV, 1975 and WAPLES, 1980] assuming the constancy of the change of reaction rate, i. e. the doubling of it by 10 °C, and, as a result of this, the change of the activation energy *vs.* temperature, are less suitable for describing the actual behaviour of the geosystem published by DOW. The decrease of the constant activation energy independent of temperature, and, as a result of this, the decrease of the reaction rate change with the increase in temperature, as reaction kinetic considerations, are more appropriate to describe the geosystem published by DOW. The outcomes of this can be summarized in the following way for geoconditions that do not change with the time:

4.1. For the relationship between the vitrinite reflectance and the actual temperature:

$$\lg R = -(\text{constant}) \cdot \frac{1}{T} + (\text{constant}).$$

4.2. For the relationship between the vitrinite reflectance and the actual depth:

$$\lg R = -(\text{constant}) f\left(\frac{1}{Z}\right) + (\text{constant})$$

4.3. For the relationship between the temperature (isometamorphic temperature) necessary for reaching the identical vitrinite reflectance values and the heating rate:

$$\lg \xi = -(\text{constant}) \cdot \frac{1}{T} + (\text{constant})$$

As for the isometamorphic temperature, the relationship used by CONNAN (1974) which uses the geological time instead of the heating rate cannot be considered as correct. As a matter of fact, the relationship of the above form is not valid between

the geological time and the isometamorphic temperature but between the heating rate and the isometamorphic temperature.

The statements published in this paper relate to reaction kinetic considerations used in LOPATIN's methods as well as to the character of the correlation equation (relationship R (TTI) and to the limits of its validity, but they do not include the constants of the correlation equation which, because of the lack of knowledge about the absolute reaction rate belonging to the reference temperature, follow from the comparison with parameters measured deriving from the geosystems. The necessity of this correlation backs up the importance of the thermohistorical reconstruction of the geosystems serving as a basis for the comparison in creating generally applicable methods that can be used for vitrinite reflectance estimations.

REFERENCES

BOSTICK, N. H. [1973]: Time as a factor in thermal metamorphism of phytoclasts. Congres International de Stratigraphie et de Geologie du Carbonifere Septieme, Krefeld, Aug. 23—28, 1971., Compte Rendu **2,** 183—193.

CONNAN, J. [1974]: Time-temperature relation in oil genesis. Amer. Ass. Petr. Geol. Bull., **58,** 2516—2521.

DOW, W. G. [1977]: Kerogen studies and geological interpretations, Jour. Geochem. Exploration **7,** 79—99.

DOW,W. G. [1978]: Petroleum source beds on continental slopes and rises. Amer. Ass. Petr. Geol. Bull., **62,** 9. 1584—1606.

GOLITSYN, M. V. [1973]: The duration of the process of coal metamorphism (in Russian), Akad. Nauk USSR Izv. Ser. Geol., **8,** 90—97.

HUCK, G. and KARWEIL, J. [1955]: Physikalisch-chemische Probleme der Inkohlung. Brennstoff-Chemie **36, 1,** 1—11.

KARPOV, P. A., *et al.* [1975]: Quatitative evaluation of temperature and geologic time as factors in the coalification of dispersed coaly remains and possibility of its application to petroleum geology. (in Russian), Akad. Nauk SSSR, Izv. Ser. Geol., **3,** 103—113.

KARWEIL, J. [1956]: Die Metamorphose der Kohlen vom Standpunkt der physikalischen Chemie. Dtsch. geol. Ges., **107,** 132—139.

KÖTTER, K. [1960]: Die mikroskopische Reflexionmessung mit dem Photomultiplier und ihre Anwendung auf die Kohlenuntersuchung. Brennstoff-Chemie **41,** 9, 263—271.

LOPATIN, N. V. [1971]: Temperature and geologic time as factors in coalification. (in Russian), Akad. Nauk SSSR Izv. Ser. Geol., **3,** 95—106.

LOPATIN, N. V. [1976]: Historico-genetic analysis of petroleum generation: application of a model of uniform continuous subsidence of the oil-source bed. (in Russian), Akad. Nauk SSSR, Izv. Ser. Geol., 8, 93—101.

SNOWDON, L. R. [1979]: Errors in extrapolation of experimental kinetic parameters to organic geochemical systems. Amer. Ass. Petr. Geol. Bull., **63, 7,** 1128—1130.

TEICHMÜLLER, M. [1971]: Anwendung Kohlen-petrographischer Methoden bei der Erdöl- und Erdgasprospektion. Erdöl u. Kohle **24,** 2, 69—76.

WAPLES, D. W. [1980]: Time and temperature in petroleum formation: application of Lopatin's method to petroleum exploration. Amer. Ass. Petr. Geol. Bull., **64,** 6, 916—926.

Manuscript received, 15 November, 1982

J. KONCZ
Hungarian Hydrocarbon Institute
Section for Geochemistry
H-8801 Nagykanizsa, Vár u. 8.
Hungary

Acta Mineralogica-Petrographica, Szeged, XXVI/1, 73—85, 1983

EXPERIMENTAL EVOLUTION OF OIL SHALES AND KEROGENS ISOLATED FROM THEM

M. HETÉNYI

INTRODUCTION

Nowadays it is generally accepted that petroleum is a product of the evolution of kerogen finely dispersed in sedimentary rocks. The quality of the products depends first of all on the type and chemical composition of kerogen. The most important quantitative feature, i. e. the genetic potential of the evolution process is also determined by the type of kerogen. To answer the question that up to the given date how the genetic potential has been realized, the indices of evolution level of the organic matter are suitable. The evolution level of the organic matter is influenced first of all by the thermal history of sediments including the kerogen, by the geological time as well as by the temperature and pressure. It is of high probability that in addition to the factors listed above the mineral matrix affects both the quantity of the degradation products and their quality. This effect should be taken into account already because of the significance of the inorganic/organic matter ratio, since in all sediments containing organic matter and even in the oil shales being of extreme composition from this point of view, the quantity of the mineral components is several times higher than that of the organic matter. This mineral phase may be of rather varied composition, further even in case of one mineral both the catalytic and retention effects can be presumed, as well. As it was stated by MONIN *et al.*, [1980]: "simulation of maturation by pyrolysis of organic matter in its mineral matrix can, some cases (low carbon content, active mineral matrices), lead to results which are more dificult to interpret."

The effect of mineral components is reflected also by the composition of the so-called lipid fractions extractable from sedimentary rocks, which may be very different depending on the relations of the fraction in question to the type of minerals. As to the investigations of SPIRO [1980] the fractions associated with clays are more aromatic and/or polar than those associated with carbonate minerals. Polar and aromatic compounds are preferentially adsorbed on clay and carbonate minerals. The aliphatic compounds are concentrated in the unadsorbed and therefore more labile fraction. As the lipid adsorption on mineral grains got a saturation level, no compositional discrimination takes place.

To elucidate the role of different mineral components in the oil and gas generation numerous laboratory experiments were carried out. A group of these experiments studied simple chemical compounds (e. g. fatty acids) in presence of clay minerals and carbonates [JURG and EISMA, 1964; SHIMOYAMA and JOHNS, 1972; ALMON and JOHNS, 1977]. In other pyrolysis experiments the kerogen was mixed with different matter: with industrial catalysts [URAND-SOURON *et al.*, 1982], with natural minerals [CONNAN, 1974; HORSFIELD and DOUGLAS, 1980; ERDMAN, 1981], further the prod-

ucts of the organic matter containing rocks and the products of artificial evolution of the kerogen isolated from these rocks, were compared [SPIRO, 1979; ESPITALIÉ *et al.*, 1980; HORSFIELD and DOUGLAS, 1980]. Most of the authors emphasized the catalytic effect of minerals, first of all of clay minerals in the oil generation. Nevertheless, this effect can be observed only at the suitable temperature. As to the results of the pyrolysis experiments of GIRAUD [1970] carried out at 280 °C, the catalytic effect of clay minerals is minimal, the composition of minerals associated with kerogen has no appreciable influence on the pyrolysis products. E. g. as to the statement of SPIRO [1979] the connection between kaolinite and organic matter can be realized in sedimentary rocks only after heating, i. e. due to the partial loss of the adsorbed water.

The catalytic effect of mineral components can be manifested in different manner. As a result of industrial catalysts admixed to kerogen the temperature of hydrocarbon generation was lowered by about 50 °C [DOURAND-SOURON, 1982]. The apparent activation energy values being low as compared to the literature data and to those calculated by CONNAN [1974] to the pyrolysis of the organic matter was attributed also to the catalytic effect of clay minerals. The catalytic effect of mineral components is reflected most obviously by the composition of the generated products. Usually, in the pyrolysate formed from pyrolized organic matter in presence of a mineral matrix the proportion of the compounds of lower molecular weight is less than in the pyrolysis products of the isolated kerogen. HORSFIELD and DOUGLAS [1980] believed that this is due to condensation and gasification of higher molecular weight constituents in the primary pyrolysate.

When comparing the pyrolyses of organic matter in its mineral matrix and of the kerogen isolated from the rock the retention effect of the mineral matrix can also be observed, and when mixing the kerogen with different minerals this effect can be verified by model experiments, as well [ESPITALIÉ *et al.*, 1980]. Due to the retention effect of the inorganic constituents less hydrocarbon can be produced from the rock sample than under the same conditions from the isolated kerogen.

Authors mentioned above called also the attention to the fact that the effect of the mineral matrix exerted on the oil generation depends on the type and quantity of the organic matter, in addition to the mineral composition. As to the observation of CONNAN [1974], in the main zone of oil generation the hydrocarbon generation is catalyzed also by the organic matter itself.

This paper aims to compare the evolution features of the high-grade oil shale and of the kerogen isolated from it, to analyze the possible reasons of differences by means of model experiments, and to throw light upon the relationships between the type of kerogen and the differences experienced during the thermal degradation in laboratory conditions of the oil shale and the isolated kerogen, respectively.

EXPERIMENTAL

Analytical methods

Experimental evolution was carried out between 300 and 500 °C under continuous N_2 flow. Products were collected on a trap cooled by air and by saline ice. The contents of the two traps were unified, the oil was separated from the water and the oil quantity was measured. The remained solid matter was extracted in Soxhlet extractor by benzene: acetone: methanole of 70:15:15 ratio. In this manner the bitumen fraction and the unconverted organic matter were separated.

The starting matter as well as the degradation products were characterized by the elementary composition. Rock-Eval pyrolysis, the CR/CT ratio, the C_{org} content and by the step-by-step oxidation by $KMnO_4$.

The measurement of H- and C-contents was carried out in the CHN—1 analysator.

The C_{org} content was determined at 1000 °C in oxygen flow by means of an instrument of Carmhograph—8 type.

The CR/CT ratio was measured after the ASTM-standard [CUMMINS *et al.*, 1972].

To characterize the type of organic matter and its evolution level the Rock-Eval pyrolysis was carried out [ESPITALIÉ *et al.*, 1977].

The determination of the chemical precursors of kerogen was carried out by step-by-step potassium permanganate oxidation [HETÉNYI *et al.*, 1978].

Description of the samples

The evolution experiments were carried out on maar-type Hungarian oil shales. The maar-type oil shales accumulated in a special environment, in the lake water developed in craters of basalt eruptions [JÁMBOR and SOLTI, 1975; BENCZE *et al.*, 1979]. These are Upper Pannonian formations of 3.05 to 5.34±0.93 my [JÁMBOR *et al.*, 1982]. The C_{org} content of the sample chosen from the maar-type oil shale of high-grade of Pula (Transdanubia, Hungary), amounts to 27.3% (sample is marked *A*). The kerogen isolated from it belongs to type I, its H/C atomic ratio is 1.7, the CR/CT ratio is less than 0.1. The organic matter consists mostly of alginite, the sample contains great amounts of remnants of the *Botryococcus braunii* alga. According to the pollen analyses the alga is well-preserved [HETÉNYI *et al.*, 1982]. The results of experimental evolution of the sample *A* and kerogen *A* were compared with the data of evolution of an other sample and kerogen (sample *B* and kerogen *B*) accumulated under similar geological conditions (Upper Pannonian, maar-type, locality: Várkesző (Transdanubia, Hungary). In case of the second sample the experimental conditions were the same. Dissimilarly to the sample *A* the sample *B* accumulated under conditions of higher biological activity. The algal remnants are more desctructed and besides them considerable amount of coalified plant remnants can be determined. The organic matter is heterogeneous, it is the mixture of kerogens of type I and II, and based on the results of all of the experiments, it is transitional between the two extreme character and seems to be of type II.

Both samples (*A* and *B*) contain immature organic matter referring to the zone of diagenesis. This is proved in both cases by the high H/C atomic ratios and by the low CR/CT ratios, as well as by the $S_2/S_3>5$ measured by Rock-Eval pyrolysis and by the T_{max} values (442 °C for sample *A* and 425 °C for sample *B*). The initial evolution level of the starting matter is indicated by the fact that by means of laboratory evolution nearly the complete evolution path can be construced.

The results of step-by-step oxidation of kerogens by basic potassium permanganate indicate that the organic matter was produced mostly from algal fatty acids [HETÉNYI *et al.*, 1979]. In sample *B* considerable amounts of humin matter was also admixed.

Results of experimental evolution

The products of experimental degradation of the kerogens of two different types (bitumen, oil and gas+water) are shown in Tables 1 and 2. As it is seen in *Fig. 1* the product distribution tendency plotted against the degradation temperature shows close correlation with the kerogen type. Much more oil and bitumen were

formed from the *A*-kerogen of type than from the *B*-kerogen of type II. Nevertheless, the remarkable hydrocarbon generation starts at $T \geqq 375$ °C in case of organic matter of type I, while at $T \leqq 350$ °C in case of the other. Based on the experimental evolu-

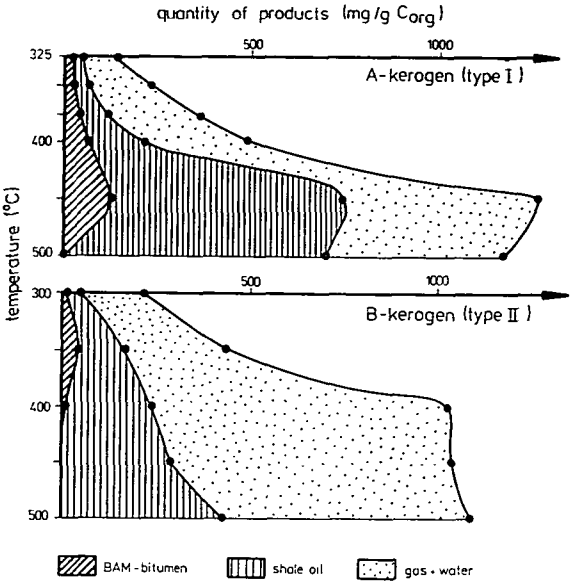

Fig. 1. Yields of pyrolysis of kerogens isolated from maar-type Hungarian oil shales
A-kerogen = a kerogen type I
B-kerogen = a kerogen type II

tion results of the studied kerogens the apparent activation energies calculated for the phase of catagenesis show considerable difference: 146 kJ/mol^{-1} and 75 kJ/mol^{-1} concerning the samples *A* and *B*, respectively. The difference of evolution features of the two kerogens is also demonstrated by the H/C atomic ratio of the unconverted kerogen, by the diagenesis coefficient as well as by the maturity values determined by Rock-Eval pyrolysis as a function of temperature (Tables 3 and 4). As it can be seen in *Fig. 2* the evolution paths obtained by the experimental evolution of the two kerogens also differ from each other. The differences in the evolution paths, in the distribution of products, in the features of the unconverted kerogen as well as in the apparent activation energies calculated for the catagenesis can be attributed to the differences between the types of the two organic matter.

When comparing the products of experimental evolution of the oil shales and of the kerogens isolated from them (Tables 1 and 5, 2 and 6) some difference can be observed between the sedimentary rock and the corresponding organic matter.

To study this problem in detail the sample *A* was chosen as a model. When comparing the tendencies of changes *(Fig. 3)* and emphasizing the shale oil as most important product from the economic point of view *(Fig. 4)* the following main differences can be observed:

— Regarding either the whole of the process, or taking the usual temperature of industrial conversion (450—500 °C) more oil is generated from kerogen than from the oil shale. (Data refer in all cases to 1 g organic carbon.)

TABLE 1

Pyrolysis of "A-kerogen" (type I) isolated from oil shale

Temperature (°C)	Period (hours)	Gas + water	Oil (mg/g organic carbon)	Bitumen
325	1	75	< 10	19
	5	86	28	21
	10	114	28	20
350	1	114	14	26
	5	177	37	30
	10	228	43	29
375	1	174	11	44
	5	246	67	51
	10	329	87	31
400	1	246	24	64
	2	245	83	86
	5	282	145	63
450	1	461	251	449
	2	522	413	339
	5	522	616	133
500	1	716	466	20
	2	641	541	29
	5	492	688	< 5

TABLE 2

Pyrolysis of "B-kerogen" (type II) isolated from oil shale

Temperature (°C)	Period (hours)	Gas + water	Oil (mg/g organic carbon)	Bitumen
200	5	76	—	56
300	5	269	35	14
350	5	264	131	38
400	5	793	226	12
450	5	745	289	< 5
500	5	669	426	< 5

— On the contrary, at lower temperatures more oil seems to be generated from the oil shale than from the kerogen.

— The maximum of the relationship between the quantities of degredation products and the degradation temperature occurs at lower temperature (400 °C) in case of the oil shale than in case of the kerogen isolated from it (450 °C).

The more intense oil production at lower temperature in presence of the mineral matrix can be explained on the one hand by the probable catalytic effect of the mineral matter, and by the degradation intermediary product, i. e. bitumen being present in the sediment and formed under natural conditions, on the other. The question may arise that the second phase of experimental evolution of the soluble organic matter, i. e. the bitumen to oil transformation would be able to modify the picture developed

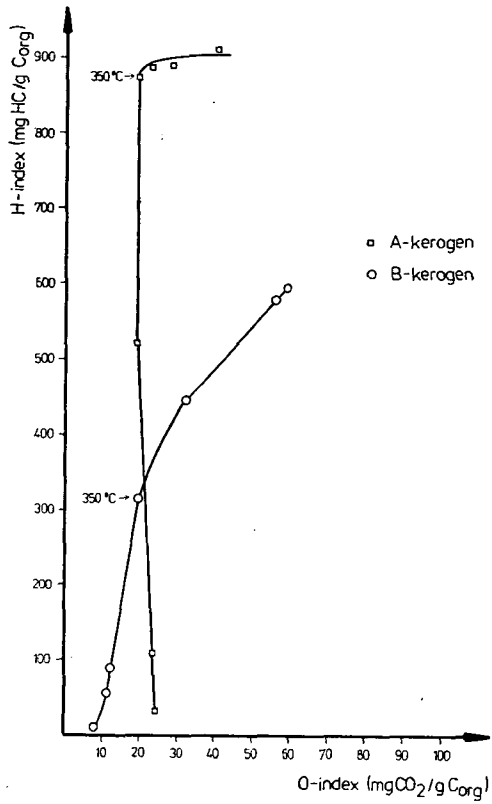

Fig. 7. Artificial evolution path of the kerogens (type I and II) isolated from maar-type Hungarian oil shales

TABLE 3

Characteristics of evolution level of unconverted "A-kerogen" at different temperature of laboratory pyrolysis

Temperature (°C)	Period (hours)	H/C atomic ratio	CR/CT	$\frac{PC}{TOC}$ (%)	T_{max} (°C)
Kerogen	—	1.70	<0.10	77	444
200	5	1.70	0.12	74	443
300	5	1.70	0.13	74	445
325	5	1.70	0.13	74	447
350	5	1.70	0.23	73	447
375	5	1.63	0.41	72	451
400	5	1.27	0.53	44	447
450	5	0.73	0.72	10	454
500	5	0.61	1.00	4	454

on the whole of evolution of the organic matter. In order to analyze the effect to be expected during pyrolysis, the soluble organic matter extracted in two phases from the oil shale *A* (chloroform extracted: Bit-A than solvent-mixture extracted: BAM-

TABLE 4

Characteristics of evolution level of unconverted "B-kerogen" at different temperature of laboratory pyrolysis

Temperature (°C)	Period (hours)	H/C atomic ratio	CR/CT	PC / TOC (%)	T_{max} (°C)
Kerogen	—	1.33	0.43	56	426
200	5	1.30	0.43	54	430
300	5	1.30	0.55	38	428
350	5	1.30	0.65	27	429
400	5	1.30	0.83	9	449
450	5	1.00	0.90	8	535
500	5	0.42	0.95	3	543

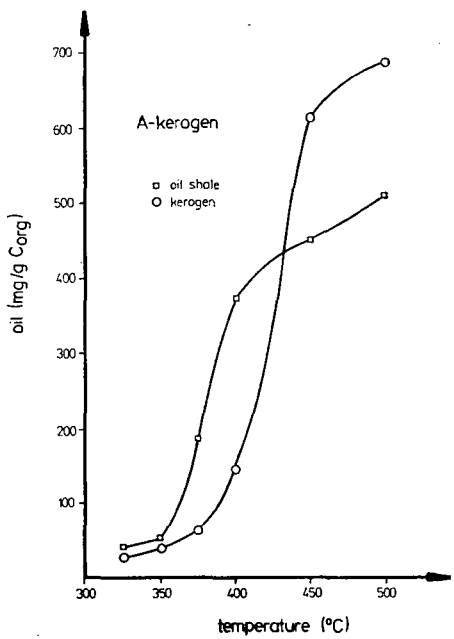

Fig. 3. Yields of pyrolysis of oil shale and kerogen isolated from the oil shale

bit.) was degraded under the same conditions as in case of degradation of the sediment and of the kerogen. The quantities of the generated oil and of the unconverted matter are shown in Table 7. Together with the corresponding data of the kerogen and oil shale the increase of oil production as a result of temperature increase of 25—50 °C are shown in *Fig. 5.* It is obvious from the figure that the measure of transformation of kerogen and of the bitumens differ from each other only at lower temperatures, later the conversion is nearly the same. The maximum can be observed in all cases at 450 °C where the bitumen conversion is nearly complete, the quantity of the unconverted matter is low. The reason of the different conversion of bitumen

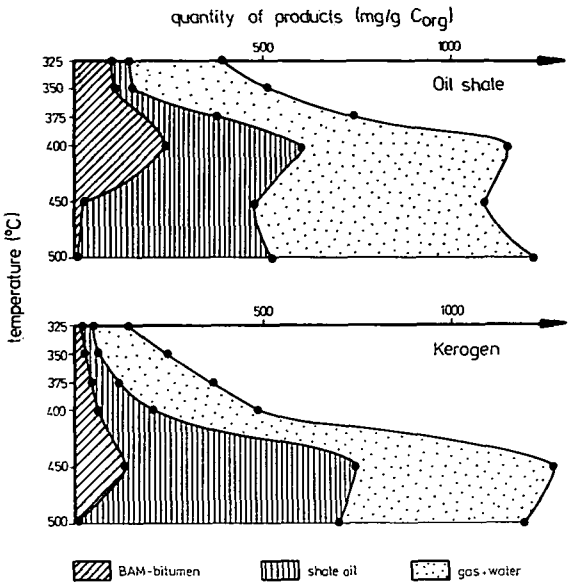

Fig. 4. Oil yielded by the artificial evolution of the Hungarian oil shale and kerogen (type I) isolated from the oil shale

TABLE 5

Pyrolysis of "A-oil shale" (Hungary, Pula)

Temperature (°C)	Period (hours)	Gas + water	Oil (mg/g organic carbon)	Bitumen
300	48	297	33	51
	96	410	33	18
	336	469	44	18
325	5	289	40	106
	10	289	40	88
	24	304	62	88
350	1	297	33	132
	5	352	51	110
	10	487	99	103
375	1	297	70	121
	5	363	187	194
	10	414	245	158
400	1	443	216	271
	5	542	374	234
	10	498	418	73
450	1	711	168	70
	2	810	216	33
	5	615	447	26
500	1	619	443	59
	2	667	542	15
	5	696	513	11

and kerogen at lower temperatures is probably the fact that in spite of all the structural similarity, the bitumen is of much simpler structure.

Thus, the activation energy needed to the subsequent transformation of bitumen is much lower, consequently, a part of the bitumen is able to transform into oil at relatively low temperature. At the same time, the conversion of the complex polymer, i. e. of the kerogen needs higher energy, especially in case of the strongly polymerized kerogen of type I. Probably, on that account a greater quantity of shale oil is generated from the oil shale at $T \leqq 400$ °C than from the kerogen isolated from it. This presumption seems to be verified by the fact that in the same temperature range nearly the same quantities of oil were generated from the kerogen *B* of type II and from the oil shale *B* (Tables 2 and 6). In the main zone of oil generation the apparent activation energy of kerogen *B* is 75 $kJmol^{-1}$, which is about the half of that of the kerogen *A* (146 $kJmol^{-1}$). Consequently, in case of kerogen *B* the lower temperature provides the suitable activation energy to the oil generation from kerogen by thermal degradation.

The catalytic effect of the mineral matrix is probably the other reason of the difference between the oil generations of the oil shale and kerogen *A* at $T \leqq 400$ °C.

TABLE 6

Pyrolysis of "B oil shale" (Hungary, Várkesző)

Temperature (°C)	Period (hours)	Gas + water	Oil (mg/g organic carbon)	Bitumen
350	1	791	67	60
	5	776	119	276
	10	791	127	216
400	1	955	201	246
	5	1067	201	149
	10	978	224	97
500	1	1261	231	15
	2	1313	254	<5
	5	1299	269	<5

TABLE 7

Oil and unconverted matter (M) yielded by pyrolysis of bitumens extracted from "A oil shale" (Hungary, Pula)
(Degradation period = 5 hours)

Temperature (°C)	Degradation of Bit – A oil (mg/g C_{org})	M (%)	Degradation of BAM – bit. oil (mg/g C_{org})	M (%)
200	5.0	96	<5.0	94
300	53.5	87	39.9	87
325	122.1	81	81.5	80
350	246.9	75	188.8	73
375	370.4	55	287.9	55
400	507.5	37	399.4	45
450	932,8	4	881.5	12
500	960.2	4	852.9	6

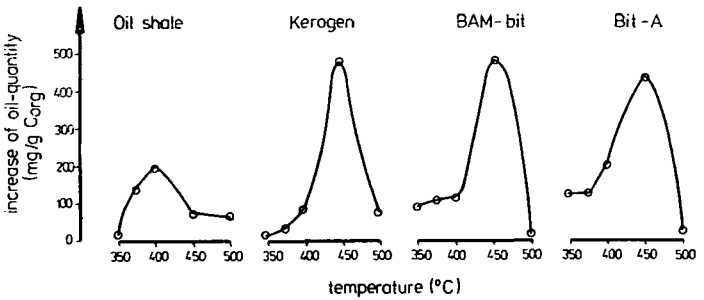

Fig. 5. Change in the oil quantity resulting by the rise of the temperature in the course of the artificial evolution

As a result of the catalytic effect too, the degradation proceeds at somewhat lower temperature in presence of the mineral matrix. This latter phenomenon can be observed in case of sample *A* containing of kerogen of type I of higher activation energy *(Fig. 3)*.

Nevertheless, in addition to the catalytic effect of the mineral components, their retention effect should also be taken into account due to the well-known high ad-

TABLE 8

Pyrolysis of mixture of "A-kerogen" and montmorillonite

Temperature (°C)	Period (hours)	Montmorillonite (%)	Bitumen (mg/g organic carbon)	Oil
375	1	0	44	11
		10	44	24
		50	55	17
		90	84	<5
	2	0	44	63
		10	42	61
		50	60	50
		90	94	26
	5	0	51	61
		10	51	67
		50	63	57
		90	98	28
500	1	0	20	466
		10	21	624
		50	33	463
		90	47	446
	2	0	29	541
		10	29	667
		50	30	533
		90	47	497
	5	0	<5	688
		10	<5	751
		50	<5	660
		90	13	627

sorption capacity of some minerals (e. g. clay minerals). The fact that what of the two opposite effects can be observed, depends on numerous conditions. The quality of the mineral component, the type of the organic matter, the ratio of the inorganic and organic phases as well as the degradation conditions (e. g. degradation temperature, time etc.) may control this dependence. The retention effect can be observed e. g. in the whole temperature range in case of sample *B*. In case of the sample *A*, however, the retention can be demonstrated only at higher remperatures where the rate of transformation of the organic matter is high enough.

In order to study the effect of the mineral components in detail, model experiments were carried out. The kerogen *A* and its mixture with montmorillonite of 9:1, 1:1, 1:9 ratio were degraded. The quantities of the generated bitumen and oil referring to unit organic carbon are shown in Table 8. It is obvious from the data that parallel with increasing montmorillonite quantity, the quantity of extractable bitumen gradually increased at both temperatures. Simultaneously, the decrease of oil quantity can also be observed indicating the fact that the retention effect of montmorillonite retards the transformation of the heavier components by retaining the bitumen, thus decreasing the quantity of the generating oil, as well. The mineral phase of low concentration as compared to that of the organic matter seems to promote the oil generation. In presence of montmorillonite of 10% usually more oil is generated from the unit organic carbon than from the pure kerogen, though the bitumen quantity remains constant.

SUMMARY

To compare the evolution features of the sedimentary rock of organic matter content and of the kerogen isolated from it experimental pyrolysis was carried out.

Samples used in the experiments are Hungarian so-called maar-type oil shales containing immature kerogen. The immaturity of the organic matter provided the possibility to construct the complete evolution paths on the basis of the results of thermal degradation.

To study the catalytic effect presumed for the mineral matrix kerogen of type I was chosen as raw material of the experiments which can be less activated than the kerogens of type II and III. Thus, the activation energy needed for the main hydrocarbon generation can be assured at higher temperature. Due to the catalytic effect of the mineral matrix greater difference can be expected at lower temperatures between the oil generation of the oil shale and the kerogen isolated from it. The apparent activation energy of the kerogen *A* calculated after the degradation experiments is 146 $kJmol^{-1}$ in the zone of catagenesis.

The results obtained for the experimental evolution of kerogen *A* and of oil shale *A* were compared with those obtained from the kerogen of type II of the maar-type oil shale *B*. The apparent activation energy of kerogen *B* is 75 $kJmol^{-1}$, i. e. about the half of the value calculated for kerogen *A*.

When comparing the oil quantities obtained by the experimental degradation of oil shales and kerogens isolated from them, two temperature ranges can be distinguished: lower and higher temperatures than 400 °C.

At lower temperature ($T \leqq 400$ °C) where only insignificant quantities of oil were generated from the kerogen *A*, considerable oil generation could be observed when pyrolizing this kerogen in its mineral matrix. This difference can be attributed partly to the catalytic effect of the mineral matrix, partly to the bitumen existing in the rock.

To analyze the catalytic effect of the mineral matrix model experiments were carried out. Kerogen was mixed with montmorillonite in different proportions. The montmorillonite of low concentration as compared to the organic matter seemed to catalyze the oil generation.

To get acquainted with the evolution features of the bitumen which can be regarded as intermediary product of degradation, experimental evolution was carried out on the bitumen extracted from the oil shale *A*. Considerable difference could be detected between the evolution features of kerogen and of the bitumen just in the afore-mentioned temperature range of $T \leqq 400\,°C$. The conversion rate of bitumen representing the smaller structural units of kerogen proved to be remarkable also at lower temperature.

The two factors, i. e. the catalytic effect of the mineral matrix and the considerable conversion of bitumen into oil at lower temperature, may be responsible for the act that the degradation processes followed at about 50 °C lower in case of the oil shale *A* than in case of the kerogen isolated from it.

According to the results of the experimental evolution of the kerogen *B* of type II and oil shale *B* which can be more easily activated in themselves, the difference mentioned above could not be observed.

In the main zone of hydrocarbon generation greater quantity of oil could be produced from kerogen than from the corresponding oil shale in the course of evolution experiments. In the degradation experiments carried out with the mixture of kerogen and montmorillonite the retention effect of montmorillonite could be detected. Parallel with increasing proportion of montmorillonite the quantity of the products in form of oil decreased. Simultaneously, the quantity of the degradation intermediary product which can be isolated in form of bitumen, gradually increased.

REFERENCES

BENCZE, G., JÁMBOR, Á., PARTÉNYI, Z. [1979]: A Várkesző és Malomsok környéki alginit- (olajpala) és bentonitkutatások eredményei. A Magyar Állami Földtani Intézet Évi Jelentése az 1977. évről. Műszaki Könyvkiadó, Budapest, 257—268.

CONNAN, J. [1974]: Time-temperature relation in oil genesis. Am. Assoc. Petr. Geol. Bull., **58,** 2516—2521.

CUMMINS, J. J. and ROBINSON, W. E. [1972]: Thermal degradation of Green River kerogen at 150° to 350 °C. U. S. Bur. Mines. Rep. Invest. **7620,** 15.

DURAND-SOURON, C., BOULET, R. and DURAND, B. [1982]: Formation of methane and hydrocarbons by pyrolysis of immature kerogens. Geochim. et Cosmochim. Acta, **46/7,** 1193—1202.

ERDMAN, J. G. [1981]: Petroleum exploration, present and future. In: Origin and chemistry of petroleum, ed. by G. ATKINSON and J. J. ZUCKERMAN, Pergamon Press, 89—111.

ESPITALIÉ, J., MADEC, M. and TISSOT, B. [1977]: Source rock characterization method for petroleum exploration. Offshore Technology Conference.

ESPITALIÉ, J., MADEC, M. and TISSOT, B. [1980]: Role of mineral matrix in kerogen pyrolysis: influence on petroleum generation and migration. Am. Assoc. Petr. Geol. Bull., **64,** 59—66.

GIRAUD, A. [1970]: Application of pyrolysis and gas chromatography to geochemical characterization of kerogen in sedimentary rock. Am. Assoc. Petr. Geol. Bull., **54,** 439—455.

HETÉNYI, M. and SIROKMÁN, K. [1978]: Structural information on kerogen from the Hungarian oil shale. Acta Miner. Petr., Szeged XXII/2. 211—222.

HETÉNYI, M. [1979]: Thermal degradation of the oil shale kerogen of Pula (Hungary) at 473 at 573 K. Acta Miner. Petr., Szeged XXIV/1, 99—111.

HETÉNYI, M. [1980]: Thermal degradation of the organic matter of oil shale of Pula (Hungary) at 573—773 K. Acta Miner. Petr., Szeged XXIV/2, 301—314.

HETÉNYI, M., TÓTH, J. and MILLEY, Gy. [1982]: On the role of temperature and pressure in the artificial evolution of organic matter of the Pula oil shale (Hungary). Acta Miner. Petr. Szeged XXV/2, 131—146.

HORSFIELD, B. and DOUGLAS, A. G. [1980]: The influence of minerals on the pyrolysis of kerogens. Geochim. et Cosmochim. Acta **44,** 1119—1131.

JÁMBOR, Á., SOLTI, G. [1975]: Geological conditions of the Upper Pannonian oil-shale deposit recovered in the Balaton Highland and at Kemeneshát. Acta Miner. Petr. Szeged XXII, 9–28.
JÁMBOR, Á., RAVASZ, Cs. and SOLTI, G. [1982]: Geological and lithological characteristics of oil shale deposits in Hungary. 3rd All. Union Meeting on the Geochemistry of Oil Shales, Tallinn.
SPIRO, B. [1979]: Thermal effects in "oil shales" — naturally occurring kaolinite and metakaolinite organic associations. Chemical Geology **25**, 67—78.
SPIRO, B. [1980]: Preferential lipid-mineral associations in some "oil shales". Chemical Geology **31**/1—2, 27—35.

Manuscript received July 7, 1983

M. HETÉNYI
Institute of Mineralogy, Geochemistry
and Petrography
Attila József University
H-6701 Szeged, Pf. 651.
Hungary

Acta Mineralogica-Petrographica, Szeged, XXVI/1, 87–97, 1983

THE GENETIC FRAMEWORK OF THE RECSK ORE GENESIS

Cs. Baksa

ABSTRACT

Many authors have dealt with the massive and stockwork gold-silver-copper-pyrite deposit at Recsk since the 1850's when the production from these deposits began. However, several points of genesis and relationships of this relatively unique mineralization have remained unrevealed. Many of the conclusions, which based solely on field data, have since outdated. In the last two decades intense exploration activities, both drilling and underground developments, have provided several new recognitions, which served as basis for a new genetic approach. These were first summarized in a special volume of the Földtani Közlöny [1975], by J. Cseh-Németh, T. Zelenka, J. Csillag, J. Földessy, K. Földessy—Járányi, and the author. Some of these conclusions have been modified or supplemented with new data in the last years. Conclusions were drawn about the setting of this occurrence in the Eocene island arc, which could be traced in SW-NE direction across the Carpathian basin [Csillag *et al.*, 1980]. Similar complexes of slightly different ages are known elsewhere in the Carpathian-Balkan region (Timok, Vardar-zone). The localisation and spatial arrangement of this deposits can be related to the plate convergence-styles through the late Mezozoic-Paleogene period [Hadži *et al.*, 1977]. Evidences were drawn about the young age of the Darno-zone [Balla *et al.*, 1982], which have questioned the earlier concepts about the Triassic formations at Recsk being part of the Central-Mountain Belt [Wein, 1969, 1978]. The Eocene Priabonian magmatism followed multiple tectonic deformation, which produced folding and fault-systems. Synchronous sedimentation (with fossiles of Nummulites fabianii stage) and Rb/Sr dates igneous rocks of $35{,}7 \pm 2-5$ m. y. [Balogh, 1975] provided reliable age determination for the mineralization. The multiple phase igneous complex includes diorite-porphyries and andesites. This suite (the Recsk Andesite Formation) is comparable with the dioritic magmatism of eusyncline belts. The ore mineralization is related to the igneous emplacement following the first submarine, volcanic phase. Alteration and mineralization zoning resembles to the diorite-model of Hollister [1978]. In the system of Krivtzov and Pavlova [1978] it is related to the eusyncline belt diorites. The succesive phases of hydrothermal mineralizations (Cu—Fe—Pb—Zn) were developed both in time and space in the order of the decreasing rate of heat flux from the peripheries toward the centre of the intrusion, and from the early peripheral metasomatic replacement and skarn deposits toward the latest central porphyry copper. A part of these ore were rejuvenated in the consequent magmatic pulses, and brought about the formation of smaller near-surface mineralization in the volcanic superstructure. Though the Cu and Mo contents within the porphyry mineralization does not correlate, the metal content contours correspond well with the geometry of the intrusion, hence, it can be considered as conformable. This arrangement is partly due to the localization characteristics, beneath the stratovolcanic pile.

INTRODUCTION

More than 130 years have elapsed since the exploration and mining commenced in the Recsk ore district. Numerous studies, papers dealing with several genetic aspects of the Recsk and Parádfürdő ore occurrences have been published in this period. Many of the ideas and suggestions have successfully survived the changes of principles and theories and contributed to the understanding of the geological setting of Recsk in the Carpathian basin. Pálfy [1929], Rozlozsnik [1939], Sztrókay [1940]; Pantó [1951, 1952], Kisvarsányi [1955], Varók, [1962], Török [1963], Vidacs [1958,

1966] and several other workers provided us valuable genetic conclusions based on the data of available surface and underground outcrops, before the deep – explorations begun. A new chapter in the history of Recsk explorations opened in 1958 with the deep drilling explorations, the results of which were summarized in 1975.

ZELENKA [1975] has interpreted the tectonic and igneous events, CSEH – NÉMETH [1975] the features and processes of mineralization, complemented by CSONGRÁDI's [1975] investigation of ore-mineralogy. FÖLDESSY [1975] and BAKSA [1975b] summarized the petrological characteristics of the volcanic and intrusive rocks, respectively. Hydrothermal alterations and skarn formation was discussed by CSILLAG [1975]. The stratigraphic and lithologic character of the sedimentary wall-rock was reviewed by K. FÖLDESSY – JÁRÁNYI [1975].

The common point in genetic interpretation of these papers was the acceptance of the theory of relationship between the igneous activity and the repeatedly activated Darnó megastructural zone [ZELENKA, 1973, 1974]. This idea was reflected by the paleographic reconstructions, suggesting the genetic link of the different mineralizations with the Eocene Priabonian tectonic evolution along this zone. This Darnó-zone is merging with the Balaton – line southeastward. Several other volcanic areas are known along this line, among others at the NE-part of the Velence Mountains, where the igneous complex shows age relations and chemistry similar to Recsk. All of these occurrences are situated on the northern boundary of the Igal-Bükk eusyncline [WEIN, 1969, 1978], in the Central-Mountains belt, and include similar mineralizations, ore indications.

An updated synthesis of this volcanic belt was given by CSILLAG and others [1980], who postulated the uniform island arc nature of these Paleogene volcanic occurrences. This volcanic arc and other earlier volcanic zones in the Carpathian-system (Banat—Timok area, Vardar-zone) can be interpreted uniformly, based on the changes of convergence styles of the Africa plate, European plate and the several microplates between them [HADŽI *et al.*, 1977]. This also explains the similar mineralization and petrologic features of these deposits, and the relative age differences.

PORPHYRY COPPER GENETIC MODELS

The thorough investigations of porphyry copper mineralizations and their plate-tectonic interpretations have simultaneously advanced. LOWELL and GUILBERT's model [1970] was followed by SILLITOE's [1972] plate-tectonic hypothesis, and HOLLISTER's [1978] comprehensive study on the geological features of porphyry copper, the studies of KRIVTZOV [1977, 1978], POPOV [1977] and others.

The model of GUILBERT and LOWELL [1970] describes the alteration and mineralization zoning patterns of porphyry mineralizations in quartz-monzonitic intrusions of the Pacific-belt. Differences and variations on other regions gave rise to the diorite-model suggested by HOLLISTER [1978], which describes the zonation pattern related to more basic intrusive environments.

KRIVTZOV [1977] has given a different classification for the porphyry mineralizations with varying petrology and chemistry:

epicratonic belt	— granite porphyry
epi-miosyncline belt	— monzonite porphyry, quartz monzonite
epi-eusyncline belt	— Na-granodiorite-porphyry phonolite-porphyry
eusyncline belt	— diorite porphyry, granodiorite porphyry.

KRIVTZOV and PAVLOVA [1978] has suggested a direct relationship between the zonation pattern of deposits and their geotectonic setting:

epicratonic belt	– K-feldspar, quartz – sericite, propylitic
epi-miosyncline belt	– K-feldspar, quartz – sericite, argillic, propylitic
epi-eusyncline belt	– quartz-sericite, argillic, propylitic
eusyncline belt	– quartz-sericite, (biotite), argillic, propylitic

zones are typical outward from the centre of the intrusion. Common minerals are the anhydrite, gypsum (almost typomorph phases) and the zeolites.

Both SILLITOE [1977], KRIVTZOV and IUGHIN [1976], and NAKOVNHIK [1968] has emphasized the importance of the advanced argillic alteration (secondary quartzite in the Russian terminology) in the lithocap region, wich is characterised by the presence of arsenic minerals and native sulphur, may indicate hidden porphyry mineralization (Recsk, Lahóca), and sometimes hosts mineralization itself.

A different problem is the question of breccia pipes, which frequently occur above intrusions in certain occurrences. According to KRIVTZOV [1977] they lack in the eusyncline belts and become increasingly abundant towards the epicratonic zone.

The mineralogical aspects of these theories will be discussed in the following sections.

THE GENETIC MODEL OF THE RECSK DEPOSIT

Recently several new aspects were revealed concerning the relationship of the Darnó-zone tectonic evolution and the Recsk ore deposition [BALLA *et al.*, 1980, 1981, 1982 and in press]. Field observations on the SW-part of the Bükk-Mts, at the Darnó-area and evaluations of drill-longs at Recsk has questioned the earlier theories about the links of the Central-Mountain-belt and the Recsk basement. The Mesozoic rocks at Recsk have found to be similarly overturned and folded, and shown similar lithological properties as the Mesozoic on the SE-side of the Darnó zone. Thus ZELENKA and co-workers (in press) have concluded that the Darnó-zone was not a paleographic boundary in the Mesozoic period, as was previously stated.

The Priabonian igneous activity was preceded by tectonic deformations (folding, horst structure) [ZELENKA, 1973, 1974, 1975] of the Triassic basement. The igneous activity was accompanied by marine transgression. The intrusive and effusive activity is centered on the horst structure. On both sides of these horst there are different basement lithologies, which now can be explained by pre-magmatic folding and faulting. This difference has later played an important role during the hydrothermal processes, since limestone dominates on the western side, while less reactive quarzite (siltstone) is the dominant lithology on the eastern contact zone of the intrusion.

The different stages of the evolution history is discussed and illustrated on *Figs. 1—10*. On these several data are plotted to enhance understanding, thus not all of them is cited in the text.

The age of the igneous activity can be quite accurately identified by both stratigraphic and radiometric data. The limestones and marls beneath and an top of the volcanic sequence belong to the *Nummulites fabianii horizon* of the Priabonian stage [BÁRDI, 1970]. The K/Ar radiometric age of the relatively fresh andesites of the Recsk Andesite Formation falls in the 34.9—35.7 (±2.5—4.9) m. y. range [BALOGH *et al.*, 1975].

The first volcanic products are the submarine effusive (to less extent explosive) a_2-type andesites, which deposited on the Triassic basement or earlier Priabonian sediments around the uplifted horst *(Fig. 1)*, filling up the peripheral subsidences.

The a_2 andesites are barren, no hydrothermal post-volcanic activity is linked to this stage, the ore indications in these volcanies are later products. The effusive centre of the a_2 andesites is not known, only the extension of the volcanics can be contoured.

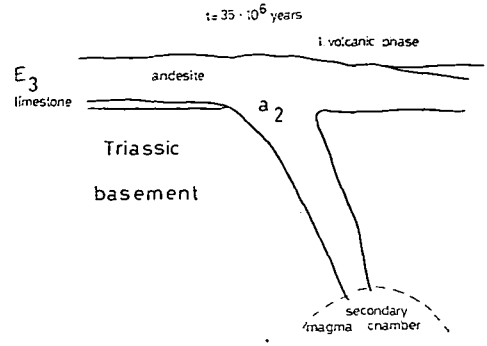

Fig. 1. The first phase of the Priabonian biotite—amphibole-andesite volcanism, intruding through and accumulating on the Triassic basement

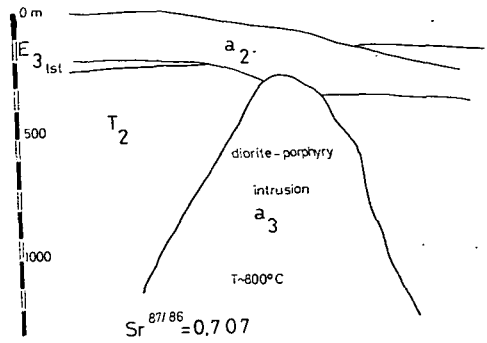

Fig. 2. Idealized section of the diorite porphyry intrusion ascending from the secondary magma chamber during the second magmatic cycle

This coincides with the position of the diorite-porphyry intrusion, which comprise the second magmatic phase *(Fig. 2)*. It thus can be concluded, that the a_3-type diorite—porphyry stock has emplaced by the partial or total destruction of the secondary magma chamber and vents of the a_2 effusives, and accompanied by the assimilation of equal volume of the Triassic host rocks. The intrusive body is 3 km long and 600—800 m wide, with an elongated shape in N—S direction, following the morphology of the uplifted basement horst. The intrusive body has complex lithology. Now only the first stage mineralized intrusives are discussed, the later, mostly barren phases are not dealt with in details, only their roles is mentioned in the appropriate sections. These later intrusives cut through the developed ore-bodies, remobilizing parts of their metal content. Upper mantle derivation is indicated for the first stage a_3-type intrusion by the Sr^{87}/Sr^{86} isotope ratios [KOVÁCS, 1972, ZELENKA, 1975]. The chemistry, petrology and setting of these intrusives [BAKSA, 1975] is better reflected by the diorite-porphyry term, than the earlier subvolcanic andesite, which was used for practical reasons. This rock-type is the most important source-rock and

host-rock of all types of mineralizations in the occurrence. As a melt, it contained almost all of the elements which generated and maintained the hydrothermal physicochemical systems resulting in the ore precipitations during cooling. The chemical and lithological properties of the intrusives are similar to the diorite-porphyries of eusyncline belts [KRIVTZOV, 1968]. This is in agreement with environment described in the island-arc reconstruction by CSILLAG *et al.*, [1980]. Thus these characteristics, and mineralogical parameters link Recsk occurrence to the diorite-model [HOLLISTER, 1978].

The Triassic wall-rocks were both mechanically and chemically affected during the a_3 intrusive emplacement. Due to the destruction by later processes, only scarce data are available for the alteration synchronous with the emplacement. The typical hornfelses are not abundant. The mechanical movements within and adjacent to the intrusion, which created the fracturization necessary for the flow of later hydrothermal systems, are related to the cooling history of the system below 800 °C. Local tectonic stress fields develop by the conversion of heat to mechanical energy, which produce zones of tension, microfissurization and brecciation. These zones provide favourable loci of alteration and mineralization. Among others LAUMULIN [1961] has dealt with the „crystallization shrinkage" of igneous melts. He suggested initial increase of volume in wall rocks during the emplacement, and shrinkage, dilatation in the contacts and lithocap of the intrusion, as well as in the adjoining wall rocks. The development of fracturization typically follows the crystallization.

OSIPOV [1974, 1978] has suggested the maximum of this volumetric shrinkage in the apical portion of stocks, creating paraboloid shaped voids, which later collapse and brecciated apical zones develop, sometimes in significant sizes. Analogous to these breccias are the so-called assimilation breccias at Recsk, which have similar position and produced by similar mechanism. These contain magmatic or hydrothermal cement material. The development alteration zoning pattern during cooling and crystallization is a function of lithological and geochemical parameters related to the geodynamic position. It has to be emphasized that rock alteration processes advanced synchronously with mineralizations, though their discussion here precedes that of the ore – formation.

The most typical alterations, which show certain zonation, are plotted on *Fig. 3.* The alterations are studied mostly by CSILLAG [1975]. 150—200 m wide skarn zone has developed on the contacts of the intrusion below −700 m depth, consisting of calc-silicate assemblages, which were formed during contac metasomatism. Outside this zone, mostly by thermal effects, local intact skarns were developed. Both endo- and exoskarns can be distinguished.

The circulation path of the migrating fluids related to the alterations is the microfissurization (stockwork structure), which pervades both the skarn and the whole intrusion. In the bottom and central parts of the intrusion the quartz-veins, phlogopite (biotite) alteration is dominant while propylitisation and endoskarns are typical to most of the intrusion. These two alterations are heavily intermingled and their distinction is sometimes problematic. The peripherical and upper zones of the intrusion have undergone intense silicic, argillic and sericitic alteration, forming a pervasive. The occurrence anhydrite and gypsum is common with every alterations, especially in the endoskarns and the propylitic zone. Argillic alteration (secondary quartzite) is typical in the apical partion of the intrusion and the lithocap zone. The alterations are related to hydrothermal processes. The zonation pattern— though it still needs improvements — does not belong to the ideal models. However, with certain generalizations — it is similar to the diorite model of the eusyncline belts.

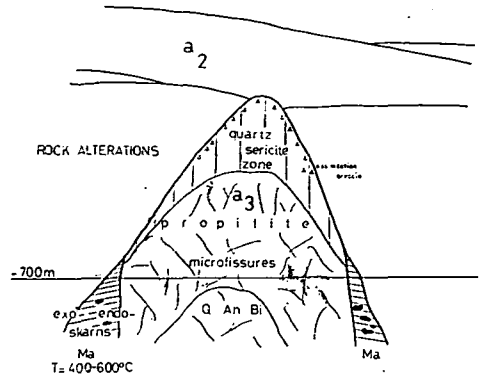

Fig. 3. Scheme of alteration zoning in the diorite porphyry intrusion. Q=quartz, Ah=anhydrite, Bi=biotite, Se=sericite, Ma=magnetite;

ORE FORMATION

Practically the ore-formation has begun with the development of the diorite-porphyry intrusions. The alteration processes, which have been related to the cooling of the intrusive, have first affected, the peripheral zones and the adjacent wall-rocks, and gradually invaded the inner zones of the intrusion towards the centre, which was the latest portion, which has been cooled down. The subsequent phases have been superimposed to the earlier ones (together with the effects of the later magmatic phases), and a complex system has been developed.

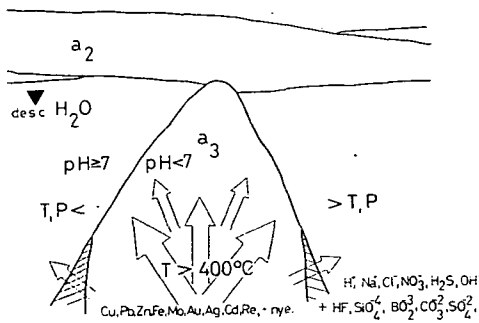

Fig. 4. The hypothetical compositions and flow paths of the fluids related to the cooling differentiation of the intrusion, the parameters of the physico-chemical conditions of the system

In my opinion, accepting this way of thinking, the activisation of the peripheral and adjacent hydrothermal systems preceded the process of pervasive metasomatism, considering the high temperatures in the central part.

The space-time model of the Recsk ore genesis can be summarized in the following empiric-logic scheme;

A. Pre-hydrothermal stage
1. Contact metasomatic magnetite deposits of the skarn zone.

B. Deposits related to the hydrothermal stage of the differentiation of the diorite porphyry intrusive:

1. Hydrothermal vein-type and metasomatic Pb—Zn—Cu—Fe ores.
2. Hydrothermal metasomatic stratabound Cu—Zn—Fe and pyrite ores.
3. Hydrothermal metasomatic Cu—Fe ores in the exo- and endoskarns of the skarn zone .
4. Porphyric hydrothermal metasomatic Cu—Fe—Mo ores within the intrusion.

C. Deposits formed in the late stage of, or following the ore-formation processes and differentation related to the cooling of the intrusion, by the remobilizations effects of later volcanic phases:

1. Hydrothermal metasomatic Cu—Fe—Pb—Zn—As—Ag ores related to the silicic zones in a_1q phase stratovolcanics.
2. Hydrothermal metasomatic stockwork, massive sulphide and hydrothermal exhalative collomorph Cu—Fe—Au—Ag—Sb—As ores related to the a_1 stratovolcanics (Lahóca-type).

This sequence indicate the temporal evolution and the genetic development too, the different stages of which is shown on *Figs. 3—10.* As it is evident from the previously described sequence, the ore deposits have no clear one-phase parageneses, rather mineral assemblages, comprised from a number of different and telescopically superimposed paragenesis, which have developed as functions of continuously changing heat fluxus of the igneous phases which have generated the circulation of fluids.

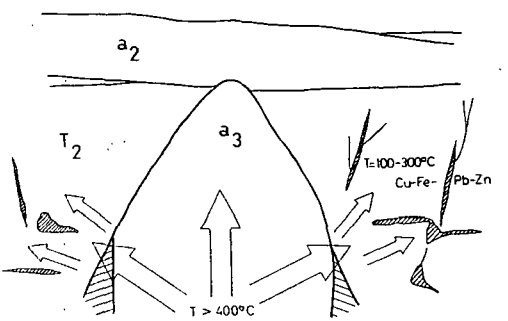

Fig. 5. Vein-type and irregular hydrothermal metasomatic polymetallic ore deposits in the Triassic wall rocks of the intrusion. The first stage of the hydrothermal ore deposition

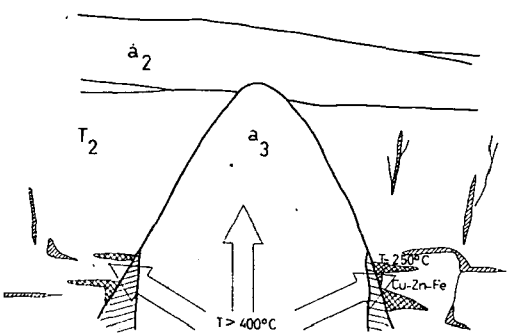

Fig. 6. Hydrothermal metasomatic polymetallic and pirit ore replacement deposits on the outer boundary of the skarn zone, along lithological contacts in the Triassic wall rocks. The second stage of the hydrothermal ore deposition

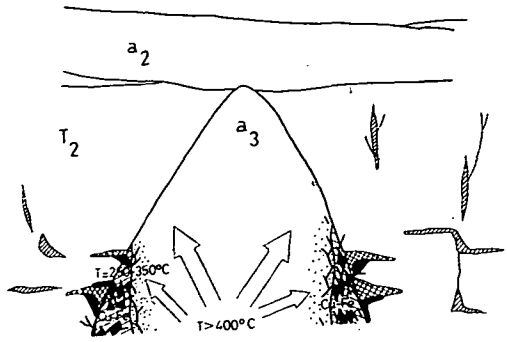

Fig. 7. Hydrothermal-metasomatic chalcopyrite–pyrite ore deposits in veins, lenses and pods in the skarn zone, replacing the silicates. The third stage of the hydrothermal ore deposition

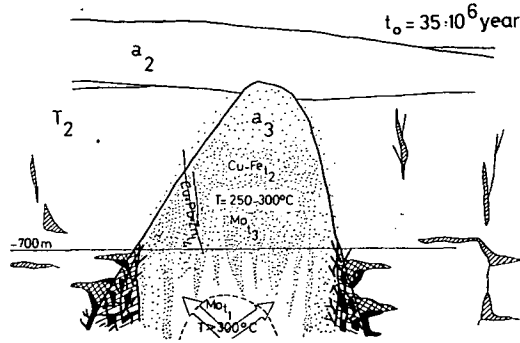

Fig. 8. Hydrothermal metasomatic Cu—Mo disseminated and vein type ores, formed in the stockwork structure of the intrusion. The fourth stage of the hydrothermal ore deposition. Also the relative times of formations ($t_1 - t_4$), for the main paragenetic types in the whole complex are shown

In the hydrothermal stage of the a_3 intrusion the ore formation has advanced from outside the intrusion inward. In the subsequent volcanic phases the formation of the related ore deposits was governed by local, though similar, factors.

The relative formation temperature data *(Figs. 3—10)* were obtained by the interpretation of decrepitation studies by CSILLAG and KOVÁCS [1972].

Thus, the last — and most important — ore formation in the physico-chemical system of hydrothermal metasomatic processes related to the diorite porphyry intrusion was the porphyry copper mineralization. During this stage, the ore mineral assemblage, which precipitated from the fluids due to the loss of their circulation energy, „freezed in" the stockwerk structure of the fracturized, porous host rock. The ore-body contours — which are in fact isograde-lines — and the alteration zone boundaries closely follow the retreating path of the thermal fronts, which generated the fluid circulation. The structural parameters of rocks (i. e. the cooling fissures of intrusives, the lithologic boundaries, lithological changes and pre-ore fissures in sedimentary wall rocks) have played important role in the shaping of these contours. The contours of porphyric ore bodies are controlled by the metal concentrations rather than lithological parameters. Two groups of the porphyric ore bodies can be distinguished according to their shape [SMIRNOV, 1974]. Conform deposits are those in which ore body contours are subparallel with the shape of the intrusive, disconform

deposits are those, in which the symmetry axis of the orebody does not fit with the axis of the intrusive. Cu and Mo distributions coincide in the disconform, and differ in the conform deposits. From this aspect, the Recsk porphyry copper mineralization shows the following characteristics:

— the isograds are subparallel with the intrusion geometry;
— the distribution of Cu and Mo shows negative correlation;
— the centre point of the Mo reserves coincide only in parts with the central depth of the Cu reserves in the explored vertical section of the intrusive body.

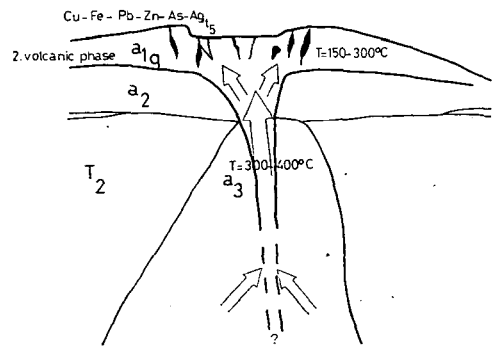

Fig. 9. Hydrothermal polymetallic ore deposits in silicic zones produced by the eruption phase of the a_1q quartz-biotite-amphibole andesite as the second phase of the stratovolcanic activity. The fifth stage of the hydrothermal ore formation

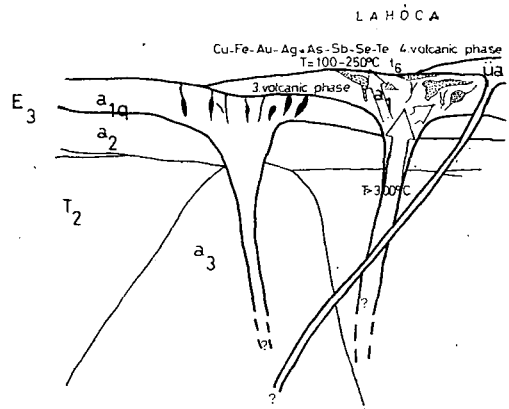

Fig. 10. The Cu—Fe—Au—Ag—As—Sb—Se—Te deposits, stocks, breccia-zones and collomorph deposits, generated by the a_1-type (Lahóca) biotite-amphibole-andesite eruptions in the third phase of the stratovolcanic activity. The sixth stage of the hydrothermal ore formation. The post-ore pyroxene-quartz-biotite-amphibole-andesite is the 4th phase of the stratovolcanic activity.

Comparing these data with the classification of SMIRNOV and POPOV [1977], the Recsk deposit belongs to the conform deposits in morphogenetic aspect. The formation of this is promoted also by the covered and quasi-closed nature of the system.

The detailed deseription of the ore-formational data and the parageneses related to each ore-forming phase is beyond the scope of this study. CSONGRÁDI [1975] and BAKSA [1975] has discussed the paragenetic sequences in the deep-level and near-surface mineralizations, respectively.

SUMMARY

The following conclusions can be drawn concerning the genesis of the Recsk deposits on the base of the cited studies and my interpretations:

— the occurrence belongs to the Paleogene volcanic arc stretching along the Balaton-Darnó line;
— the main phases of mineralizations ending with the porphyry copper formation, are related to the hydrothermal stages of the differentiation of the diorite-porphyry intrusion (a_3);
— the two younger volcanic cycles have resulted in late-stage near-surface mineralizations, which are considered as rejuvenated ores.

In comparison with other porphyry copper mineralizations in the world, it can be suggested, that the Recsk deposit was formed during dioritic magmatism of an eusyncline belt. It shows similarities with the diorite-model in the zonation of the source intrusive rocks and ore-distribution. Morphogenetically it can be termed as conform deposit. Its classification was made easy by the completeness of the cluster of ore deposits, though the sequence of superimposed ore forming stages have meant difficulties in the interpretation.

ACKNOWLEDGEMENTS

This study were not be written without the constructive assistance and cooperation of geologists working in the Recsk exploration for more than ten years. Special thanks are due to J. FÖLDESSY, who advised the separation of the different magmatic cycles, and to J. CSILLAG for providing laboratory results and valuable discussions about the topic of the study.

REFERENCES

BAKSA, Cs. [1975a]: Új enargitos-luzonitos-pirites ércesedés a recski Lahóca-hegy É-i előterében Földt. Közl., **105**, 1, 58—74.

BAKSA, Cs. [1975b]: A recski mélyszinti szubvulkáni andezittest és telérei. Földt. Közl., **105**, 612—624.

BAKSA, Cs. [1975c]: A recski Lahóca-hegy É-i előterében feltárt újabb enargitos-luzonitos-pirites ércesedés földtani, teleptani vizsgálata. Ph. D. Thesis, p. 120. ELTE TTK, Manuscript, Budapest.

BAKSA, Cs., CSEH–NÉMETH, J., FÖLDESSY, J. and ZELENKA, T. [1980]: The Recsk Porphyry and Skarn Copper Deposit Hungary. European Copper Deposits. Belgrade p. 73—76.

BAKSA, Cs., CSILLAG, J., FÖLDESSY, J., ZELENKA, T. [1981]: A Hypothesis about the Tertiary Volcanic Activities of the Mátra Mountains, NE Hungary. Acta Geol. Ac. Sci. Hung., **24**, (2—4), 337—249.

BAKSA, Cs., CSILLAG, J., DOBOSI, G. and FÖLDESSY, J. [1981]: Rézpala indikáció a Darnó-hegyen Földt. Közl., **111**, 59—66. Budapest.

BAKSA, Cs., J. CSEH-NÉMETH, J. CSILLAG, J. FÖLDESSY and T. ZELENKA [1982]: The relationship of the structure and metallogeny of Northern Hungary (IAGOD VI. Symposium, Tbilisi 1982. (in press)

BALLA, Z., BAKSA, Cs., FÖLDESSY, J., HAVAS, L. and SZABÓ, I. [1981]: Mezozoos óceáni litoszféramaradványok a Bükk-hegység dél-nyugati részén. Ált. Földt. Szemle No **16**, 35—88., Budapest

CSILLAG, J. [1975]: A recski terület magmás hatásra átalakult képződményei. Földt. Közlöny **105**, Suppl., 646—671, Budapest.

CSILLAG, J., FÖLDESSY, J., ZELENKA, T. and BALÁZS, E. [1980]: The plate tectonic setting of the Eocene Volcanic Belt in the Carpathian Basin. Proc. of the 17th Assembly of the ESC, Budapest, 589—599.

CSEH-NÉMETH, J. [1975]: A recski mélyszinti szinesfémérc-előfordulás és annak teleptani, ércföldtani képe. Földt. Közl., **105**, Suppl., 692—708, Budapest.

CSONGRÁDI, J. [1975]: A recski mélyszinti szinesfémércesedés jellemzése ércmikroszkópi vizsgálatok alapján. Földt. Közlöny **105**, 672—691, Budapest.

FÖLDESSY, J. [1975]: A recski rétegvulkáni andezitösszlet. Földt. Közlöny **105,** Suppl., 625—645. Budapest.
FÖLDESSY JÁNOSNÉ [1975]: A recski mélyszinti alaphegységi üledékes képződmények. Földt. Közlöny **105,** Suppl., 598—611., Budapest.
HADŽI, E., ALEKSIĆ, V. PANTIĆ, N. and KALENIĆ, M. [1977]: The plate movements in south-eastern Europe during the Alpine cyclus. Metallogeny and Plate Tectonics in the Northeastern Mediterranean (ed: by S. JANKOVIĆ), 231—248, Belgrade.
HOLLISTER, V. F. [1975]: An appraisal of nature and source of porphyry copper deposits. Miner. Sci. Eng., No. 3.
HOLLISTER, V. F. [1978]: Geology of the porphyry copper deposits of the Western Hemisphere. New York, Soc. Mining Engineers AIME, 219.
KRIVCOV, A. I. [1977]: Tipi rajonov mednoporfirovovo orugyinenija. Geologija rudnüh meszt. No. **4,** 1977.
LOWELL, J. D., GUILBERT, J. M. [1970]: Lateral and vertical alternation — mineralization zoning in porphyry ore deposits. Econ. Geol., **65,** No 3.
NORTON, D. [1979]: Transport phenomena in hydrotermal systems, the redistribution of chemical components around cooling magmas. Bull. Mineral., **102,** 471—486.
PAVLOVA, I. G. [1978]: Medno porfirovoje mesztorozsgyenyija. Moszkva, Nyedra 1978, 275.
POPOV, V. Sz. [1977]: Geologija i genezisz medno — i molibden — porfirovüh mesztorozsgyenih. Moszkva, Nauka.
SILLITOE, R. H. [1972]: A plate tectonic model for the origin of porphyry copper deposits. Econ. Geol., **67,** 184—197.
SILLITOE, R. H. [1973]: The tops and bottoms of porphyry copper deposits. Econ. Geol., **68,** 799—815.
WEIN, GY. [1978]: A Kárpát-medence kialakulásának vázlata. Ált. Földt. Szemle **11,** 5—28., Budapest.
ZELENKA, T. [1975]: A recski mélyszinti szinesfémérc-előfordulás szerkezeti-magmaföldtani helyzete. Földt. Közl., **105,** 582—597., Budapest.
ZELENKA, T. [1973]: New data on the Darno megatectonic zone. Acta. Geol. Ac. Sci. Hung., **17,** 155—162.
ZELENKA, T. [1974]: Isztorija megatectonicseszkovo i magmato-geologicseszkovc razvitija szevero-vosztocsnoj Matri. Acta Geol. Ac. Sci. Hung., **18,** p. 377—385.

Manuscript received, 5 May, 1983

Cs. BAKSA
National Ore and Mineral Mines
H-1406 Budapest, Pf. 34., Hungary

Acta Mineralogica-Petrographica, Szeged, XXVI/1, 99—108, 1983

THE METALLOGENIC PROVINCE OF BANAT AND ITS PLATE-TECTONIC POSITION IN THE BALKAN PENINSULA

C. I. SUPERCEANU

ABSTRACT

The metallogenic province of Banat represents one of the most interesting mineralization zones of the European continent. The present work represents the first attempt to classify all of the ore deposits of Banat from the plate-tectonic viewpoint, taking into consideration the tectonomagmatic premises which defined the structure of the thin Carpathian section.

The superposition of the Alpine metallogeny over the Protezoroic-Paleozoic basement is primarily responsible for the complexity and the diversity of the mineralization of the Banat metallogenic province. The suggested classification separates the Banat into two subprovinces, which are:

— The Old-Carpathian province, with Proterozoic and Paleozoic ensimatic ore deposits.

— The Laramide province of banatites, with porphyry copper, iron and copper tactites.

INTRODUCTION

The present work represents the first attempt to classify all known ore deposits from Banat, taking into consideration the plate-tectonic premises which define the structure of this Carpathian section.

Metallogenic relations between the ore deposits of Banat and those in eastern Serbia were also unterlined by VON COTTA, [1864, and 1878]. The problem of the petrochemical, geotectonic and metallogenic relations between Banat and those in Serbia, was clarified by SCHNEIDERHÖHN [1928]. He considered that both zones belong to the same copper province.

PETRASCHECK [1942] studied the metallogenic province in the Srednogorie Mountains in Bulgaria and later he extended his researches to the foot of the Caucasus at Hopa. Recent work published by DONATH [1952], CISSARZ [1967], POLLAK [1966], SUPERCEANU [1969], GIUŞCĂ [1967] a.o. brought many important contributions to the exact form of this metallogenic province.

The superposition of the Laramide subduction and metallogeny over the Proterozoic — Paleozoic crustal units, constitutes the main cause for the complexity and diversity of the mineralization from the metallogenic province. The classification suggested separates the Banat area into two subprovinces, which are:

— The Old-Carpathian province, with the Danubian Autochton, the Getic-, and Supragetic crustal units.

— The Laramide banatitic province.

THE OLD-CARPATHIAN PROVINCE

This province consists of Proterozoic-Paleozoic crustal units, which were regenerated by the Laramide subduction of the Moesian plate. The geotectonic evolution of the Banatian South-Carpathians was controlled by the subduction of the Archean

Carelian microcontinent, and consists of the basement of the Moesian Plate, below the mobile zone of the South-Carpathians. The differentiated major crustal domains of the Old-Carpathian province are as follow:

— the middle pericontinental-paleooceanic Danubian Autochthon
— the western Getic and Supragetic crustal units
— the Moesian plate, in the east *(Fig. 1)*.

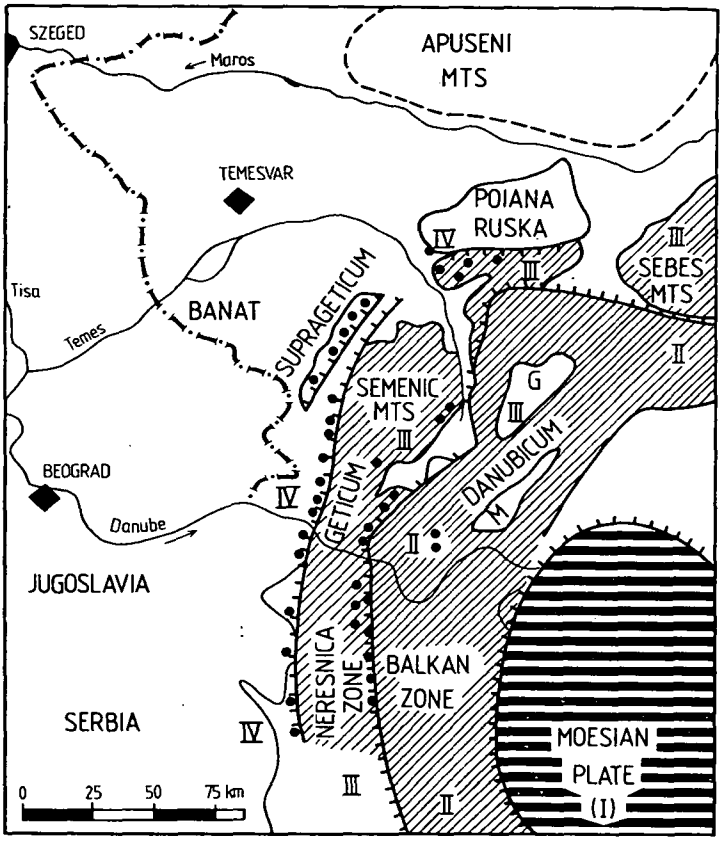

Fig. 1. The metallogenic province of Banat and eastern Serbia, and the concentric arrangement of geotectonic—metallogenic units around the Moesian plate

I The Moesian plate
II The pericontinental—paleooceanic Danubian Autochthon
III The Getic crustal nappe
G = Godeanu sheet
M = Mehedinţi sheet
IV The Supragetic unit
● Laramide — banatitic ore deposits

Metallogeny of the pericontinental-paleooceanic Danubian Autochthon

The Danubian Autochthon is a pericontinental crust, thereby constituting a lateral transition between the paleooceanic crust of the west and central part of the Danube and the continental crust of the Moesian plate which at that time was part of

the margin of the European continent [GRUBIC, 1974]. The Proterozoic Danubian pericontinental crustal unit, with important fossil upper mantle intercalations, with an intensive ophiolitic magmatism, occupies the southern and eastern part of Banat (Almăj, Cerna, Ţarcu, Muntele Mic and Retezat Mountains).

Proterozoic and Bretonic ensimatic ore deposits. This Danubian Autochthon contains Proterozoic metasomatic-metamorphosed deposits of iron and manganese carbonates intercalated in the carbonatitic level of the Jelova zone at Rudăria-Bănia (Fe—Mn carbonates), Topleţ (oxides, silicates, apatite) [PAPP, 1915], Sadova, Ilova, Căleanu Mountains (magnetite) and other areas. The ensimatic ore deposits of the ultrabasic magma derived from the upper mantle are localized in the Jelova—Mărul zone (dunites, wehrlites, peridotites, serpentinites, hypersthenites, gabbros and amphibolites). The Bretonic ophiolites contain chromite bodies (hundreds of occurrences) Cu—Ni mineralizations, Ni-bearing serpentinites, magnesite deposits in the Tisoviţa-Eibenthal-Plavişeviţa, Bretonic serpentinite-gabbro lopolith, numerous chrysotile and apmhibole asbestos occurrences in the Rudăria — Urda Mare Proterozoic ultrabasic lineament in magnetic serpentinite (with Pt) ranges *(Fig. 2., 4)*.

Ensialic mineralizations. The Danubian Autochthon contains ensialic mineralisation which was derived the Assynthian granites (Sfîrdinul and Cherbelezul plutons) generated from sialic mobilization up the converging margins of the Moesian plate and the Eurasian plate. The ensialic mineralization of the Danubian Autochthon are represented by the polymetamorphic iron deposit (Jablaniţa), barite lenses (Topleţ), numerous pegmatites, aplites with red feldspar and Cu, Ti, Zr, Mo, Sn mineralizations (Rudăria, Putna, Prigor) and red carbonatites with apatite, magnetite, sphene, pyrite, chalcopyrite (Rudăria) as well as Alpine quartz veins (crystals, with Cu—Pb—Zn mineralization) derived from the granite pluton of Muntele Mic (Sadova, Ilova, Arjena and Ţarcu Mountains). Pegmatites and aplites with molybdenite occur at Rudăria and Bucova. [VENDL, 1939] *(Fig. 2)*.

Periplatformal sedimentary deposits. The Paleo-Mesozoic Svinecea-Sviniţa cover contains Bathonian (limonitic) oolitic iron deposits [PAPP, 1915] at Rudăria — Bănia — Debeli Iug — Sviniţa in the Almăj Mountains and in the Stara Planina (eastern Serbia).

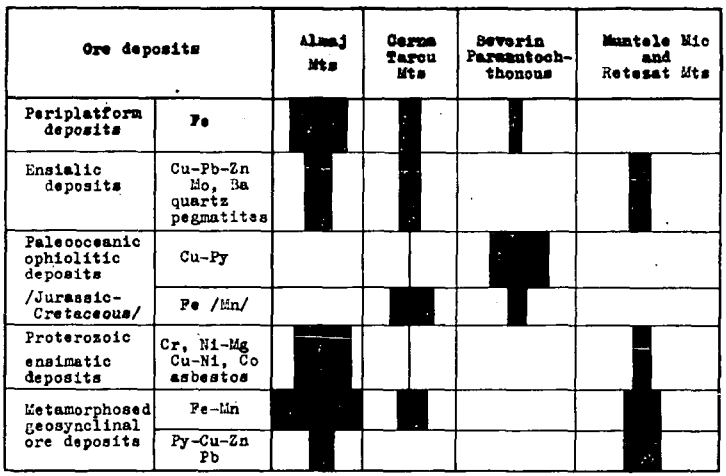

Fig. 2. Metallogenic types and ore deposits in the geotectonic units of the Danubian Autochthon

Jurassic ophiolitic ore deposits. The Upper Jurassic paleooceanic ophiolite province, is developed in the eastern external part of Banat (Severin Para-autochthon) and extends into Serbia in the Miroc Planina zone. The simatic ophiolite complex is a relict of the Upper Jurassic — Lower Cretaceous paleomicroocean ("mesoparatethys", after GRUBIC, 1974) elongated in a NE — SW direction, created by the divergence of the Eurasian plate and the lately formed Getic island arc. These relicts of oceanic crust consists of ophiolites throughout the Sinaia-Azuga beds (diabases, spilites, serpentinites, dunites, basic tuffs and cherts) named the Severin .Para-autochthon [CODARCEA, 1940], where it contains the following ore deposits:

— The volcanogenic-hydrothermal, massive pyrite-copper deposit at Baia de Aramă ($\delta S^{34} - 3.2‰$, upper mantle origin), Balta and Ponoarele.
— Disseminated magnetite nodules (5—15 cm) with Cu, Co, Fe sulphides in serpentinites at Podeni (Sulița and Plătica Mountains), Isverna, Obîrșia Cloșani, and chrysotile asbestos occurrences.
— Exhalative-sedimentary iron and manganese mineralization (Balta Cireșul).

This ophiolitic complex extends to Eastern Serbia, to the known Deli Jovan Mountains, which is considered a typical contemporaneous and fossil oceanic crust, with chromite and Cu—Bi—Au mineralizations. The Danubian Autochthon continues southwards into Serbia, passing in the Balkan zone, where it contains iron deposits connected with granites (Rudna Glava, Trnaica), copper-bismuth mineralization (Aldinaț, Jasicovo), tungsten (Tanda), molybdenum (Gornjane), gold (Deli Jovan) and Pb—Zn—Ag—Sb mineralization *(Fig. 5)*.

Metallogeny of the crustal Getic nappe

The Getic crystalline area is a typical Proterozoic continental crustal unit and has been developed by the central and northeastern Banat (Semenic, Pioana Rusca and Godeanu Mountains, *Fig. 1)*. The Getic crystalline formations were folded and metamorphosed during the Dalslandian metamorphism [SAVU, 1978]. The Getic meso-katazonal polymetamorphic crystalline schist (gneisses, mica schists, amphibolites) anticline include in the axial zone the Sichevița-Poniasca-Gosna granite pluton and numerous pegmatites generated through the Dalslandian anatectic migmatization in the deeper parts of the sialic crust and the collision and subduction processes of the Moesian plate under the Carpathian mobile zone *(Fig.1)*. The Dalslandian Getic crystalline area contains the following deposits:

Regional-metamorphic, kyanite deposits, in kyanite-staurolite mica schists (Semenic Mountains), sillimanite gneisses (eastern Semenic and Godeanu Mountains) and graphite occurrences (Bozovici).

Geosyncline-metamorphosed ore deposits. The Getic nappe contains Proterozoic geosyncline-polymetamorphic iron deposits (magnetite) Armeniș, Băuțari, Valea Fierului, connected with the Dalslandian initial magmatism (amphibolites) and crystalline dolomites, in the lower Getic nappe level, manganese deposits (silicates, carbonates, jakobsite) in the northern part of the Semenic Mountains (Delinești, Lindenfeld, Rugi, Ohabița) connected with amphibolites and quartzite (median level of the Getic crystalline basement) *(Fig. 3)*.

Ensialic deposits. A characteristic feature of the Getic continental crust are the numerous Dalslandian pegmatites, oriented NE—SW N—S and concentrically situated around the boundaries of the Moesian plate. These anatectic migmatization pegmatites (hundreds of occurrences) with feldspar, muscovite, beryl, columbite, tantalite, montebrasite, apatite, and other minerals are situated at Teregova, Armeniș,

Mehadica, Topleţ, Pătaşi, Crîjma, Băuţeri; concordant and discordant in the lower gneiss level. Kyanite and graphite pegmatite occur at Dalci (eastern Banat).

Polymetamorphic tactites, with diopside, epidote, phlogopite, biotite and Cu, Pb, Zn, Mo mineralization at Armeniş, Sadova, Godeanu Mountains, in contact zones between aplites, pegmatites with crystalline dolomites.

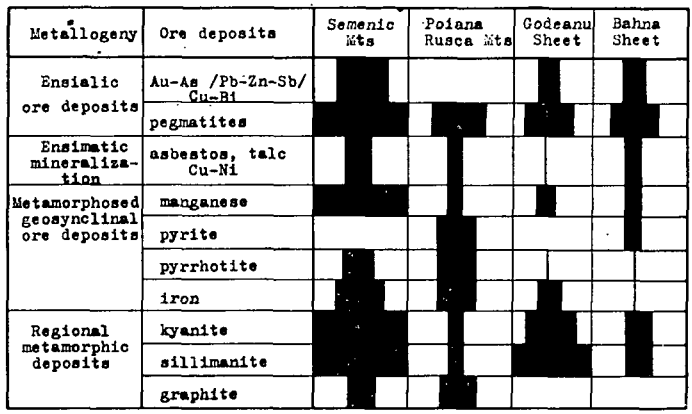

Fig. 3. Metallogeny and ore deposits in the geotectonic units of the Getic crystalline mass

The hypothermal gold mineralizations (veins, lenses) in gneisses with quartz, arsenopyrite and Pb—Zn—Sb mineralizations at Văliug Bozovici and Cocora Mountains (Godeanu Mountains) connected with the acid differentiates of the Proterozoic granite [CODARCEA, 1972]. In the upper Buceaua ensimatic level, the Getic nappe contains nickel ore veins (chrysoprase a. o.) at Bozovici (Lighidia, Agris, Tăria valley).

The Getic crystalline area continues southwards, passes the Danube into eastern Serbia and crosses into the Neresnica zone, which also contains numerous pegmatites and Au—W (scheelite), Sn, Pb—Ag—Zn—Sb mineralization (Vlagoev Kamen, Tanda, Bosilkovac, Zeleznic, Brodite, Seliste) [CISSARZ, 1967]. *Fig. 5* presents the comparison between the metallogeny of Neresnica and the Getic Semenic zones.

Metallogeny of the Supragetic crystalline

The Supragetic intra-Carpathian epizonal schists zone contains Hercynian and Caledonian crustal units (Locva Mountains, Dognecea Mountains and the northern part of Poiana Rusca) *(Fig. 1)*. This geotectonic unit contains in the south geosyncline (volcanogenic-sedimentary) iron-carbonate deposits (Teliuc, Ghelar, Vadul Dobrii), connected with albite-chlorite schists (Devonian, initial diabase volcanites) [KRÄUTNER, 1970] and metamorphosed hematite deposits (Poieni, Tomeşti, Iazuri, Lahn-Dill type) [PAPP, 1915]. The northern part of Poiana Rusca contains in the Padeş schists level, volcanogenic-hydrothermal metamorphosed lead — zinc deposits (Rammelsberg-type) at Muncelul Mic, Muncelul Mare with metarhyolites and copper mineralization at Veţel *(Fig. 3. 4.)*.

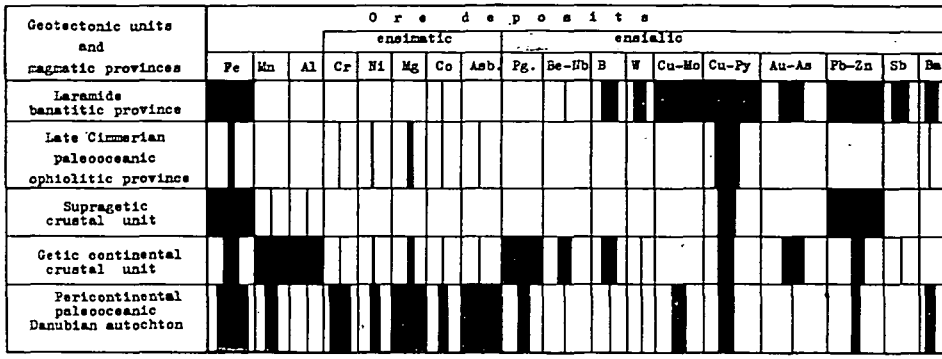

Fig. 4. The principal plate tectonic — metallogenic units of the Banat and the extension of ore deposits

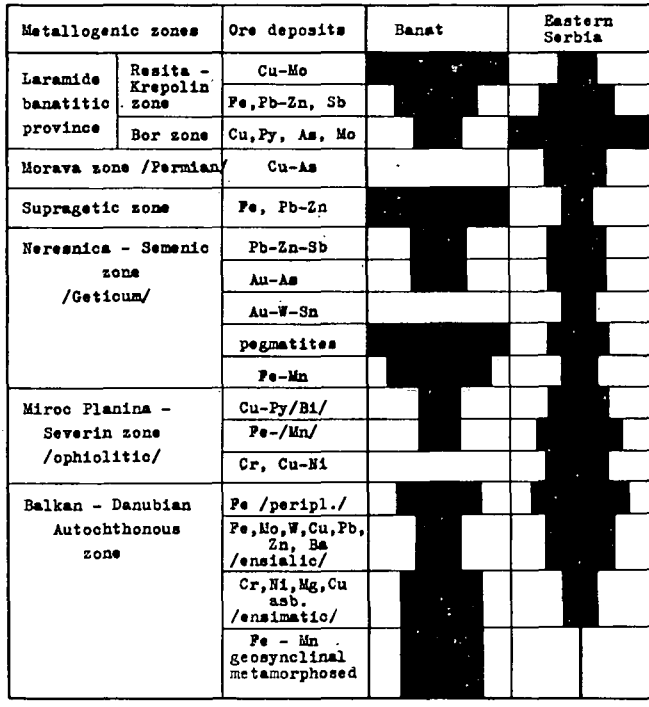

Fig. 5. The metallogenic zones and extension of ore deposits in Banat and eastern Serbia

THE LARAMIDE — BANATITIC PROVINCE

The Laramide province of the banatites forms the northwestern part of the Tethyan panglobal copper-molybdenum belt. The seismo-tectonomagmatic lineaments of the banatitic province are tectonically generated on the marginal zones on the deep fractured Proterozoic-Paleozoic crustal scales (Geticum, Suprageticum, Danubicum) as a result of the Laramide subduction *(Fig. 1)*. The copper tactites and

porphyry copper deposits are localized in the Laramide igneous rocks (mainly in subvolcanic granodiorites and monzodiorites) and the contacts with the Mesozoic limestones of Reşiţa zone.

The origin of the hybrid, copper rich banatitic multiphase and polyfacial magmatism is genetically related to the Laramide subduction of the pericontinental and paleo-oceanic crust of the Danubicum and the Moesian plate under the Geticum island arc. Further in the Backzone of the subduction, under the Reşiţa-Krepolin fault zone *(Fig. 1)* banatitic magmas were generated by the same process but at greater depth (plutonic granodiorites).

The Sr^{87}/Sr^{86} and Al_2O_3/K_2O ratio of banatites indicates contamination of initially upper mantle simatic material by remelted pericontinental crust material (magmatic crust/mantle mixture). The generation of the calc-alkaline banatitic igneous complex and the associated ore deposits occurred also with the partial melting of subducted oceanic crust and the penetration, along deep fracture (West- and East-Banatian Lineaments, oriented N—S and NE—SW, above the Banatian Benioff-zone. The important seismo-tectonomagmatic lineaments of the banatitic province (Carpathian longitudinal deep fractures) concentric with the boundaries of the Moesian plate, are as follows:

The west Banatian main lineament ("Oraviţa lineament")

This lineament, oriented N—S *(Fig. 1)* is a deep crustal fracture with seismic geothermal and magmatic-metallogenic manifestations in the western part of the Reşiţa zone, in tectonic contact with the Suprageticum (epizonal schists), contains two segments:

The Bocşa-Surduc Segment (NE—SW) with plutonic banatites (granodiorites, granites, diorites, gabbros) generated the classical pyrometasomatic iron deposit at Ocna de Fier (including ludwigite, copper, lead-zinc and gold mineralization) [CODARCEA, 1931; KISSLING, 1968] and the lead-zinc deposit at Dognecea (in hedenbergite skarns). The gabbros with (vanadium-bearing) titanomagnetite disseminations explored at Surduc, are derived from the upper mantle.

The Oraviţa — Moldova Nouă Segment (N—S) with subvolcanic banatites (porphyric quartz-monzodiorites, granodiorites) generates copper tactites and porphyry coppers:

The Moldova Nouă ore deposit complex (at Danube, 40 km NW from Majdanpek) with the great porphyry copper deposits of Suvorov Valley (open pit) in silicified argillitized and sericitized porphyritic quartz diorites. The mineralization contains chalcopyrite impregnations and veinlets, bornite, pyrite, molybdenite, tetrahedrite and titanomagnetite. The Moldova Nauă mining district contains copper-pyrite tactite bodies at Suvorov (paragenesis: pyrite-chalcopyrite–magnetite) realgar-auripigment occurrences (Florimunda Mine) and Cu—Pb—Zn mineralizations at Vărad ar Danube [GHEORGHIŢĂ, 1970].

The Stinăpari Plateau. The stratiform copper tactite deposits ("Manto type") are found between Jurassic limestones and a horizontal banatite sill (porphyritic biotite-hornblende granodiorite). The copper ores of the Stinăpari Plateau are characterized by the high temperature paragenesis: pyrite-charlcopyrite-pyrrhotite-magnetite-hematite in andradite-epidote tactites. The Cu—Mo mineralization of porphyry type has been reported in the banatite.

Sasca Montana. The well known ancient copper tactite deposit of Sasca Montana (George valley) is a classical pyrometasomatic copper deposit (Clifton Morenci

type) with the paragenesis: bornite-digenite-chalcocite-tetrahedrite-molybdenite in garnet-vesuvianite tactites. The colloform textures between bornite-chalcopyrite-digenite-tetrahedrite-sphalerite-melnicovite are uncommon in pyrometasomatic copper deposit around the world [SUPERCEANU, 1969]. The molybdenite of high rhenium content (0.13%Re) and associated with colloform tetrahedrite, melnicovite, jordisite, chalcopyrite and bravoite, formed at low temperature.

Ciclova Montana. The copper tactite deposit at Ciclova, connected with sienodioritic, monzodioritic and sienogabbroidal banatites contains pyritic copper bodies (Lobkowitz Mine), gold-bearing arsenopyrite bodies with scheelite and Co, Bi, Te, Ni, Mo mineralization (Baron and Speis ore bodies) in polyascendent garnet-diopside-wollastonite- and berylium-bearing vesuvianite skarns (0.2—2.5% BeO), accompanied by sulphurous geothermal springs (Lobkowitz Mine) and porphyry copper.

Oravița an old mining district with the Clementi Mine, Cu—Mo mineralizations in banatites, aplites, veins and skarns [SUPERCEANU, 1975], Racovița valley (Cu—Mo—Co-scheelite) and the Rochus Mountains with Cu—Co—Ni—Bi—Te—Au—W (scheelite) mineralization (Elisabeth Mine).

The Maidan (Bradisorul de Jos) area, with porphyritic Cu—Mo mineralization in pyritized and silicified porphyritic biotite-granodiorite (Fruntea, Miclea Mountain, Maidan banatite open pit) and hydrothermal pyrite-arsenopyrite (cobalt-bearing)-galena-sphalerite-antimonite-berthierite veins in crystalline schists (Perciului and Cuptorului valley).

The gabbro enclaves (with vanadium-bearing titanomagnetite disseminations) especially the spheroidal olivine gabbro nodules (0.1—2.0 m^3) in the banatites (Surduc, Bocșa, Oravița), the Fe—Co—Ni mineralization in skarns and the cobalt content in the pyrites and arsenopyrites is an argument for the prinordial upper mantle origin of the banatitic magma.

The west Banatian main lineament, which continues southward from the Danube in Serbia, passes to the Ridanj — Krepolin lineament, with the Cu—Fe deposits (Ridanj-Golubac), Kukaina (Pb—Zn—Au—Ag), Mo (Reșcovița) and Brezovac-Osanica (Sb) in subsequent banatitic dacites.

The East Banatian Lineament (Rudăria-Majdanpek lineament)

This NE—SW oriented metallogenic lineament is concentric with the boundaries of the Moesian plate and delimits the Danubian Autochthon and the Getic crustal units. The Geticum were subducted at the Danubicum *(Fig. 1)* with generation of banatitic hydrid magma. The banatites are represented by shallow consolidated subsequent subvolcanites (porphyritic quartz-monzodiorites, porphyritic quartz-diorites, dacites, andesites and tuffs).

The east Banatian lineament is continued southwards into Serbia *(Fig. 1)* to the Timoc (Bor) eruptive complex and copper province, with the re-known copper deposits at Bor, Majdanpek, Veliki Krivali a.o. The East-Banatian lineament contains the following ore deposits:

The Liubcova ore deposit is located 30 km north of Majdanpek and is connected by porphyritic quartz-monzodiorites and contains the pyritic copper tactite deposit at Illeci Mountain in Upper Cretaceous (Cenomanian) marble, associated with porphyry coppers. The tactite ore contains pyrite, chalcopyrite, pyrrhotite, sphalerite, hematite and other minerals. In Prasnic valley there are the gold-bearing arsenopyrite occurrences. The porphyry mineralisation contains pyrite, chalcopyrite,

bornite and molybdenite in silicified and epidotized porphyritic hornblende–monzodiorites.

The Sopotul Vechiu — Ravensca district contains the pyritic complex and barite mineralizations at Purcar Mountain and Nasovăţ valley in epidote-bearing porphyritic quartz-monzodiorites and andesites in contact with the Cenomanien marbles of the Culmea Sicheviţii Cretaceous syncline in epidote-garnet skarns. Porphyry copper mineralizations are identified at the Purcar Mountain.

The Lăpuşnicul Mare ore deposit contains porphyry copper in the Cornilor Mountains, in silicified quartz-diorites and epidote hornfels with pyrite, chalcopyrite, pyrrhotite, specularite and arsenopyrite.

Borlovenii Vechi. The pyritic occurrences at Borloveni, in the Nera valley (Botul Calului, Nergăniţa valley and Bănieşu valley) contains pyrite, pyrrhotite, chalcopyrite and arsenopyrite ores in andradite skarns, generated by subvolvanic andesites, in contact with crystalline schists.

The Luncaviţa-Mehadia area in eastern Banat contains small porphyry copper mineralizations in silicified and chloritized-sericitized andesites and quartz-diorites [GUNNESCH, 1975] in the Dalia and Satului valley.

The Poiana Mraconia — Dubova zone in southern Banat, in the internal part of the Danubicum, contains:

— Porphyry Cu—Mo mineralization in porphyritic biotit-granites and granodiorites, accompanied by molybdenite-bearing aplites and pegmatites. Accentuate analogies with the Clementis molybdenum mineralization from Oraviţa [SUPERCEANU, 1975] exist. Important occurrences of Poiana Mraconia, Faţa Strîmba, Stafetsky valley a.o.

— Iron tactite mineralization, with hematite, magnetite, pyrrhotite in epidote-garnet tactites (Satului valley, Dubova).

— Caledonian stratiform pyritic Cu—Pb—Zn—As—Sb—Au-ankerite-barite in the crystalline schists of the Corbu zone with crytalline limestone intercalations Poiana Mraconia [NICKMANN, 1900].

THE POSITION OF BANATITIC PROVINCE IN THE TETHYAN PANGLOBAL COPPER—MOLYBDENUM BELT

The Laramide banatitic province is a northwestern part of the Tethyan (Eurasian) copper-molybdenum belt. It is located at the southern of the Eurasian plate up to 10.000 km. The Laramide-Pyrenean and late volcanic copper deposits are associated with the volcanic-intrusive complexes, composed of the calc–alkaline suites. The behind trench lineaments and the island arc environments are principal geotectonic conditions for metallogenic provinces [SUPERCEANU, 1971].

This copper belt consists besides numerous of porphyry copper deposits, massive stratiform copper deposits, copper tactites and replacement Cu—Fe—Pb—Zn—Sb deposits accompanied by gold.

The main metallogenic provinces of this copper belt are as follows: the Banat province, the Eastern Serbian (with porphyry copper at Majdanpek, Veliki Kriveli, massive replacement copper deposits at Bor), the Srednogorian province (Medet, Assarel, Elacite, Radka), the Eastern Pontids (Murgul, Bakirkay, Ulutas), the Lesser Caucasus (Young Alpidic porphyry Cu—Mo deposits at Ancavan, Agarac, Kadjaran, Daskakert and others), the Iranian province (Talmesi, Meskani, Sar Cheshmeh), the Pakistan province (Chagai, Saidak, Robak) and the Tibetan-Burmese province (Monywa) on Sumatra in connexion with the Pacific copper belt.

The Tethyan belt is comparable with the Pacific copper belt, which contains numerous great porphyry copper deposits in the western Canada Rocky Mountains, Mexico, Chile, Peru and Philippines.

REFERENCES

CISSARZ, A. [1967]: Eine neue Lagerstättensystematik auf geotektonischer Grundlage und ihre Anwendung auf jugoslavische Lagerstätten. Zb. Rud. Geol., Fac., **9—10**, 18—34.

CODARCEA, A. [1932]: Geologische und petrographische Studien des Gebietes von Ocna de Fier — Bocşa Montana (Banat). An. Inst. Geol. Rom., **15**, 1—270.

CODARCEA, A. [1940]: Vues nouvelles sur la tectonique du Banat Meridicnal et du plateau de Mehedinţi. An. Inst. Geol. Rom., **XX**, 1—74.

CODARCEA, A. [1972]: Die Mineralschätze des Banates und ihre Verwertung. Ses. Acad. R. S. Romania, 1—15., Bukarest.

COTTA, B. v. [1864]: Erzlagerstätten im Banat und Serbien. Verl. Braumüller, Wien.

COTTA, B. v. [1878]: Forsetzung der Banater Erzlagerstättenzone nach Serbien. Berg u. Hütt. Ztg. 37.

DONATH, M. [1952]: Majdanpek, eine neue Grosskupferlagerstätte in Jugoslavien. Z. f. Erzbg. u. Met., V, 3, 80—90.

GIUSCA, D., GIOFLICĂ, G., SAVU, H. [1967]: Caracterizarea petrologică a provinciei Banatitice. An. Com. Geol., **XXXV**,

GHEORGHIŢĂ, I. [1975]: Studiul mineralogic şi petrografic al regiunii Moldova Nouă. Stud. Tehn. Ec., I, **11**.

GRUBIC, A. [1974]: Eastern Serbia in the light of the new gobal tectonics. Metallog. and concepts of the geotect. develop. in Jugosl., 179—213.

GUNNESCH, K. [1975]: Beiträge zum Studium der Banatitischen Eruptivgesteinen im Gebiet Liubcova — Lăpuşnicul Mare (Südbanat) D. d. S. Inst. Geol., **XI**, 104—189.

KISSLING, A. [1968]: Mineralogische und petrographische Studien in der Exoskarnzone von Ocna de Fier (Banat). Ed Ac. R. S. R. 1—130.

KRÄUTNER, H. G. [1970]: Die hercynische Geosynklinalerzbildung in den Rumänischen Karpathen und ihren Beziehungen zu der hercynischen Metallogenese Mitteleuropas. Mineral. Dep., **5**, 323—344.

NICKMANN, R. [1900]: Erzlagerstätten in Poiana Mraconia und Facea Strîmba in Krasso—Szőrenyer Comitat. (Manuscript, 1—3, Orschowa.)

PAPP, K. [1915]: A Magyar Birodalom Vasérc és Kőszénkészlete. Budapest.

PETRASCHECK, W. E. [1942]: Gebirgsbildung, Vulkanismus, und Metallogenese in den Balkaniden und Südkarpathen. Fort. d. Geol. u. Pal., **XIX**, 47.

POLLAK, W. [1966]: Kupfererzlagerstätten in der Türkei. Schr. d. GMBD. **18**, 89—97.

SAVU, H. [1978]: Dalslandian metamorphous formations in the Southern Carpathian. Rev. Roum. Geol., **22**, 7—17.

SCHNEIDERHÖHN, H. [1928]: Die Jungeruptive Lagerstättenprovinz in Serbien, Siebenbürgen und das Banat. Zbl. Min. A, 404—406.

SUPERCEANU, C. I. [1969]: Die Kupfererzlagerstätte von Sasca Montana im S. W. Banat und ihre Stellung in den alpidisch—ostmittelmeerischen Cu-Mo Erzgürtel. Geol. Rdsch., **58**, 3, 798—861.

— — — [1971]: The Eastern Mediterranean — Iranian alpine copper-molybdenum belt. Soc. Mining Geol. Japan, Sp. Issue **2**, 393—398. (Proc. IMA—IAGOD).

— — — [1975]: Die Kupfer-Molybdänvererzungen der Clementis Grube im Kontaktgebiet von Orawitza (Banat). Mineral. Dep., **10**, 305—314.

VENDL, M. [1939]: Die Mineralschätze Ungarns. Sopron.

Manuscript received, 10 December, 1982

CAIUS I. SUPERCEANU
Department of Natural Sciences
Timişoara University, Bd. V. Pîrvan 4. Romania

Acta Mineralogica-Petrographica, Szeged, XXVI/1, 109—114, 1983

GENETICAL TYPES OF THE TITANIUM MINERALIZATIONS IN THE METAMORPHIC AND BASIC ROCKS OF THE RHODOPE MASS IN SERBIA (YUGOSLAVIA)

V. VUJANOVIĆ and M. TEOFILOVIĆ

INTRODUCTION

Various types of titanium mineralizations in the Serbian portion of the Rhodope geotectonic unit are described in this paper. The data presented are based on complex field and lab. examinations carried out in the 1973—1980 period. Field work including the sampling of the ores and the rocks were mainly carried out by V. VUJANOVIĆ and M. TEOFILOVIĆ, and laboratory examinations by mineralogists and chemists. Ore microscopic examinations were performed by V. VUJANOVIĆ, petrographic ones by V. ĆEBIĆ, chemical analysis by Z. ČERVENJAK and V. OCOLOKJIĆ and spectrographic ones by S. MAKSIMOVIĆ and M. ARSENIJEVIĆ. X-ray diagrams were explained by V. VUJANOVIĆ and M. VUKASOVIĆ.

The geologic-tectonic study was done by M. TEOFILOVIĆ.

The collected data, the synthesis as well as the petrologic, geochemical, mineralogical and metallogenetic study were carried out by the authors.

RHODOPE MASS

The Rhodope geotectonic unit *(Fig. 1)* starts east of Beograd, south of the Danube (i.e. of the Pannonian Basin) passing throughout Serbia in the SSE direction about 300 km. in lenght (air distance). In SE Serbia and NE Macedonia Rhodope mass turns eastward passing over Bulgaria ending in Asia Minor.

The Rhodope geotectonic unit was mainly formed during Hercynian movements in form of a complex anticlinorium which was relativelly stable throughout later geological events. In fact, in the Posthercynian and especially within the period of the Alpine movements the Rhodope mass represented a mountain barrier which separated the eastern Balkan (Carpatho-Balkan range) from the western one (Dinarids), both of which were raising during the Alpine orogenesis [K. PETKOVIĆ and P. PAVLOVIĆ, 1976].

The crystalline core of the Rhodope mass consists prevailingly of high crystalline schists and also of the lower ones. The former include migmatite gneisses, para—and ortho-amphibolites, amphibole schists, biotite, mica and two mica schists, marbles, cipolines, quartzites etc. In the stratigraphic column these rocks are multiply alternating. The formation described is Prepaleosoic and is overlain by schists of lower crystallinity such as various types of phyllites and "green schists" which are often felsparized and, in a lesser degree, by limestones and quartzites [K. PETKOVIĆ and P. PAVLOVIĆ, 1976].

Most of the mountains in the Rhodope mass in Serbia are built up of the described crystalline schists, such as the mountains Crni Vrh, Juhor, Stalać Hills,

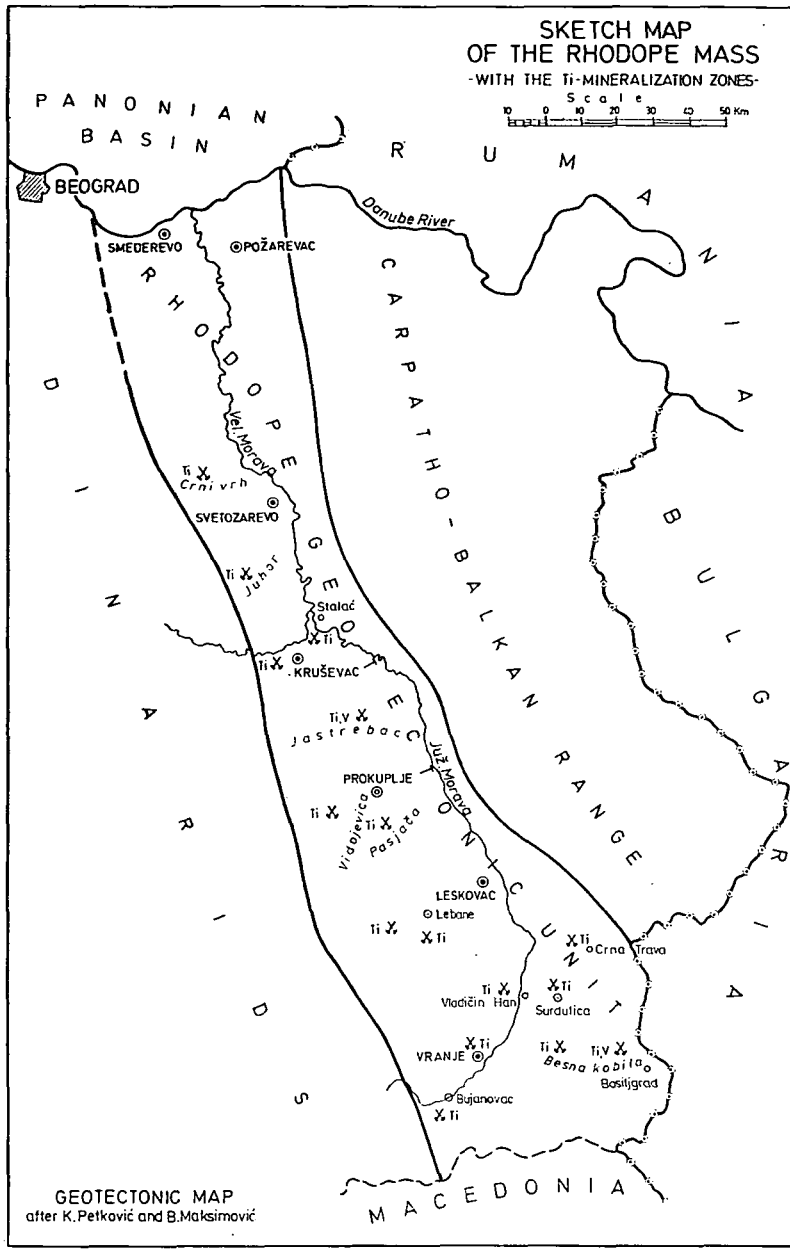

Fig. 1

Jastrebac, Vidojevica, Pasjača, and the Jablanica and the Vranje areas, further on Crna Trava, Besna Kobila, Kriva Feja, the vicinity of Bosiljgrad and others.

Along the eastern and western borders of the Rhodope anticlinorium in Serbia, deep dislocation lines were formed in which basic magmatites intruded. They occasionally occur in the Rhodope mass in form of occurrences or as relativelly large

massifs. These rocks intruded throughout the late Caledonian and the young phases produced the Posthercynian gabbros. In the Saalian and Pfalzian phase of the Hercynian orogenesis various types of granitoids were formed, accompanied by aplites and pegmatites [K. PETKOVIĆ and P. PAVLOVIĆ, 1976].

During the Alpine movements strong granitization of the metamorphic, granitoid and gabbroic rocks took place and by this process the large migmatite complex was produced within the whole Rhodope mass in Serbia. Throughout the granitization processes the granitoids were alkalized, dacites and andesites were felsparized or granitized, whereas meta-gabbros were alkalized or converted into diorites, quartz-diorites and plagiogranites.

In the Tertiary/Quaternary period the latest granitization took place and produced the mineralizations of the titanium metasomatic front, and this was followed by the later alkaline metasomatism. These titanium mineralizations are the most widespread in the whole Rhodope mass in Serbia.

TITANIUM MINERALIZATIONS

Examinations described have demonstrated that the highest concentrations of titanium show such rocks as meta-gabbros, granitized gabbros, amphibole gneisses and amphibolites, occasionally also biotitized and garnetized schists, whereas serpentinites, as a rule, show very low contents of the mentioned metal.

On the basis of the field investigations and the laboratory examinations numerous titanium mineralizations have been detected throughout the Rhodope mass in Serbia, including a number of titanium deposits.

The mineralizations described, depending on their genetical features, occur in various rocks and differ in size and way of appearance.

In general, there exist four genetical types of the titanium occurrences such as:

1. Titanium minerals as accessory constituents in the gabbroic and metamorphic rocks. The dominant titanium mineral has usually been ilmenite, but occasionally also rutile, or sphene or both of them. In the gabbroic rocks these minerals often occur as minute grains, or crystals (ilmenite, rutile), which are often elongated with cleavages of Fe—Mg minerals. The relatively coarse ilmenite grains are in many cases partly or totally transformed into leucoxene, in much less degree in rutile and sphene.

In some localities also ilmenite-hematite and hematite-ilmenite have been recognized, accompanied by some hematite-rutile. The primary accessory minerals had been ilmeno-hematite and hemato–ilmenite, later transformed into the above cited associates. The latter as a rule occur in the gabbroic rocks, the amphibolites and in the „greenschists". Hematite from the associates described is usually cream-white, showing rate internal reflections as well as lower reflectivity, indicating the presence of some unexsolved $FeTiO_3$. In the dioritized amphibolites situated near the town of Lebane, beside ilmenite-hematite and hematite-ilmenite also accessory sphene occurs namely as numerous minute "droplets" forming relativelly large patches. The primary hemato–ilmenite and ilmeno–hematite, as well as the sphene "droplets" are high-temperature products of the remobilization of the accessory titanium, and the latter process took place during the dioritization of the amphibolites.

Finally, in some cases also Ti-magnetite has been recognized as the accessory mineral, sometimes accompanied by some magnetite.

2. The titanium mineralizations in the gabbroic rocks are detected in many cases in the studied region and are genetically related to these rocks. The dominant titanium mineral has always been ilmenite frequently converted into leucoxene or

into rutile and sphene. As a rule, ilmenite is coarse but rarely also crystalline. In the polished sections ilmenite concentrations may reach up to 80%, and its average contents in the ore bodies is up to 10%. The average vanadium contents in this type of deposit reach up to 0.15%.

In the gabbroic rocks ilmenite is rarely associated with the other metallic minerals like magnetite and Ti-magnetite and the latter minerals are scarce. Occasionally sulphide assemblages may occur sparsely, namely in form of small grains disseminated in the host rock. These assemblages include pyrrhotite, pyrite, pentlandite, cubanite, valleriite, chalcopyrite and quartz.

The largest deposit of this type is the Bodevik, situated on the top of the Jastrebac mountain, north of the town of Prokuplje, south Serbia, where the ore body may be traced about 0.5 km in lenght, is 200 m large and sinks 200 m at least. The average contents of TiO_2 are about 5%, those of vanadium 0.13%.

3. The occurrences of leucoxene have been detected in the vicinity of the town of Bosiljgrad, SE Serbia, namely in the granitized gabbro. This gabbro appeared in form of large massif in which the Ti-mineralizations were present occasionally. The primary titanium mineral was ilmenite, and its associates were not detected. The gabbro described is of Paleozoic age and throughout the Alpine tectonics it was metamorphized and granitized, whereas the ilmenite was mostly converted into leucoxene. The late granitization (granitization II) which is of Tertiary/Quaternary age introduced some titanium (ilmenite, sphene) and caused the greisenization of the granitized gabbroic rocks introducing tourmaline and the associates [V. VUJANOVIĆ and M. TEOFILOVIĆ, [1979, *a, b*]. In the first phase of the granitization of gabbros granitoids were formed and the dominant conversion of the ilmenite took place within this process.

The newly formed granitoids show increased concentrations of the "basic" elements like *vanadium* (up to 1000 ppm), *nickel* (up to 190), *cobalt* (up to 320) and chromium (up to 105 ppm), as well as the micro-residues of the altered primary gabbro. The main titanium deposit of this type was detected in the Leska Mahala village, where the leucoxene ore body is exposed in a lenght of about 270 m, is 80 m large and sinks more than 40 m. In no direction the ore body is thinning out so far.

The ore body shows average TiO_2 contents of about 6% and averages of vanadium of 500 ppm. However, the leucoxene concentrations may reach up to 30% or more in the specimen. The groundmass of the leucoxene is represented by sphene or by rutile, or by both, containing numerous inclusions and residues of the ilmenite. In some cases inclusions and minute grains of rutile and ilmenite have also been seen in the sphene matrix. Although the sphene is as a rule grey-white (!), the examinations of the mineral show its normal chemical composition as well as the X-ray diagrams. Leucoxene is usually coarse (up to 2 mm in size). Its grains are often rounded as a result of resorption of the primary ilmenite during the granitization of the gabbro. Contrary to the titanium minerals of the metasomatic type (see below), the leucoxene does not contain traces of columbium, lanthanium, tin or other "acid" elements, except for the increased contents of zirconium (0—250 ppm), and the traces of lead (up to 14 ppm). Both of the latter elements were introduced under the influence of the granitization processes. The manganese contents in the leucoxene reach up to 500 ppm, those of chromium up to 40 ppm, including the traces of nickel and cobalt. These elements are genetically related to the primary gabbroic rock and the ilmenite.

In the leucoxene ore body also sparce chrom-spinel has been observed. This mineral has been the accessory constituent in the primary gabbro, partly resorbed later during granitization processes and in a considerable part also magnetitized.

The sulphide assemblage has also been detected in the leucoxene ore body, and is hydrothermal in origin. The predominant sulphide minerals are pyrrhotite and pyrite and the associates are scarce sphalerite and chalcopyrite. This paragenesis is very young and genetically related to the latest granitization processes, which also attacted the described gabbro massif (granitization II). This conclusion may also be supported by the fact that the mentioned sphalerite contains a number of the "acid" elements such as *cadmium* (up to 4500 ppm), *silver* (up to 150 ppm) and *bismuth* (up to 70 ppm).

The increased contents of *titanium* in the sphalerite (up to 150 ppm) may be explained by remobilizing the said element from the primary gabbro or the ilmenite.

4. The titanium mineralizations which are the products of the Ti-metasomatic front are genetically connected with the young granitoids. The case is of the rocks of the Tertiary/Quaternary age which metasomatically intruded in the crystalline rocks introducing titanium minerals in many places in the mentioned rocks. This type of titanium mineralizations is usually disseminated showing high concentrations in many places (up to 8% TiO_2). However, the bulk of these mineralizations is usually small with variable contents of titanium. The disseminated titanium mineralizations may appear within a large area with numerous "points" of the increased concentrations of the metal (the mountains of Juhor, Crni Vrh, Jastrebac, Pasjača, Vidojevica, Lebane, Crna Trava; further on the areas of the towns of Bosiljgrad and Vranje etc.). The only minerals are ilmenite and sphene, with rutile sporadically. Minerals are relativelly fine-grained or crystalline. In many cases the sphene is almost exclusively in form of elongated crystals (up to 0.2 mm in size) which often are double-twinned. The twin lamellations in the ilemnite and the rutile could be only rarely seen.

Although veinlets of titanium minerals have been observed, metasomatic replacement structures are dominating. Namely, the titanium minerals penetrated along the rock-forming grain contacts, or along the cleavages in them, as well as along the schistosity of the rock. The enclosures of the rock forming minerals in the newly formed titanium minerals have usually been seen in the localities in which the titanium concentrations are high. Thus, in some areas in the Rhodope mass (Juhor, Crni Vrh, Vidojevica, Pasjača, Lebane, Surdulica area etc.) a strong sphenization of the crystalline schists took place (up to 40% of sphene in the specimen), namely along their schistosity and newly formed sphene encloses numerous rock grains. However, strong ilmenitization of the crystalline rocks has only rarely been seen. Intense ilmenitization and sphenization are best expressed in amphibolites and amphibol migmatite gneisses, i.e. in the lower levels of the stratigraphical column.

The paragenetical relationships between the titanium minerals are very simple. The oldest is ilmenite, the youngest is sphene. However, rutile also often appears as sparse transformation product of ilmenite and in such cases it is the latest titanium mineral.

The high concentrations of the ilmenite as a rule caused the retreating of the sphene and vice versa; this fact may support the conclusion that both ilmenitization and sphenization have been separate processes caused by identical granitoids.

The way of occurrence of titanium minerals of the discussed type is uniform along the whole Rhodope mass in Serbia, i.e. not depending on the area or on the host rock.

During the titanium metasomatism some associates were also introduced, thus ilmenite, rutile and sphene often contain the increased concentrations of such elements as *lanthanium* (up to 2000 ppm), *tin* (up to 316 ppm), *columbium* (up to 2000 ppm) and *zirconium* (up to more than 1%), with some *tantalum, hafnium* and *vanadium,* as well as the increased contents of *nickel, cobalt* and *chromium.* However,

the latter elements are probably partly remobilized from the surrounding crystalline and gabbroic rocks.

During the sphenization processes beside the influx of calcium also its remobilization is supposed, namely from the limestones, marbles and cipolines which are included in the metamorphic complex. In connection to this conclusion we would point out the fact that young calcite is very widespread within the Rhodope mass, forming in some cases carbonatite-sövite masses (Jastrebac mountain). After the titanium metasomatism also an intense alkaline one took place developing throughout the whole Rhodope mass in Serbia. This process which also developed within the Tertiary/Quaternary period was observed within the formation of the crystalline schists sometimes also in the granitoids and the gabbros. This metasomatism introduced a number of felspars such as orthoclase, anorthoclase, microcline, albite, oligoclase, oligoclase-andesine, andesine and rarely andesine-labradorite, with the frequent and strong silification and biotitization of the schists including also an usually moderate muscovitization. All of the minerals described are younger than those of the Ti-metasomatic front (ilmenite, sphene and the associates) and the latter are often replaced by the former. The felspars and the biotite are preserved as a rule.

The alkali-metasomatism is varying in chemistry throughout the Rhodope mass in Serbia. In northern portions potassium metasomatism is dominating and in the central and the southern part the soda and calcium metasomatism. In the latter part of the Rhodope mass the potassium metasomatism is prevailing only is some areas notably in the Mačkatica molybdenum district (Surdulica), where considerable parts of dacites are totally granitized by the influx of orthoclase, anorthoclase and the associates.

The latest mineral assemblages in the region are sulphidic, which are hydrothermal and also genetically related to the late granitoids [V. VUJANOVIĆ, 1978]. The case is of the disseminated copper occurrences which are widespread within the whole Rhodope mass in Serbia, notably in the crystalline schits, sometimes also in the granitoids and the gabbros. These mineralizations are, as a rule, scarce and include pyrite, pyrrhotite and chalcopyrite which may be associated with some sphalerite, bornite, valleriitie, pentlandite, chalcocite, covellite and marcasite. The non metallic minerals are quartz and calcite sometimes also barite and fluorite.

REFERENCES

PETKOVIĆ, K. and PAVLOVIĆ, P. [1976]: Geologija Srbije-Tektonika. — Univerzitet u Beogradu, p. 445—454. Beograd.

VUJANOVIĆ, V. [1978]: The disseminated copper mineralizations in the Serbian—Macedonian (Rhodope) mass of Serbia. — Bull. du Museum d'Historie Naturelle, Serie A., p. 101—112, Beograd.

VUJANOVIĆ, V. and TEOFILOVIĆ, M. [1979*a*]: The occurrences of tourmalinization in the Bosiljgrad area (SE Serbia). — EXTRAIT des Comptes Rendus des Séances de la Société Serbe de Géologie p. 85—98. Beograd.

VUJANOVIĆ, V. and M. TEOFILOVIĆ, [1979*b*]: The titanium-sulphide-graphite association and the occurrences of greisenization in Klisura Mahala area (Bosiljgrad, SE Serbia). — EXTRAIT des Comptes Rendus des Séances de la Société Serbe de Géologie, p. 133—137., Beograd.

Manuscript received, 8 December, 1982

V. VUJANOVIĆ
M. TEOFILOVIĆ
Knez Danilova 36
Beograd, Yugoslavia

Acta Mineralogica-Petrographica, Szeged, XXVI/1, 115—123, 1983

MINERAL CHEMISTRY OF HORNBLENDES FROM THE CHARNOCKITES OF KARNATAKA, INDIA

B. MAHABALESWAR and I. R. VASANT KUMAR

ABSTRACT

Calciferous amphiboles found in the charnockites of Karnataka have been analysed for major elements. The majority of the analysed amphiboles are contained within a narrow range of $Fe^{tot}/(Fe^{tot}+Mg)$ values. They show all the chemical characteristics of high alumina, high titanium and high alkali hornblendes from other granulite facies area. They can be termed ferroan pargasitic hornblendes according to the nomenclature of LEAKE [1978]. The variation of Si—Al in the hornblendes is attributed to influence of pressure, whereas the Ti variation is due to a combination of independant parameters namely, temperature of metamorphic crystallisation and oxygen fugacity. The Al^{iv} and Al^{vi} relationship in the hornblendes has been considered as a function of Ti substitutions.

INTRODUCTION

Calciferous amphiboles are formed in a wide range of temperature, pressure and chemical environment in both metamorphic and magmatic rocks. Their chemistry is complex because of numerous ionic substitutions. This factor hinders the specific identification of amphiboles by conventional petrographic methods. Furthermore, recent investigations in some metamorphic areas have shown that there are significant differences in hornblende chemistry between different regional metamorphic terrains i.e. different metamorphic facies series [SHIDO and MIYASHIRO, 1959; RASSE, 1974; FABRIES, 1968]. With this in mind the authors have undertaken the chemical investigation of amphiboles found in the charnockites from the Sivasamudram and Kanakapura areas. The charnockites of these areas are considered to be typical for these rocks and afford an opportunity to understand the chemical complexities of the amphiboles present. A comparison of chemistry of the amphiboles of the present study with those of others found in different metamorphic environments is made in an attempt to understand the differences between the chemistry of the amphiboles formed under different metamorphic environments.

LOCATION

The Sivasamudram and Kanakapura areas described in this investigation are located 65 to 115 km. southwest of Bangalore city. They are bounded by latitudes 12°15′ and 12°34′ and longitudes 77° and 77°34′. The area largely consists of charnockites, granulite and amphibolite facies gneisses and granites.

ANALYTICAL METHODS

Compositional determination of the amphiboles of charnockites were facilitated by energy dispersive spectrometry (EDS) at Department of Mineralogy and Petrology, University of Cambridge, Cambridge, U.K. Analysis were done on carbon-

coated polished thin sections an on energy dispersive spectrometry unit with a Harwell Si(Li) detector and pulse processor. The results were calculated using a computer programm employing iterative spectrum stripping techniques [STATHAM, 1976]. Correction procedures applied were those of SWEATMAN and LONG [1969].

CHEMICAL CHARACTERISTICS OF AMPHIBOLES

The analyses of 15 hornblendes are given in Table 1. The structural formula of the hornblendes have been calculated on the basis of 23 oxygen atoms, according to the methods of the Subcommittee on amphiboles [LEAKE, 1978]. Classification of the hornblendes, as suggested by the Subcommittee, is on the basis of the number of $(Ca+Na)_B$ and Na_B. Following this classification, the amphiboles of the areas belong to the calcic amphibole group, and on the basis of $Mg/Mg+Fe^{2+}$, fall within the field of ferroan pargasitic hornblendes *(Fig. 1)*.

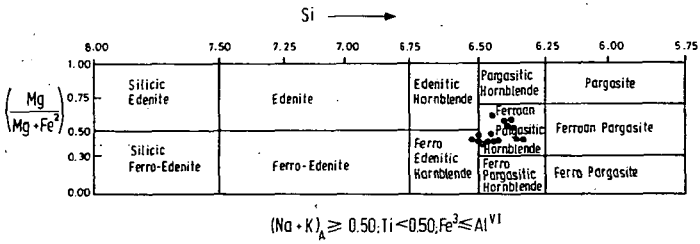

Fig. 1. Classification of amphiboles [after LEAKE, 1978]

Hornblendes from the charnockites show all chemical characteristics of well known high Ti, high Al and high alkali hornblendes from other granulite facies areas [ENGEL *et al.*, 1964; BINNS, 1965; LEELANANDAM, 1970; DAVIDSON, 1971 and COOLEN, 1980].

The majority of hornblendes represent a narrow range of $Fe^{tot}/Fe^{tot}+Mg$ values extending from 0.46 to 0.57. These hornblendes are olive green to brownish green and brown in colour.

The Ti content of the hornblendes vary considerably. The maximum Ti content of the hornblendes of the present study (3.09 wt% TiO_2) is higher than reported elsewhere from these areas [ANANTHA IYER *et al.*, 1976] but is slightly lower than the maximum Ti values reported from hornblende-pyroxenite xenoliths in basalt pipes [e.g. DAWSON and SMITH, 1973]. The variation in Ti values appears to depend upon the type of mineral adjacent to the hornblende; hornblende grains surrounding opaque oxides always contain less Ti than hornblendes which are associated with pyroxene [*c. f.* COOLEN, 1980].

The Al^{iv} values are close to 2.0 *(Fig. 2)* accompanied by low Al^{vi} values. Compositional zoning within individual grains of hornblende is generally lacking.

Al AND Si VARIATION AND THE INFLUENCE OF PRESSURE

LEAKE [1965, 1971] recognised that hornblendes in magmatic and contact metamorphic rocks generally have lower Al^{vi} and Si contents, than hornblendes in regional metamorphic rocks. He suggested that Al^{vi} content is pressure dependent and showed

TABLE 1

Chemical composition and structural formula of hornblendes

	CHR11	CHR	CHR3	326	326	121	540	110	141	139	183	56a	25	167	72	
SiO_2		41.75	42.50	42.27	41.11	41.87	42.50	42.75	41.68	42.30	42.65	42.40	41.60	41.80	42.40	42.60
Al_2O_3		11.50	11.63	11.59	11.80	11.17	11.74	11.38	11.73	11.40	11.26	12.32	11.70	11.97	11.90	11.90
TiO_2		3.09	2.95	2.80	1.42	1.76	2.90	2.76	2.16	2.58	1.94	2.10	1.02	1.42	0.96	1.09
FeO		19.06	18.35	18.15	16.86	15.37	17.52	18.75	17.01	19.86	17.76	16.60	18.57	18.76	18.85	18.90
MnO		0.16	0.18	0.27	—	0.16	0.18	0.16	0.10	0.17	0.16	0.24	0.27	0.10	0.20	0.25
MgO		8.24	8.54	8.84	10.55	10.46	10.65	8.24	9.96	8.03	8.36	10.76	8.62	8.62	8.73	9.15
CaO		11.34	11.31	11.35	10.49	11.31	11.25	10.70	11.12	11.12	11.88	12.40	11.97	11.87	11.60	11.50
Na_2O		1.67	1.63	1.43	1.22	1.22	1.65	1.43	1.69	1.35	1.46	1.60	1.52	1.65	1.35	1.30
K_2O		1.35	1.30	1.29	1.35	1.30	0.70	0.92	1.15	0.85	1.20	0.65	0.80	1.05	1.10	1.30
Total		98.16	98.39	97.99	94.79	94.62	99.09	97.09	96.60	97.66	97.67	99.67	96.07	97.24	97.09	97.99

TABLE 1 contd.

Structural formula on the basis of 23 oxygens

	CHR11	CHR	CHR3	326	326	121	54B	110	141	139	183	56a	25	167	72	
Si		6.360	6.391	6.511	6.381	6.469	6.376	6.502	6.363	6.440	6.523	6.352	6.414	6.400	6.466	6.439
Al^{iv}		1.640	1.609	1.489	1.619	1.531	1.624	1.498	1.637	1.560	1.477	1.648	1.586	1.600	1.534	1.561
T		8.000	8.000	8.000	8.000	8.000	8.000	8.000	8.000	8.000	8.000	8.000	8.000	8.000	8.000	8.000
Al^{vi}		0.425	0.449	0.616	0.540	0.504	0.447	0.545	0.468	0.486	0.541	0.526	0.543	0.549	0.609	0.561
Ti		0.356	0.334	0.317	0.166	0.205	0.207	0.319	0.247	0.292	0.220	0.117	0.120	0.156	0.109	0.127
Mg		1.882	1.931	2.029	2.440	2.408	2.395	1.878	2.280	1.827	1.917	2.417	1.999	1.974	1.997	2.086
Fe^{2+}		2.337	2.286	2.038	1.854	1.883	1.951	2.258	2.005	2.395	2.266	1.940	2.338	2.321	2.285	2.226
C		5.000	5.000	5.000	5.000	5.000	5.000	5.000	5.000	5.000	4.944	5.000	5.000	5.000	5.000	5.000
Fe^{2+}		0.084	0.016	0.300	0.312	0.103	0.237	0.113	0.155	0.126	—	0.135	0.068	0.066	0.115	0.159
Mn		0.027	0.027	0.035	—	0.021	0.027	0.019	—	0.018	0.018	0.027	0.037	0.009	0.027	0.036
Ca		1.846	1.823	1.873	1.745	1.986	1.810	1.742	1.822	1.818	1.945	1.986	1.981	1.947	1.896	1.859
Na		0.043	0.134	—	—	—	—	0.127	0.023	0.038	0.037	—	—	—	—	—
B		2.000	2.000	2.208	2.057	2.110	2.074	2.000	2.000	2.000	2.000	2.148	2.052	2.022	2.038	2.054
Na		0.450	0.330	0.428	0.363	0.366	0.486	0.293	0.471	0.364	0.403	0.468	0.463	0.496	0.403	0.381
K		0.274	0.253	0.254	0.268	0.256	0.063	0.167	0.220	0.164	0.239	0.126	0.167	0.184	0.220	0.253
A		0.724	0.583	0.682	0.631	0.622	0.559	0.457	0.691	0.528	0.642	0.594	0.630	0.680	0.623	0.634

that the maximum possible Al^{vi} in calciferous and sub-calciferous amphiboles increase regularly as Al^{iv} increases.

KOSTYUK and SOBOLEV [1969] on the basis of statistical analysis, distinguished a variety of paragenetic types of calciferous amphiboles in metamorphic rocks. They concluded that increasing pressure causes a slight increase in Al^{vi}, whereas increasing temperature causes a slight increase in Al^{iv} and alkalies. The postulated Al^{iv} increase with temperature is in contradiction to detailed investigations of SHIDO and MIYASHIRO [1959], ENGEL and ENGEL [1962], BINNS [1965] and BARD [1970]. These authors

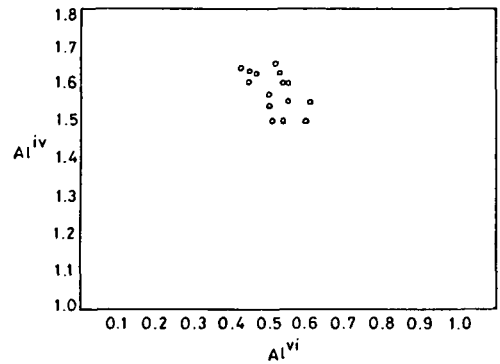

Fig. 2. Plots of Al^{iv} and Al^{vi} for the amphiboles

recognised slight increase of alkalies and Ti and sometimes significant decrease of Al^{vi} and Fe^{2+} with increasing metamorphic grade. This may be interpreted as a change from tschermakitic composition in the low grade amphibolite facies versus pargasitic composition in the hornblende granulite facies [RASSE, 1974]. From the above resume it is clear that the Al content has a complex dependence upon temperature, pressure and chemical environment, which makes it difficult to use it as an indicator of metamorphic grade. Nevertheless the Al^{vi} and Si contents together permit a rather good distinction between hornblendes of low pressure type and high pressure type of regional metamorphism.

The Al^{vi} and Si contents of the hornblendes of the present study are plotted in *Fig. 3* along with Al^{vi} and Si content of hornblendes from some petrographically well known regional metamorphic terrains. The diagonal solid line in *Fig. 3* is taken from LEAKE [1965] and indicate maximum possible Al^{vi}. It can be seen that the hornblendes of the present study are relatively low in Al^{vi} and Si and plot well below the line of maximum possible Al^{vi}, similar to the hornblendes from low pressure regional metamorphic facies series from the Central Abukuma Plateau, Japan [SHIDO and MIYASHIRO, 1959], Broken Hill district, New South Wales [BINNS, 1965] and Adirondack mountains, New York [ENGEL and ENGEL, 1962]. On the contrary, the hornblendes from the Grampian Highlands, Scotland [SHIDO and MIYASHIRO, 1959], the Sanbagawa belt, Japan [BANNO, 1964] and the Holenarsipur schist belt, Karnataka [ANANTHA IYER *et al.*, 1976] plot between the broken line and the line of maximum Al^{vi} in *Fig. 3*, which is indicative of their formation at higher pressures probably above 5 kbs [RASSE, 1974].

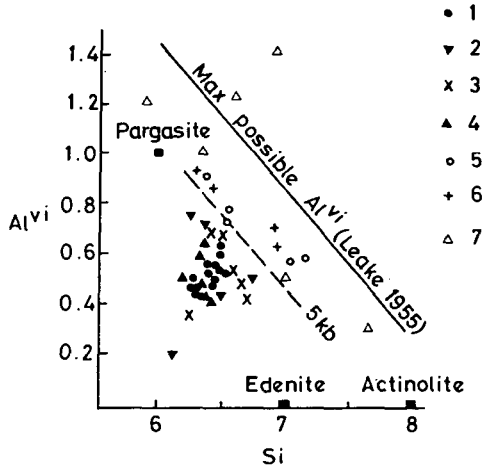

Fig. 3. Relation between Al^{vi} and Si of hornblendes of
1) the present study
2) Central Abukuma Plateau
3) Broken hill district
4) Adirondack Mountains
5) Grampian Highlands
6) Sanbagawa belt
7) Holenarsipur schist belt

Ti CONTENT OF HORNBLENDE AND ITS RELATION TO METAMORPHIC GRADE

Though KOSTYUK and SOBOLEV [1969] were able to distinguish different paragenetic types of hornblende corresponding to different metamorphic facies and rock composition by making use of the diagrams Al—Fe+Mn/Fe+Mg, Na+K−Al−(Na+K) and $Al^{iv}-Al^{vi}$, it is impossible to relate a hornblende of a definite composition to a definite paragenetic type, since overlapping of hornblende composition is large. So the most satisfactory parameter that can be used to distinguish different paragenetic hornblendes is the Ti content. A comparison of the Ti contents of hornblendes from rocks of different metamorphic facies has shown that variation in Ti content is related to metamorphic grade.

In *Fig. 4* the Ti content of the hornblendes of the present study and Ti content of hornblendes from rocks of different metamorphic facies is represented. Although there is some overlapping in Ti contents regarding neighbouring metamorphic facies, there is a clear trend of increasing Ti with metamorphic grade. The broken line in *Fig. 4,* indicates maximum possible Ti in hornblende of respective metamorphic facies.

Ti AND Al VARIATIONS AND THE INFLUENCE OF OXYGEN FUGACITY

Several authors have evaluated Ti and Al^{iv}/Al^{vi} variations in hornblende in terms of difference in bulk chemistry, modal content, T and P conditions of metamorphism [RASSE, 1974; BINNS, 1965; HELZ, 1973 and GRAPES *et al.,* 1977]. However, the observed features of the hornblendes of the present study, namely, *1.* no relation-

ship between the whole rock Ti content and the Ti content of hornblendes; *2.* the consistency in the $Fe^{tot}/Fe^{tot}+Mg$ of the hornblendes; *3.* lower Ti content in hornblendes associated with Fe—Ti oxides than those associated with pyroxene; *4.* high whole rock oxidation ratios, defined as $Fe^{3+}/Fe^{3+}+Fe^{2+}$ molar ratios, tend to be related to relatively lower Ti values in the hornblendes *(Fig. 5)*, have made the authors to believe that the Ti variations in the hornblendes of the present study is due to a combination of independent parameters namely, temperature of metamorphic crystallisation and oxygen fugacity.

The influence of oxygen fugacity is noted on minor scale as shown by the low Ti contents of hornblende that surrounds Fe—Ti oxides but also much larger scale as shown by a correlation of low Ti with relatively high whole rock oxidation ratios. Both the relationships are consistent with data of HELZ [1973] who has demonstrated experimentally that an increase in fO_2 at constant whole rock oxidation ratio and

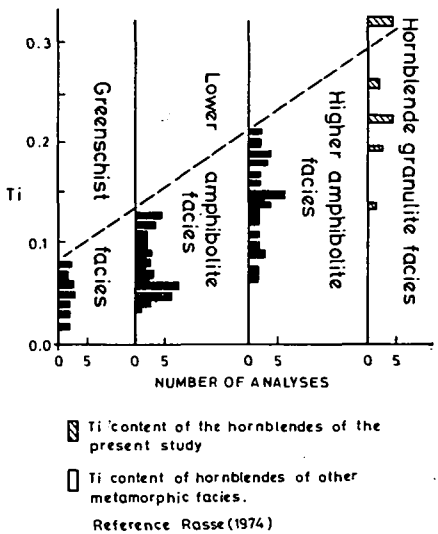

Fig. 4. Histogram of Ti content of hornblende of the present study and hornblendes in rocks of metamorphic facies

temperature reduces the Ti content of hornblende in favour of Fe—Ti oxides. Hornblende around Fe—Ti oxides in the charnockites of Sivasamudram and Kanakapura areas apperently form microdomains of relatively high fO_2. HELZ [1973] has also demonstrated that the Ti content of hornblende increase with rising temperature in the range of 700°—1000°, in agreement with the inferences of BINNS [1965] and RASSE [1974]. The relations between Ti and temperature, however, is shown to be highly dependent upon fO_2. HELZ [1973] observed distinct positive correlation in quartz-fayalite-magnetite buffered experiments. In hematite-magnetite buffered ones, on the other hand, the Ti content of hornblende was rather low, showing to increase with rising temperature.

The observed positive correlation between Ti and Na + K and Al^{iv} and Na + K in a near 1 : 2 and 1 : 1 cation ratio, respectively *(Figs. 6. and 7)* are consistent with a model of titanotschermakite substitutions in the hornblende structure expressed as Ti, 2Al, Mg, 2Si, coupled with an increasing occupation of the *A* site [ROBINSON *et al.*,

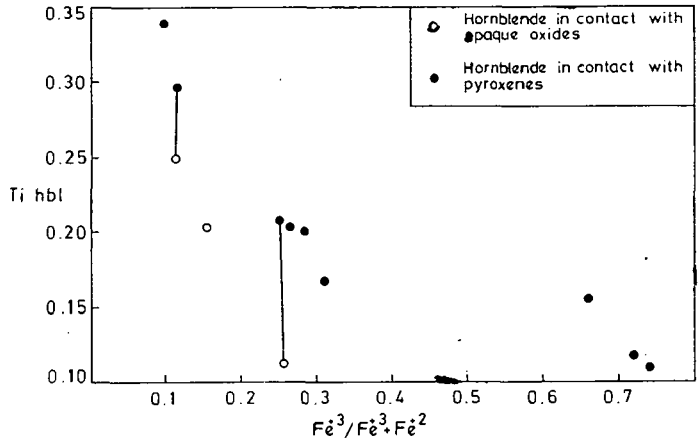

Fig. 5. Plot of Ti content of hornblende and whole rock oxidation ratio expressed as molar ratio $Fe^{3+}/Fe^{3+}+Fe^{2+}$

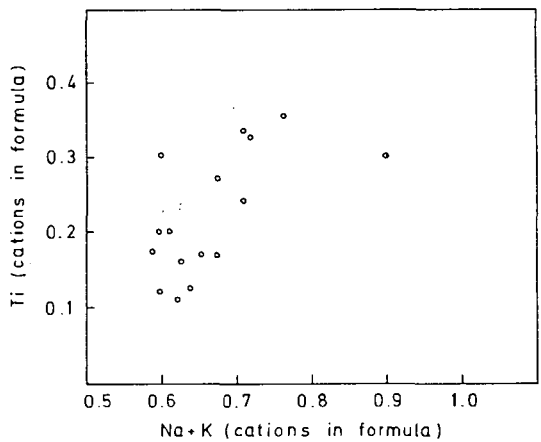

Fig. 6. Plot of Ti and total alkalies for hornblendes showing positive correlation in near 1:2 cation ratio

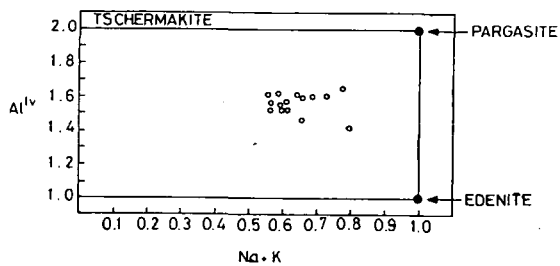

Fig. 7. Plot of Al^{iv} and total alkalies for hornblende

1971; GRAPES *et al.*, 1977; COOLEN, 1980 and VAN LAMOEN, 1980]. However, the above substitution is more complex than described above because of the generally complementary relation between Ti and Al^{vi}. Nevertheless, the $Al^{iv}-Al^{vi}$ relationship in the hornblendes of the present study may be regarded as essentially a function of Ti substitutions. Similar relationships are discussed by VAN LAMOEN [1980] and COOLEN [1980] who stressed the point that substitution of this type strongly influence the Al^{iv}/Al^{vi} ratio in hornblende, a ratio currently being used to indicate pressure estimates of metamorphism [RASSE, 1974 and MORTEANI, 1978].

CONCLUSIONS

Hornblendes from the charnockites of Karnataka show all the characteristics of previously published high Ti, high Al and high alkali hornblendes from other granulite facies areas. The hornblendes of the present study are of low pressure type which can be clearly demonstrated by $Al^{vi}-Si$ content of these hornblendes. The variation in Ti content of the hornblendes is due to a combination of independent parameters namely, temperature of metamorphic crystallisation and oxygen fugacity. The $Al^{iv}-Al^{vi}$ relationships in the hornblendes of the present study has been regarded as essentially a function of Ti substitutions.

ACKNOWLEDGEMENTS

We are indebted to DR. C. SIVAPRAKASH, Department of Mineralogy and Petrology, Cambridge University, Cambridge for providing electron microprobe analyses. We are grateful to DR. C. R. L. FRIEND, Oxford Polytechnic, Oxford and PROF. C. NAGANNA, Head of the Department of Geology, Bangalore University, Bangalore, who critically reviewed the manuscript.

REFERENCES

ANANTHA IYER, G. V. and NARAYANAN KUTTY, T. R. [1976]: Geochemistry of amphiboles from the Precambrian of Karnataka. Jour. Geol. Soc. India **17**, 17—36.

BARD, J. P. [1970]: Composition of hornblendes formed during the Hercynian progressive metamorphism of the Aracena metamorphic belt (SW Spain). Contrib. Mineral. Petrol., **28**, 117—134.

BANNO, S. [1964]: Petrologic studies on Sanbagawa crystalline schist in the Bessi-Ino district, Central Shikoku Japan. J. Fac. Sci. Uni. Tokyo, Sect II., **15**, 203—319.

BINNS, R. A. [1965]: The mineralogy of metamorphosed basic rocks from the Willyama complex Broken Hill district, New South Wales, Part I. Hornblendes. Mineral. Mag., **35**, 306—326.

COOLEN, J. J. M. M. [1980]: Chemical petrology of the Furua granulite complex, Southern Tanzania. GUA papers of geology, **1**, 13, 1—246.

DAVIDSON, L. R. [1971]: Metamorphic hornblendes from basic granulites of the Quirding district, Western Australia. N. Jb. Mineral. Mh., 344—349.

DAWSON, J. B. and SMITH, J. V. [1973]: Alkalic pyroxenite from the Lashine Volcano, Northern Tanzania, J. Petrol., **14**, 113—131.

ENGEL, A. E. J., ENGEL, C. C. and HAVENS, R. G. [1964]: Mineralogy of amphibole interlayers in the gneiss complex, North West Adirondack mountains, New York. J. Geol., **72**, 134—156.

ENGEL, A. E. J. and ENGEL, C. C. [1962]: Hornblendes formed during progressive metamorphism of amphibolites, North West Adirondack mountains, New York. Geol. Soc. Am. Bull., **73**, 1499—1514.

FABRIES, J. [1968]: Nature des hornblendes et type de metamorphism. Pap. Proc. 5th Gen. Meet. Cambridge (Engl), 204—211.

GRAPES, R. H., HASHIMOTO, S. and MIYASHITA, S. [1977]: Amphiboles of a metagabbro-amphibolite sequence, Hidaka metamorphic belt, Hokkaido. J. Petrol., **18**, 285—306.

HELZ, R. T. [1973]: Phase relations of basalts in their melting range at $P_{H_2O} - 5$ kb as a function of oxygen fugacity. Part I. Mafic phases. J. Petrol., **14**, 249—306.

KOSTYUK, E. A. and SOBOLEV, V. S. [1969]: Paragenetic types of calciferous amphiboles of metamorphic rocks. Lithos **2,** 67—82.
LAMOEN, H. van [1980]: Ti zoning in corona hornblende of a metamorphosed iron ore from Susimaki, South West Finland. Neues Jahrb. Miner. Mh., 88—96.
LEAKE, B. E. [1965]: The relationship between tetrahedral aluminum and maximum possible octahedral aluminum in natural calciferous and sub-calciferous amphiboles. Am. Mineral, **50,** 843—851.
LEAKE, B. E. [1971]: On aluminous and edenitic hornblendes. Mineral Mag., **38,** 389—407.
LEAKE, B. E. [1978]: Nomenclature of amphiboles. Am. Mineral., **63,** 1023—1052.
LEELANANDAM, C. [1970]: Chemical mineralogy of hornblendes and biotites from the charnockitic rocks of Kondapalli, India. J. Petrol., **11,** 475—505.
MORTEANI, C. [1978]: High-aluminum amphiboles from the Penninic rocks of the Western Tauern window (Tyrol, Austria). Neues Jahrb. Mineral. Abh., **133,** 132—148.
RASSE, P. [1974]: Al and Ti contents of hornblende: Indicators of pressure and temperature of regional metamorphism. Contrib. Mineral. Petrol., **45,** 231—236.
ROBINSON, P., ROSS, M. and JAFFE, H. W. [1971]: Composition of the anthophyllite-gedrite series, comparisons of gedrite and hornblende and the anthophyllite-gedrite solvus. Am. Mineral., **56,** 1005—1041.
SHIDO, F. and MIYASHIRO, A. [1959]: Hornblende of basic metamorphic rocks. Univ. Tokyo J. Fac. Sci., II, **12,** 85—102.
STATHAM, F. J. [1976]: A comparative study of techniques for quantitative analysis of the X-ray spectra obtained with Si(Li) detector. X-ray Spectrom., **5,** 16—28.
SWEATMAN, R. R. and LONG, J. V. P. [1969]: Quantitative electron probe microanalysis of rock forming minerals. J. Petrol., **10,** 332—379.

Manuscript received, 12 May, 1983

B. MAHABALESWAR AND I. R. VASANT KUMAR
Department of Geology,
Bangalore University, Bangalore 560 056
INDIA

Felelős kiadó: Grasselly Gyula

Készült: monószedéssel, íves magasnyomással, 10,8 A/5 ív terjedelemben,
az MSZ 5601—59 és 5602—55 szabvány szerint
84-928 — Szegedi Nyomda — Felelős vezető: Dobó József igazgató

Illustrations

Figures should be used only where they are essential to elucidate the text.

The illustrations should be numbered according to their sequence in the text, and in the text references should be made to each figure.

All illustrations should be given separately, not stuck on sheets and not folded. The number of the figure and the authors name should be noted on the reverse side of the photograph and on the lower frontside of drawings, indicating at the same time the top of the figure where it is necessary.

Captions for all figures should be given typewritten on a separate list at the end of the manuscript. Drawn text in the figures should be kept to a minimum.

Drawings should be made on tracing paper by Indian ink. The thickness of the lines and the size of the lettering should be big enough to allow a necessary reduction.

Photographs of good contrast and intensity on glossy paper are only acceptable. Colour photographs or drawings cannot be accepted.

Use bar scale on all illustrations instead of numerical scales that must be changed if reduction is necessary.

References

All references to publications made in the text should be made by quoting the author's name (without initials) and year of publication in parenthesis.

The list of references at the end of the manuscript should be arranged alphabetically by author's names and chronologically per author.

If the referred publications are written by more than two authors, in the text only the name of the first author should be indicated, the other co-authors are denoted by "et al.", however, in the list of references the names of authors and all co-authors should be mentioned.

In the list of references all references should be written, e.g. Balogh, K., A. Barabás [1972]: The Carboniferous and Permian of Hungary. Acta Miner. Petr., Szeged, XX/2, 191—207.

At references to books beside the author's name, year of publication, title and the publishing house should also be mentioned.

In the case of references for symposium volumes, special issues or multi-authors books, the following system should be used: Roser, B. P., C. W. Childs, and G. P. Glasby [1980] : Manganese in New Zealand. In: I. M. Varentsov and Gy. Grasselly (Editors): Geology and Geochemistry of Manganese, Vol. II. Akadémiai Kiadó, Budapest, 199—211.

Manuscripts that are not adequately prepared will be returned to the author(s).